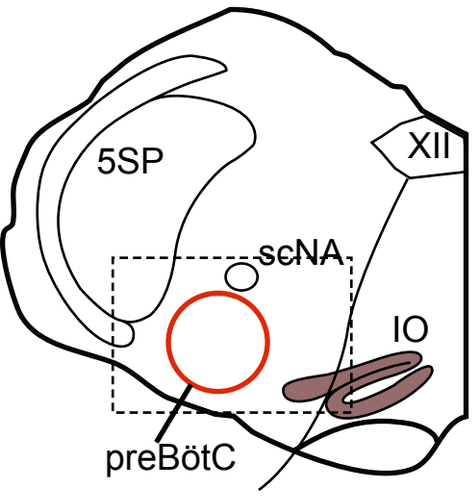

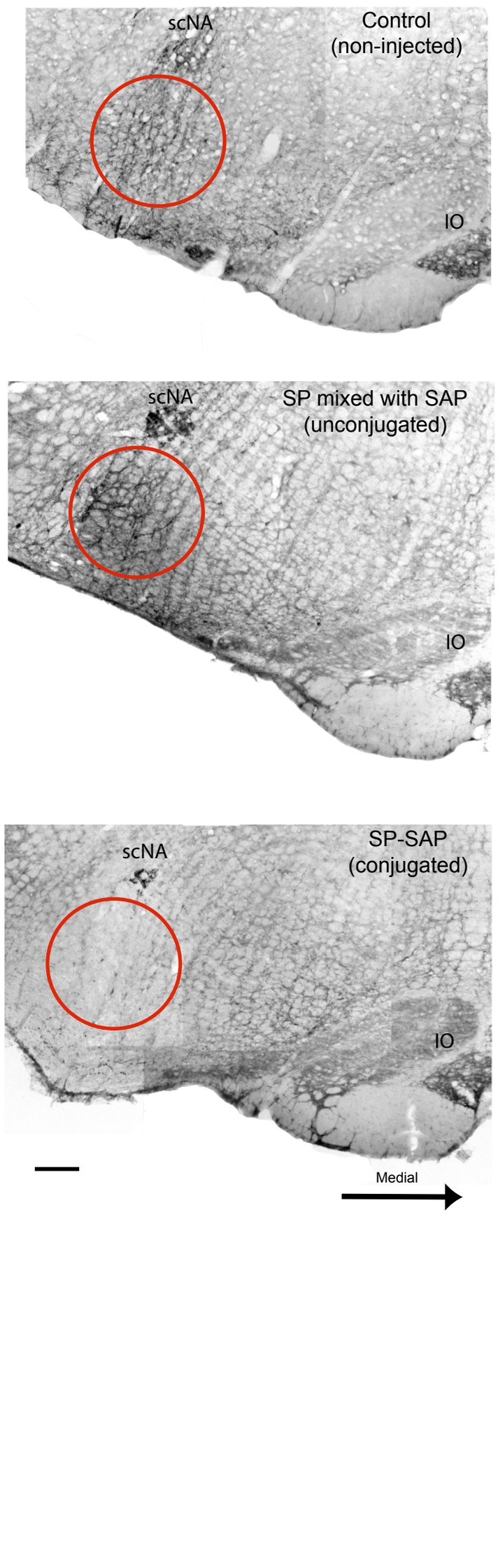

Supplementary Figure 1 SP-SAP specifically ablates NK1R neurons within the preBötC. Schematic of transverse medullary slice denotes extent of preBötC (circle) and surrounding area (rectangle) analyzed for NK1R neurons. All histological analyses were carried out > day 10 post injection, when the rats exhibited an ataxic breathing pattern. *In vivo*, neuronal death following SAP-induced lesions occurs o ver a period of days with most targeted cells ablated by day 7 post injection[14]. Lesions were confined to the preBötC where NK1R immunopositive staining was significantly reduced or completely absent. In some additional cases with identical outcomes (n=3), a small number of neurons within the nucleus ambiguous (NA) were damaged; thus we can not exclude that the pathological changes in breathing observed here (see also[13]) may be partly attributed to a small amount of upper airway motoneuronal damage within the NA, or the destruction of a small number of NK1R bulbospinal neurons that are also located within this area[17]. However, such changes would be unlikely to account for the disturbances of rhythm. There was no significant neuronal loss in other regions examined (e.g., solitary tract and motor nucleus of vagus), similar to the results reported in our previous study using the same injection protocol[13]. An ataxic breathing pattern did not develop in rats with destruction of <50% of preBötC NK1R neurons (n=3). These rats were monitored up to 20 days post-injection, during which time respiratory disorders did not increase significantly in frequency during sleep or wakefulness (P>0.05). scNA, compact nucleus ambiguous; IO, inferior olive; XII hypoglossal nucleus; 5SP, trigeminal nucleus. Scale bar, 200 µm.

CONTROL(pre-injection)

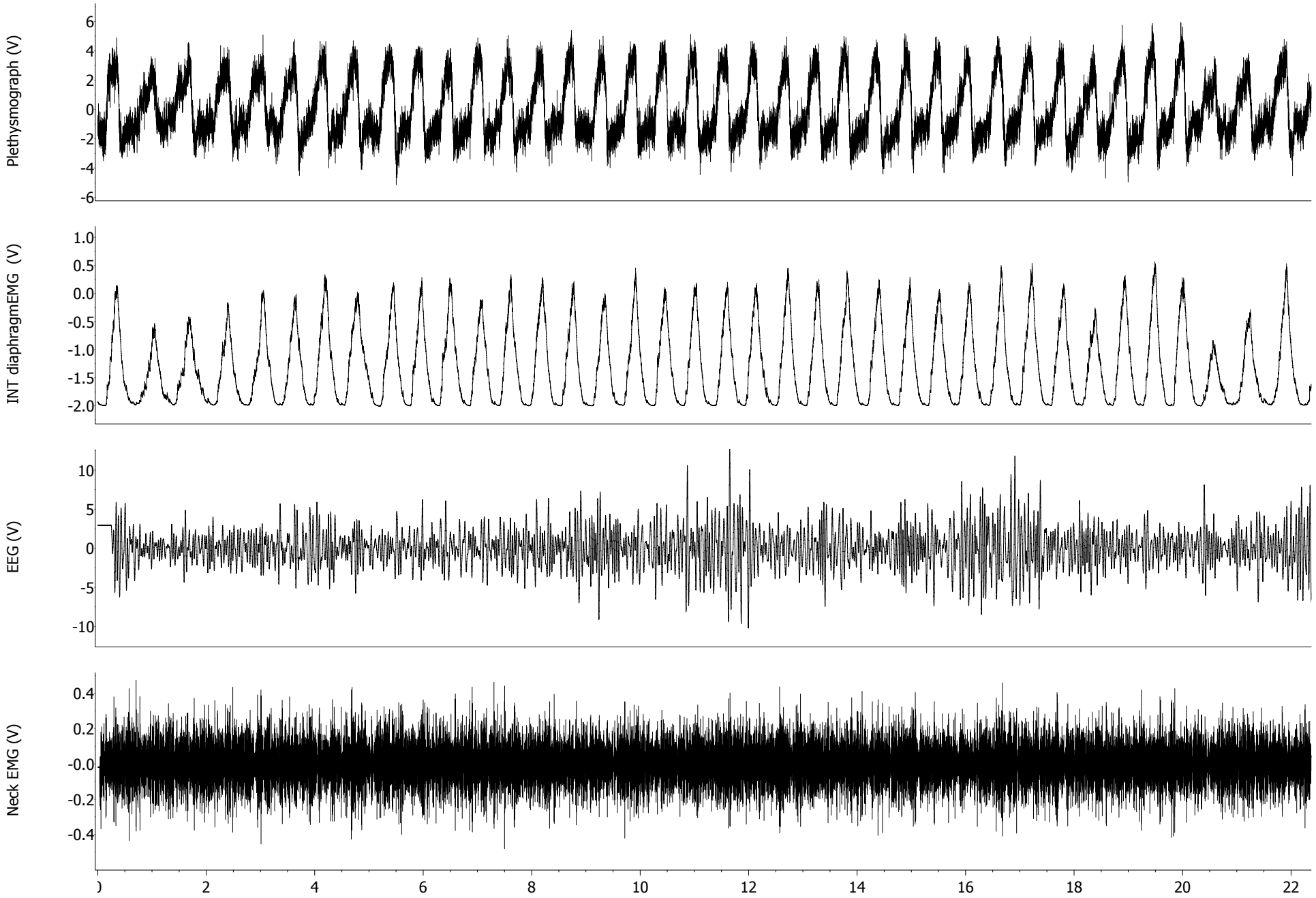

CONTROL(pre-injection)

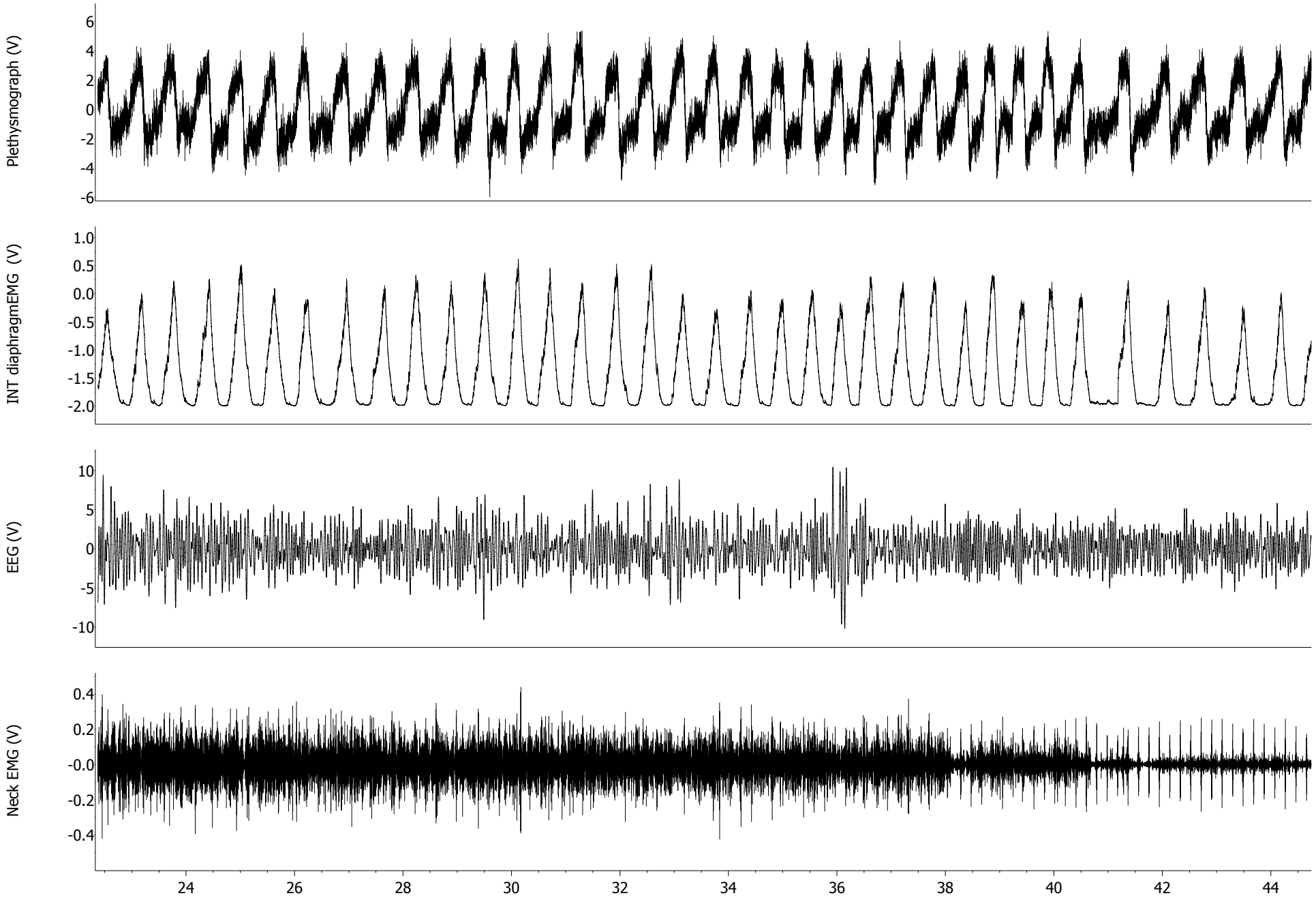

CONTROL(pre-injection)

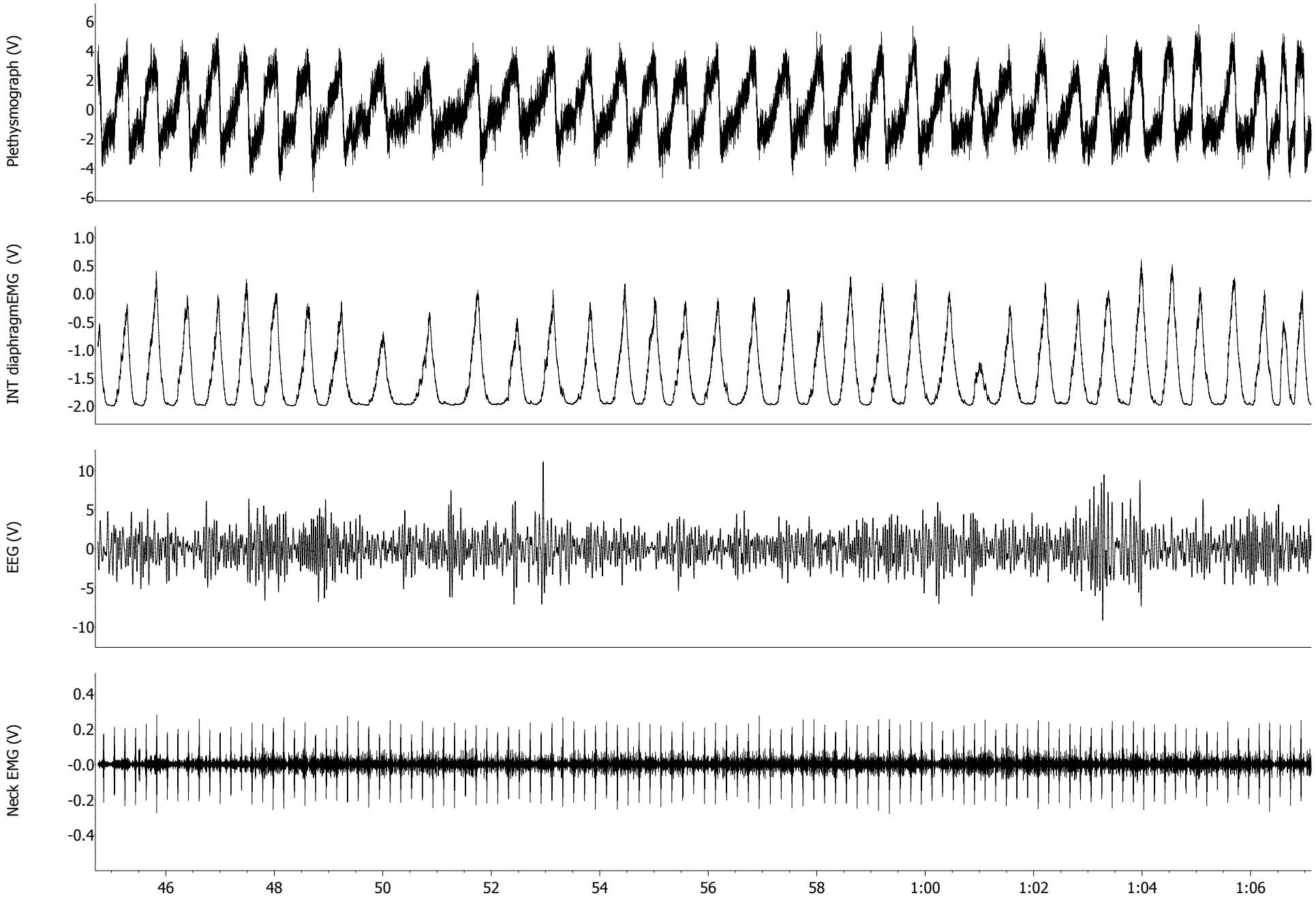

CONTROL(pre-injection)

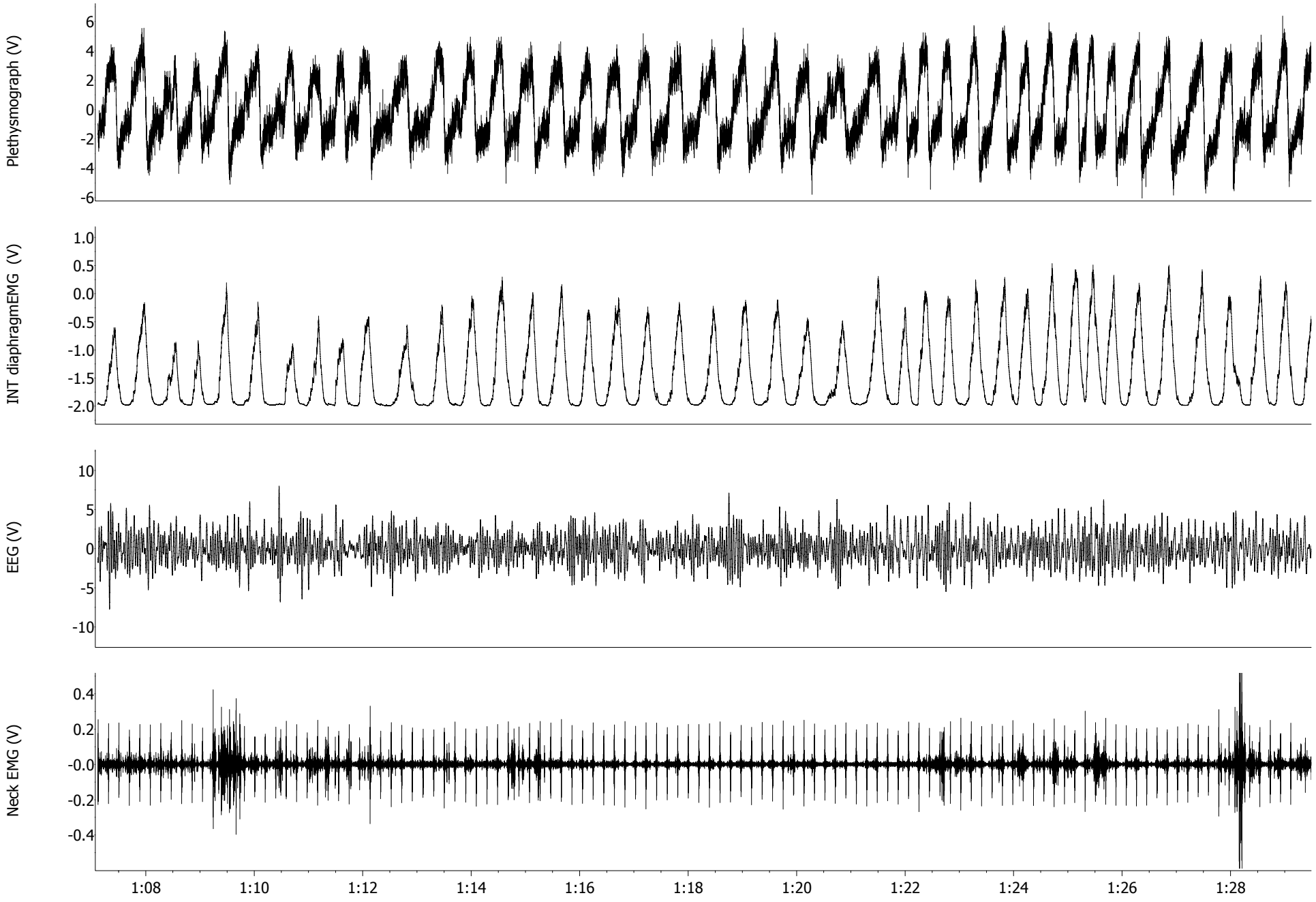

CONTROL(pre-injection)

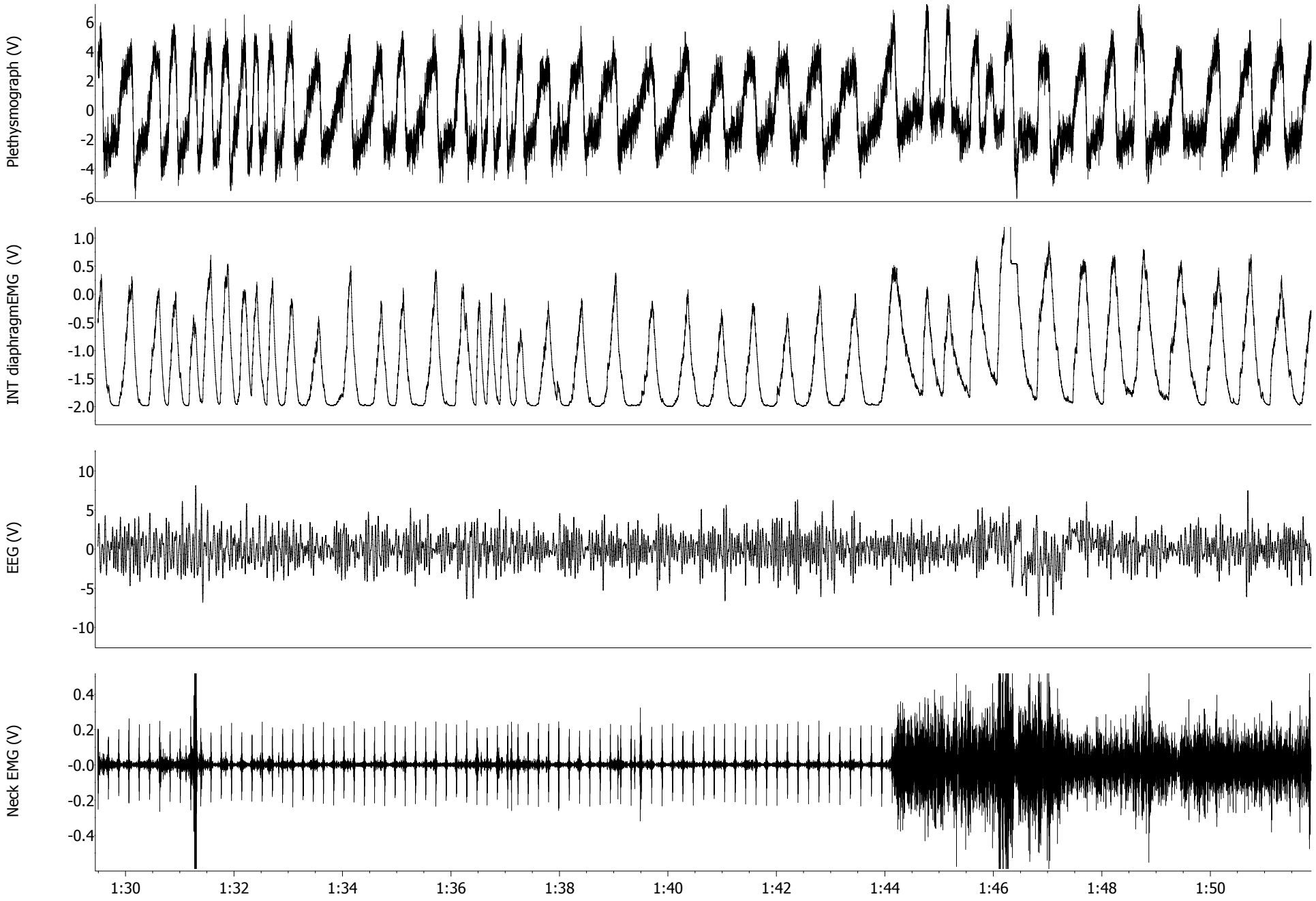

CONTROL(pre-injection)

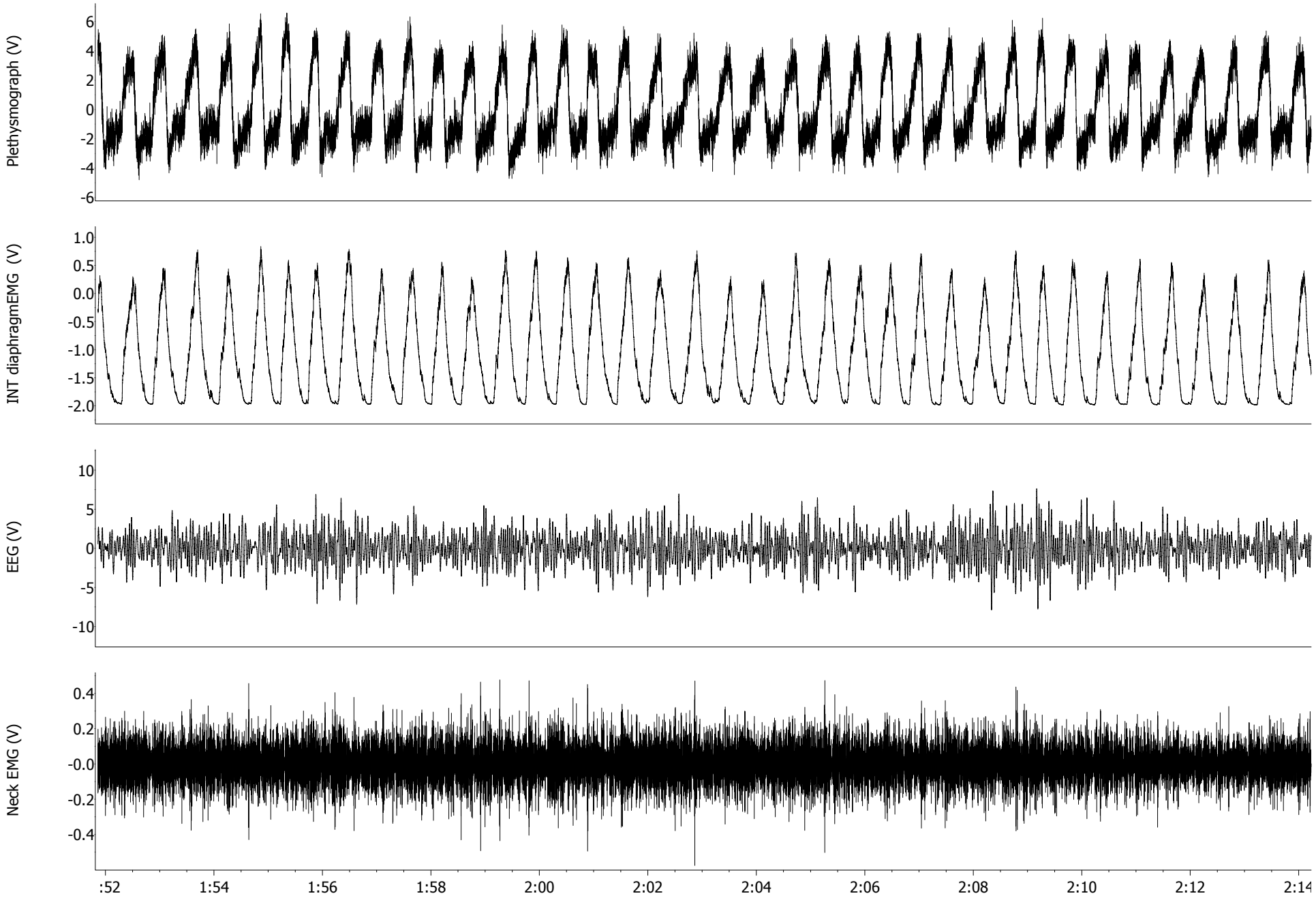

CONTROL(pre-injection)

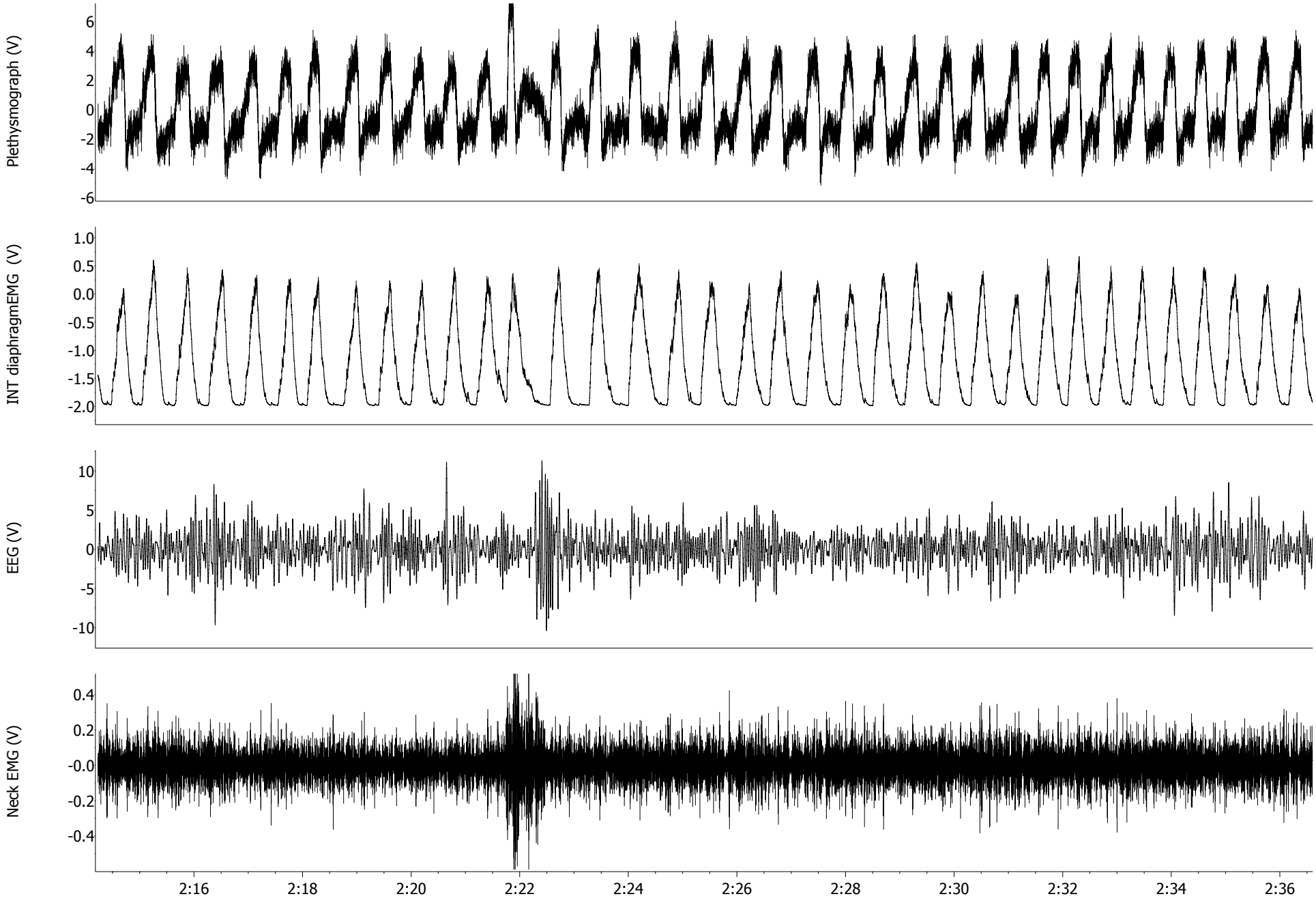

CONTROL(pre-injection)

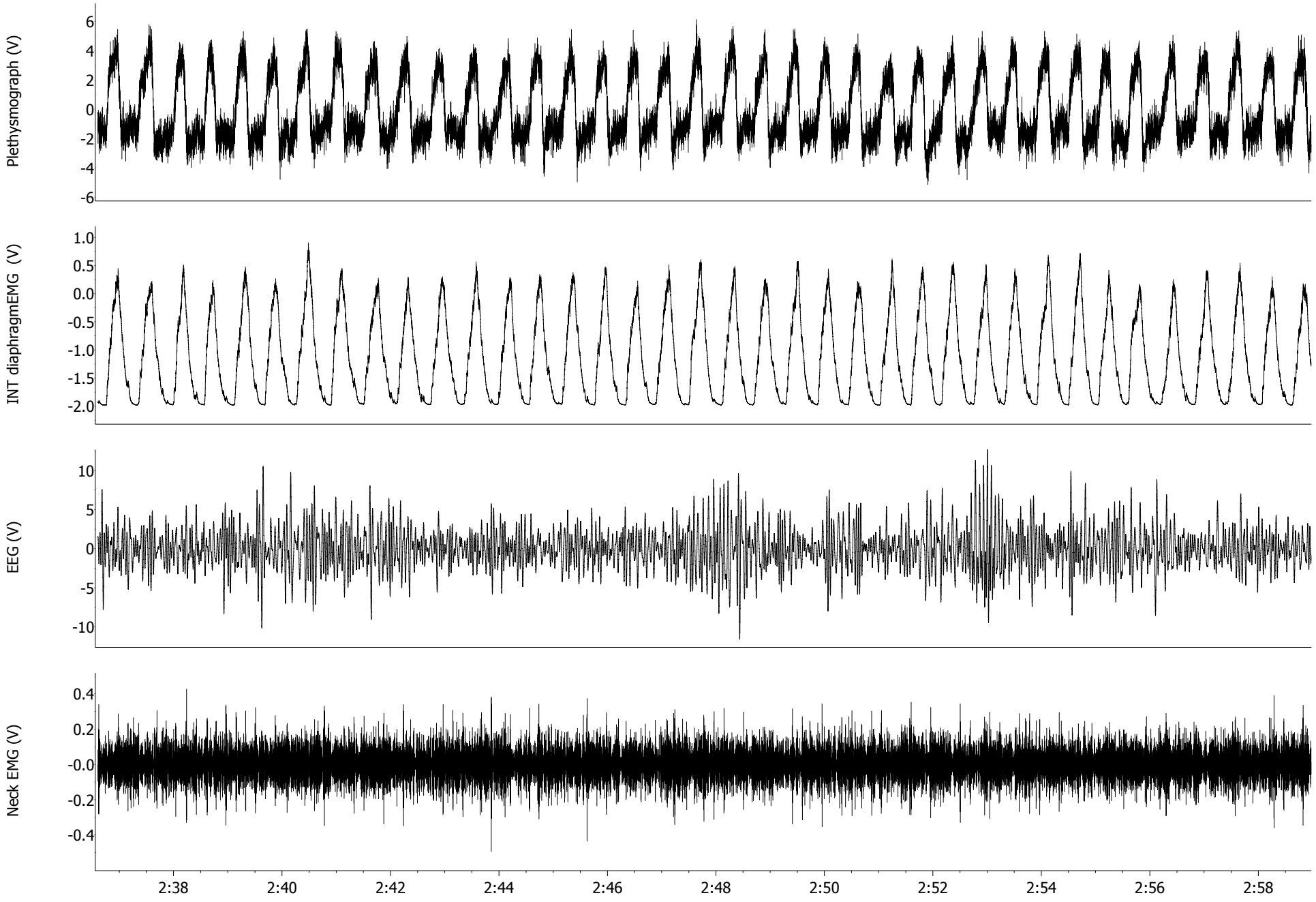

CONTROL(pre-injection)

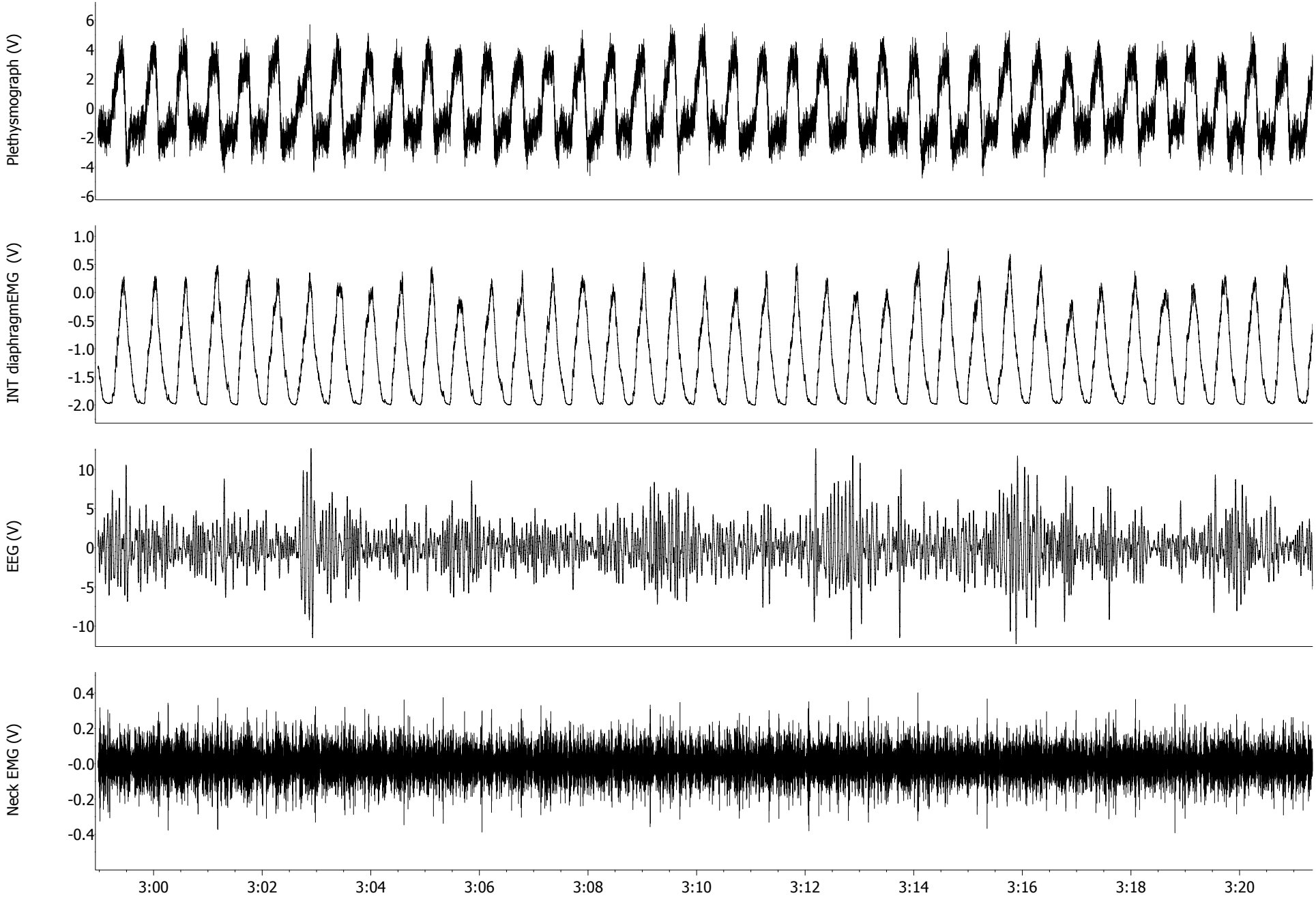

CONTROL(pre-injection)

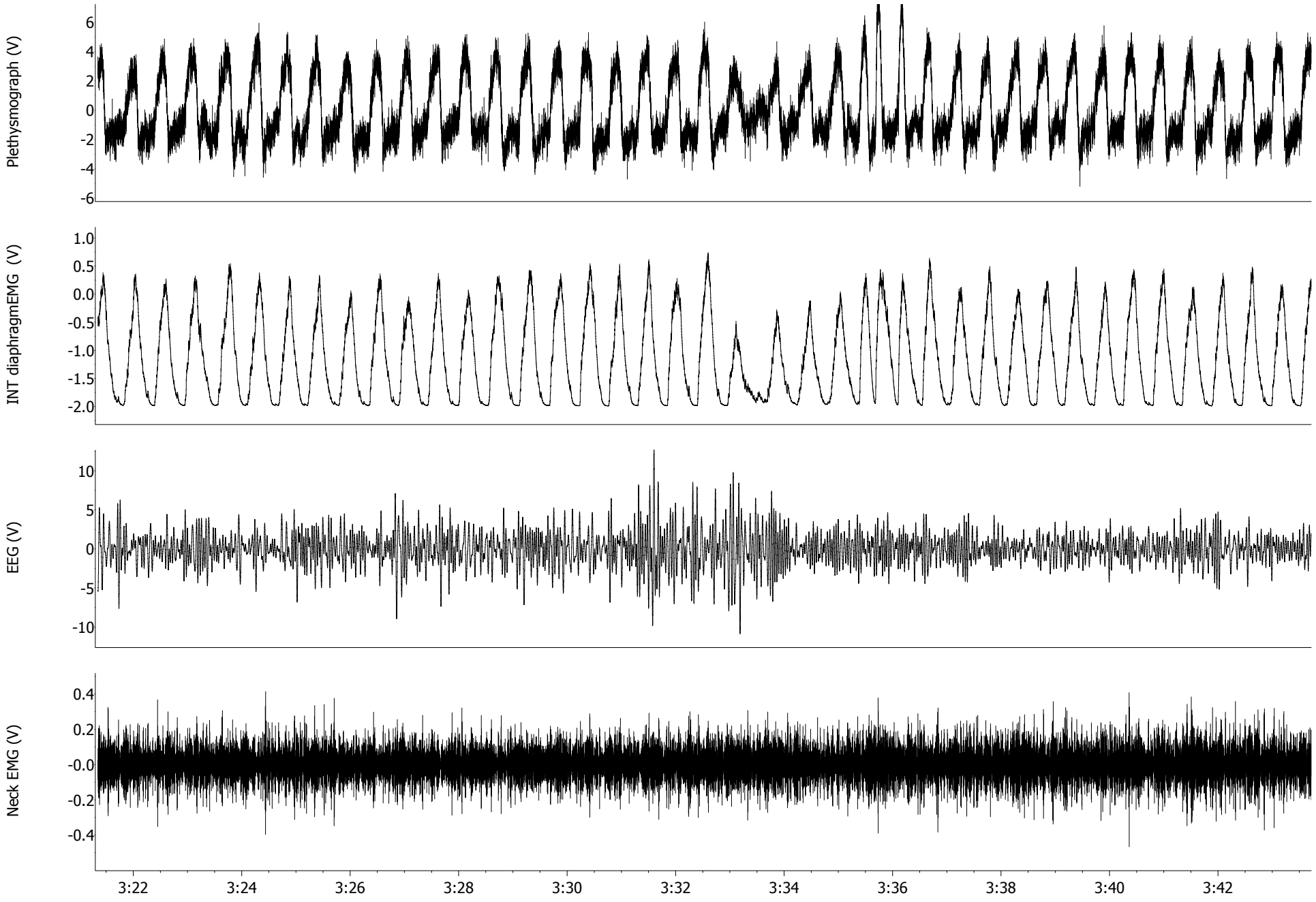

CONTROL(pre-injection)

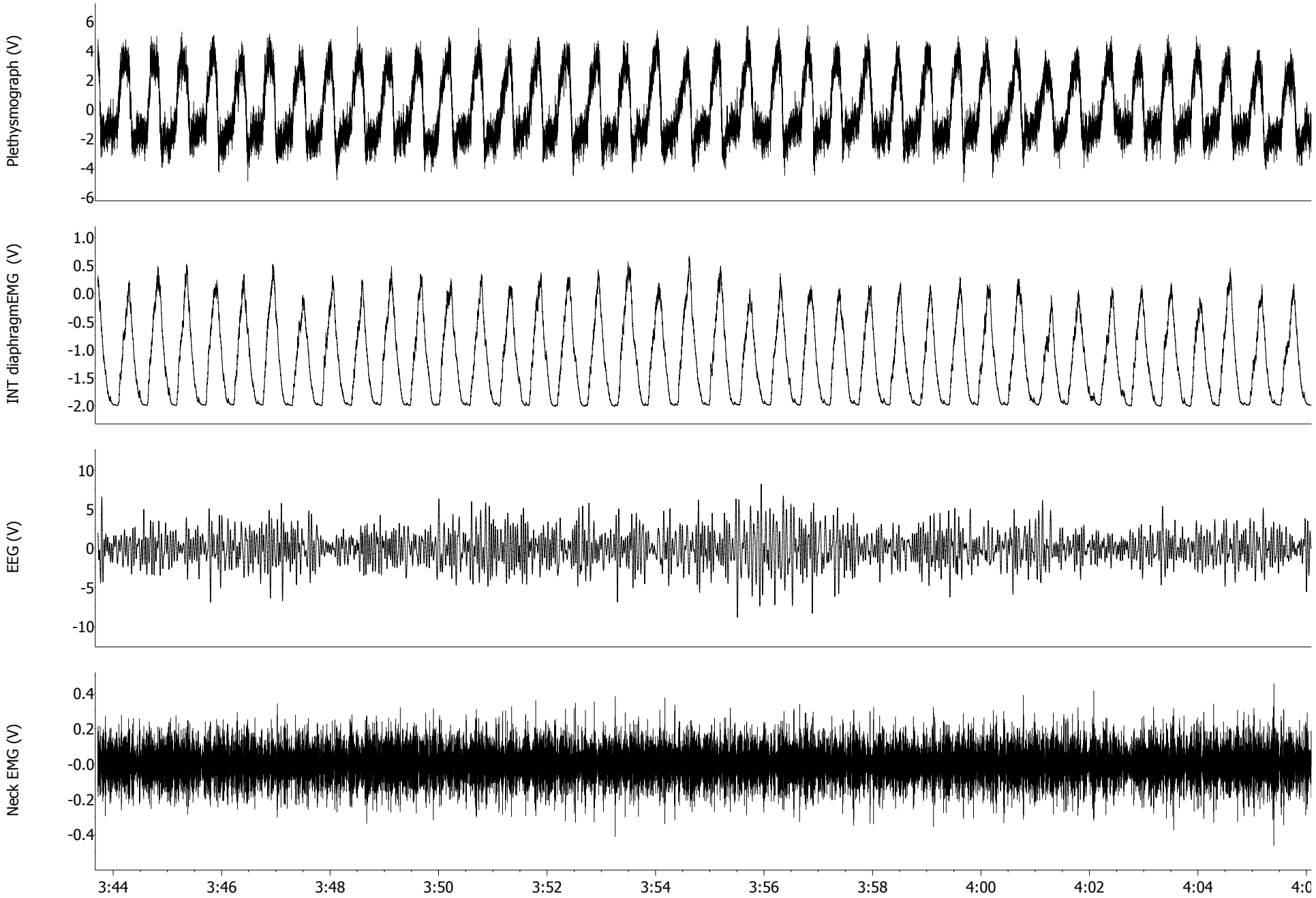

CONTROL(pre-injection)

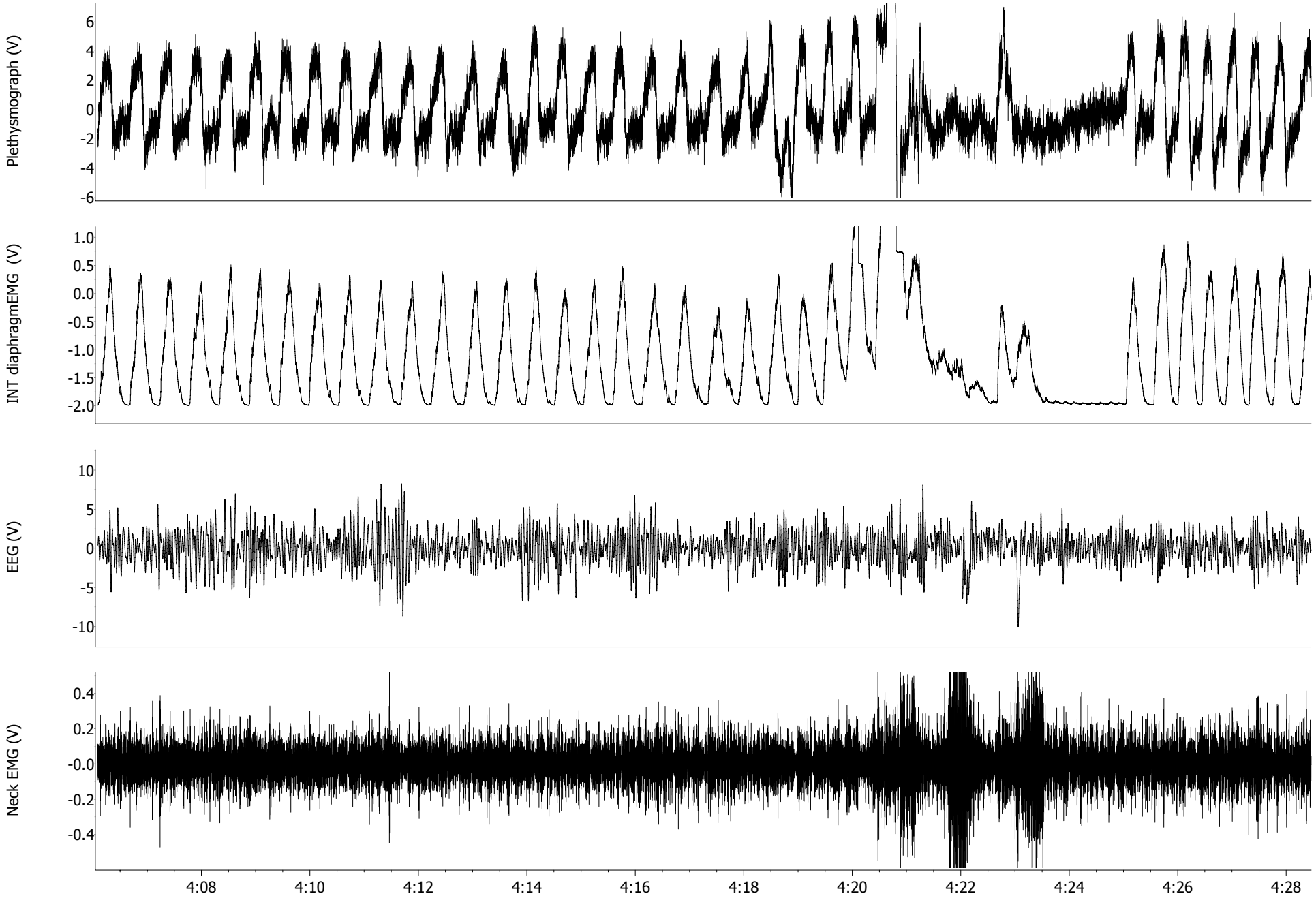

CONTROL(pre-injection)

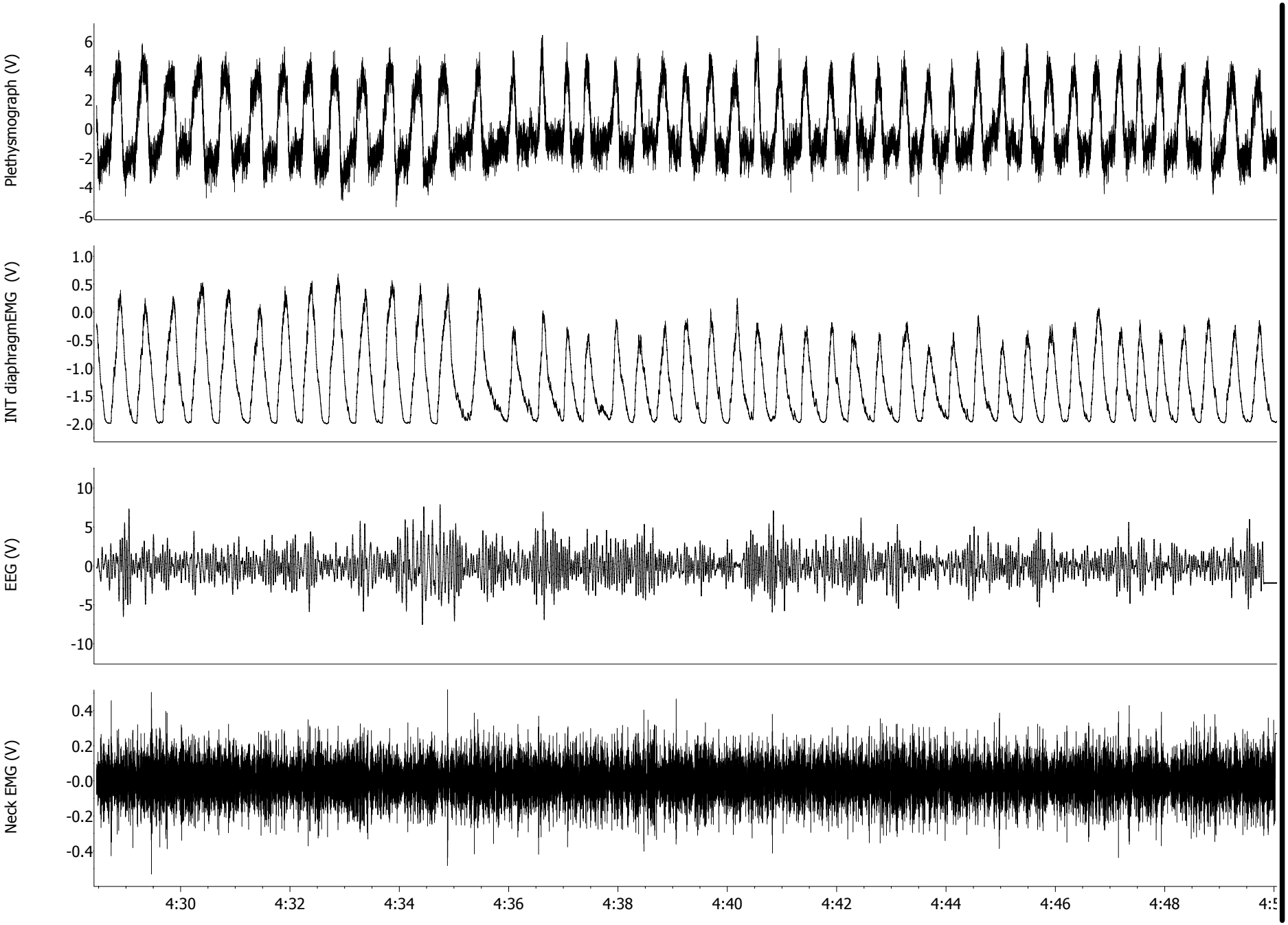

Supplementary Figure 2: Continuous 5 minute physiological recordings pre-injection (control). Tracings of plethysmograph, integrated diaphragm EMG, EEG and raw neck EMG. Respiratory pattern was regular during wakefulness and sleep.

DAY4 Post-injection

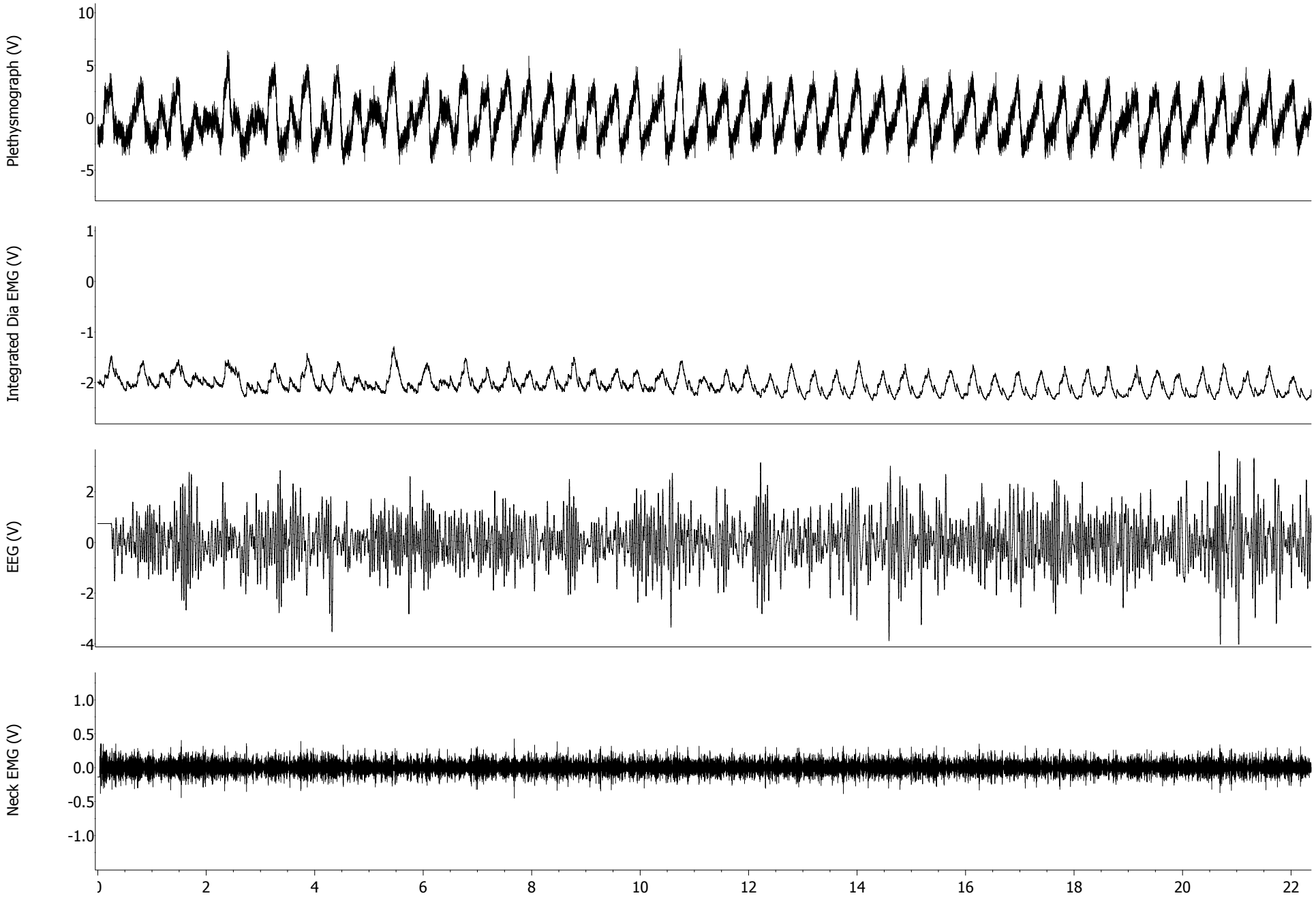

DAY4 Post-injection

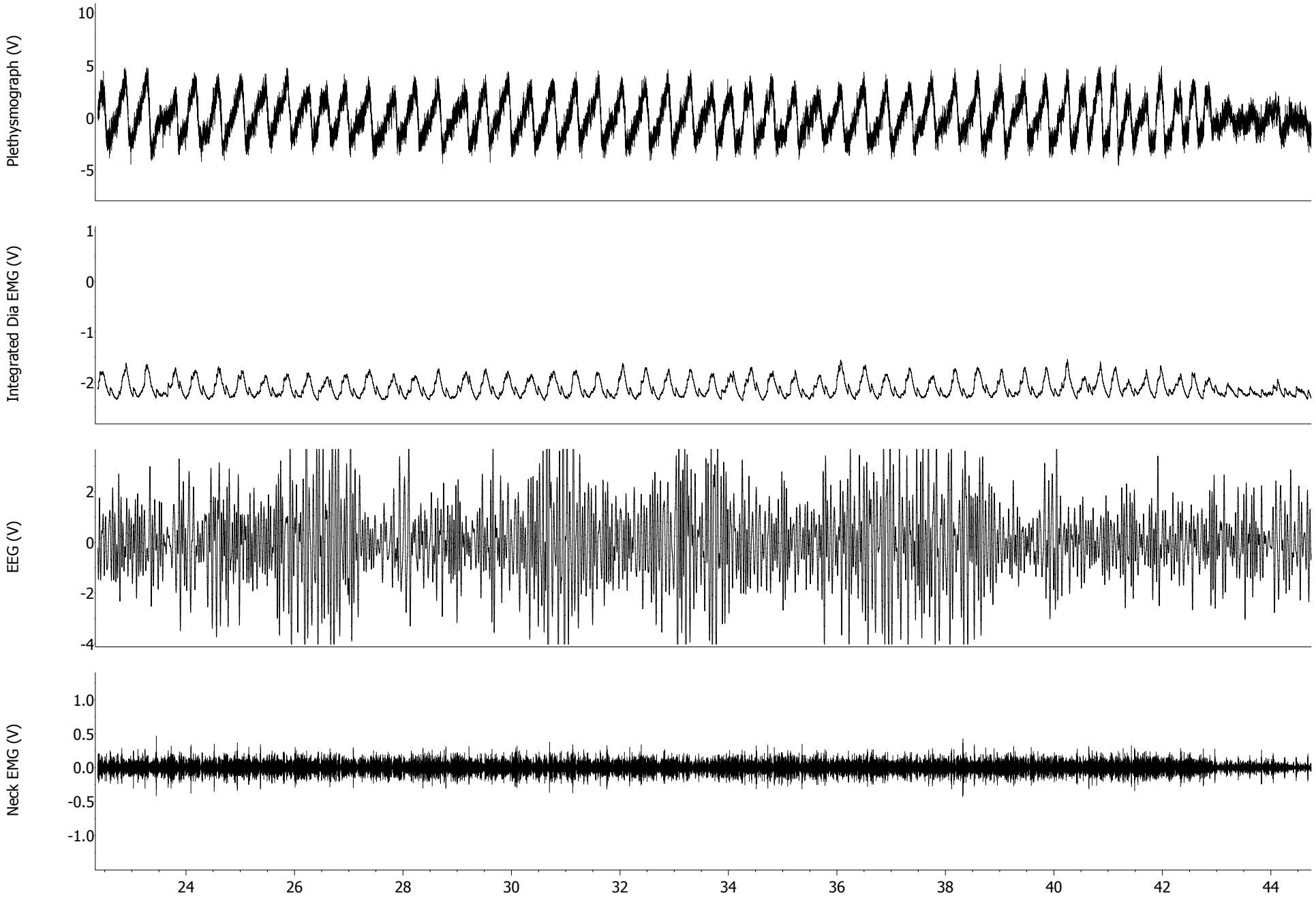

DAY4 Post-injection

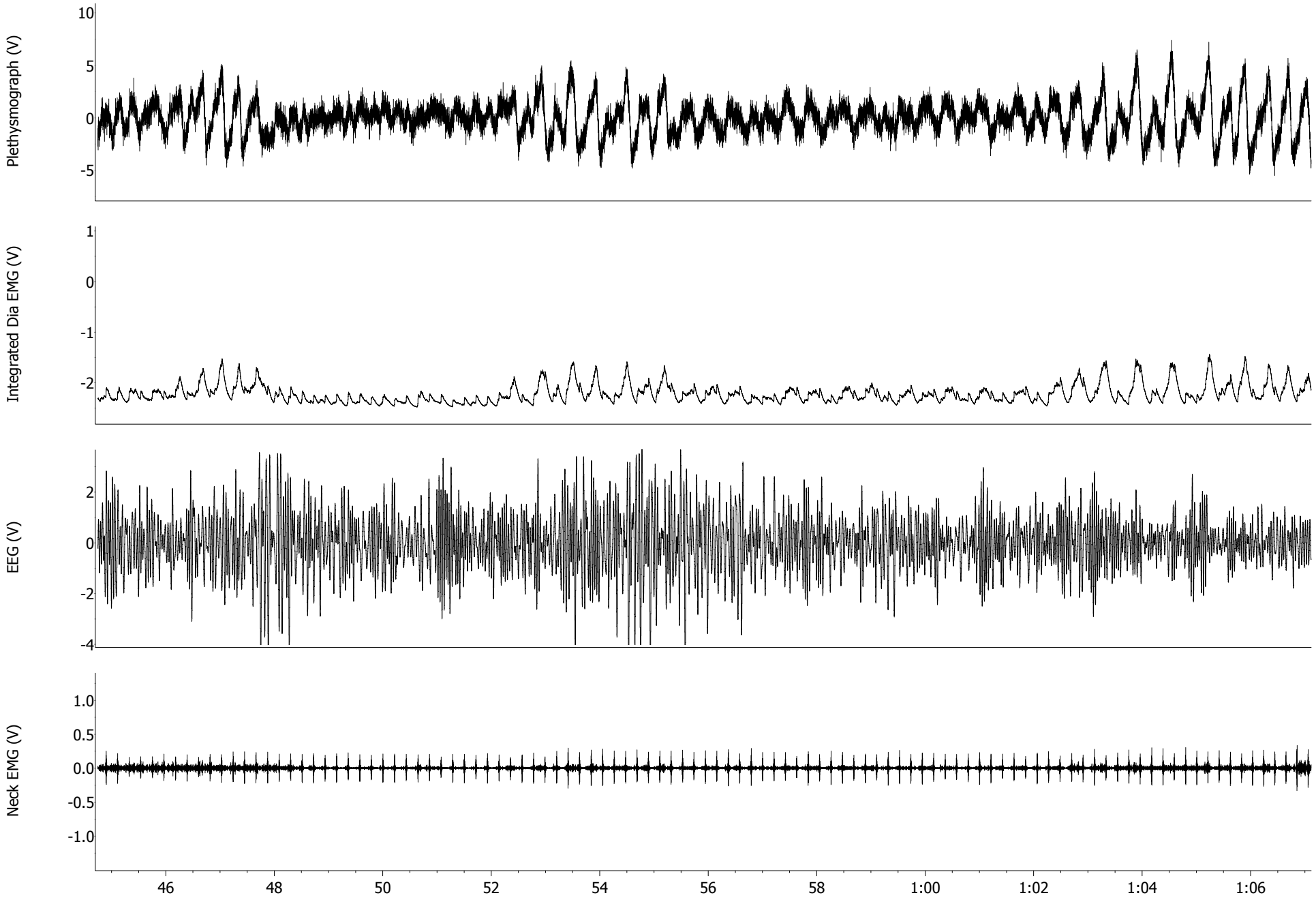

DAY4 Post-injection

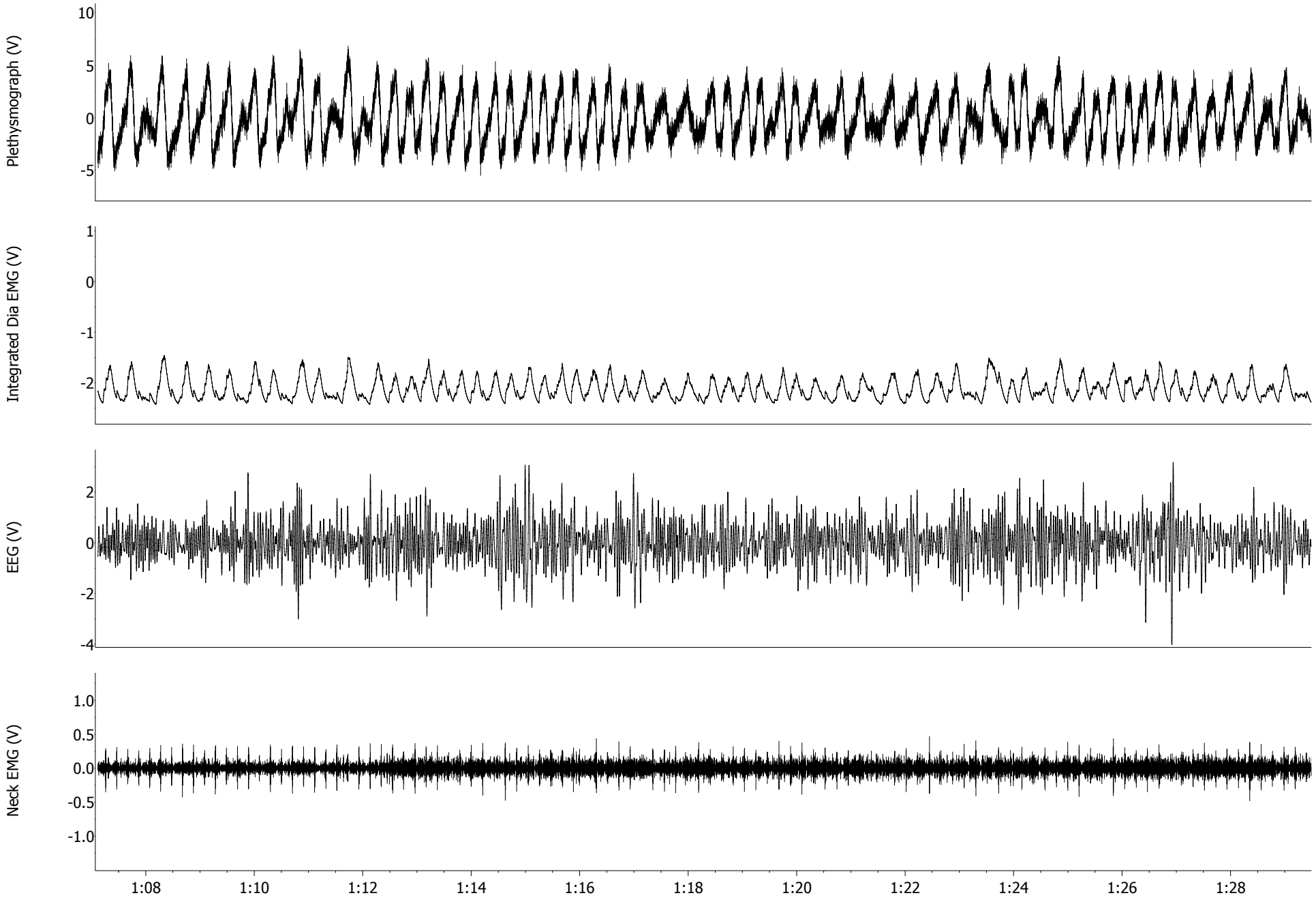

DAY4 Post-injection

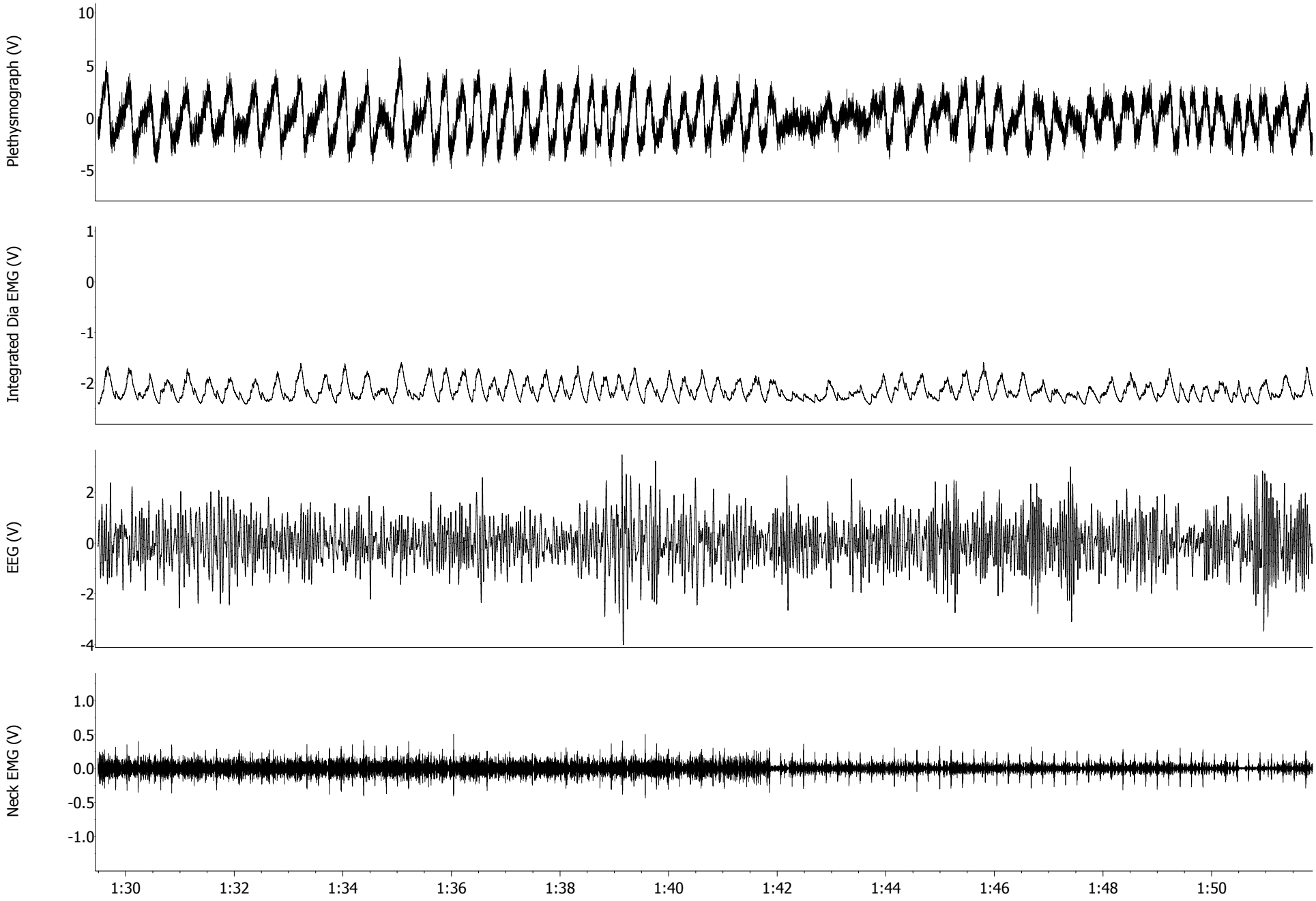

DAY4 Post-injection

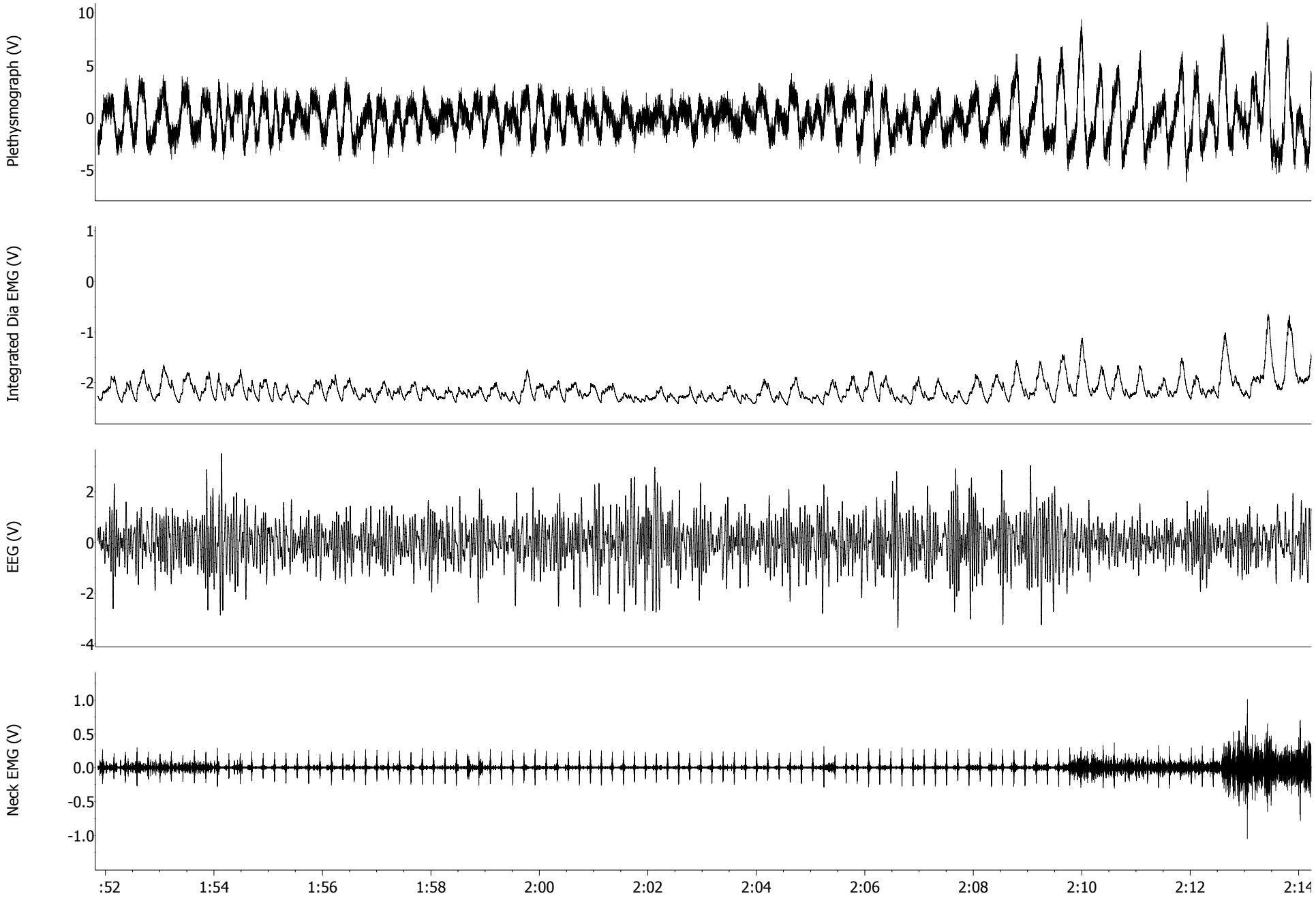

DAY4 Post-injection

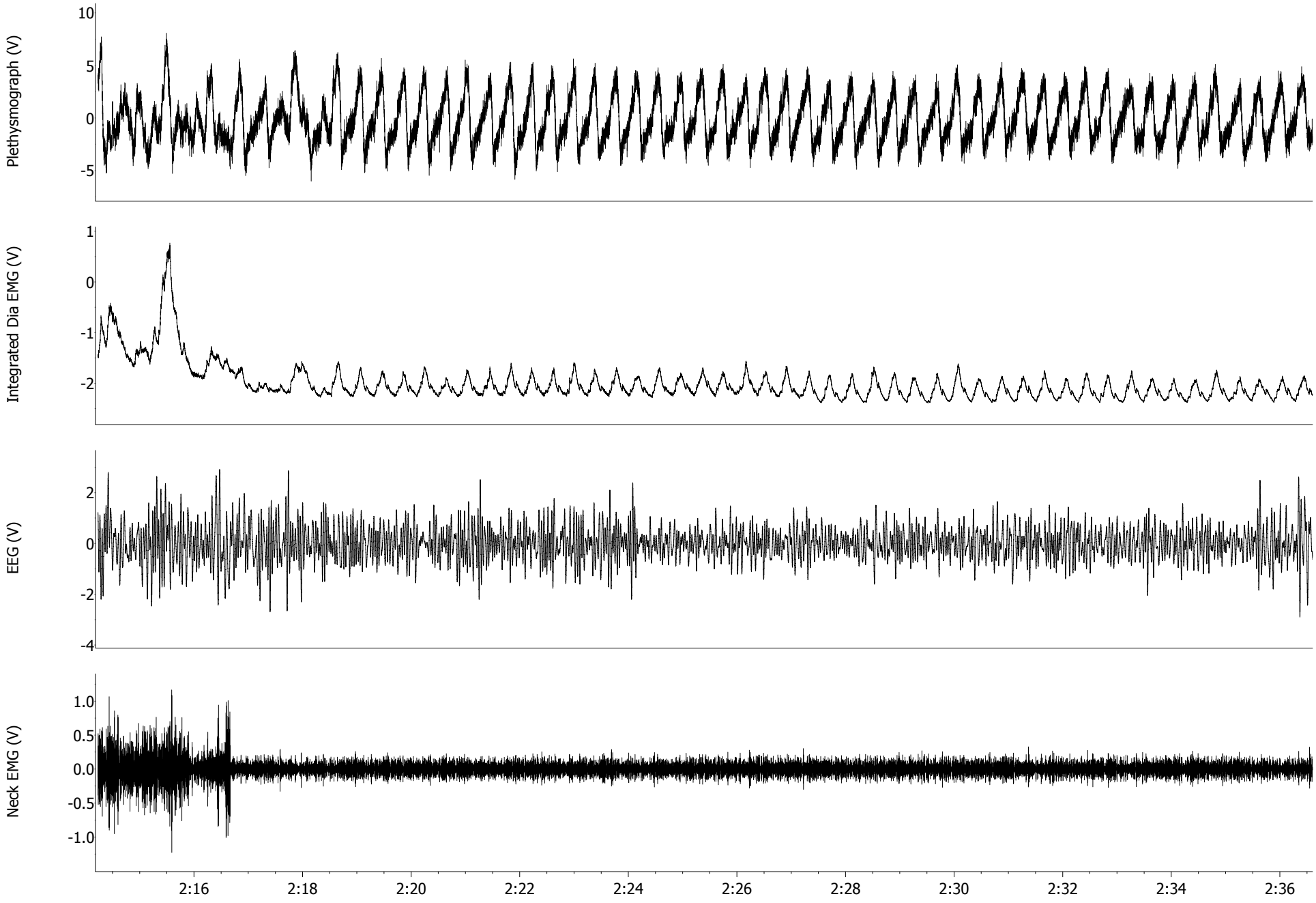

DAY4 Post-injection

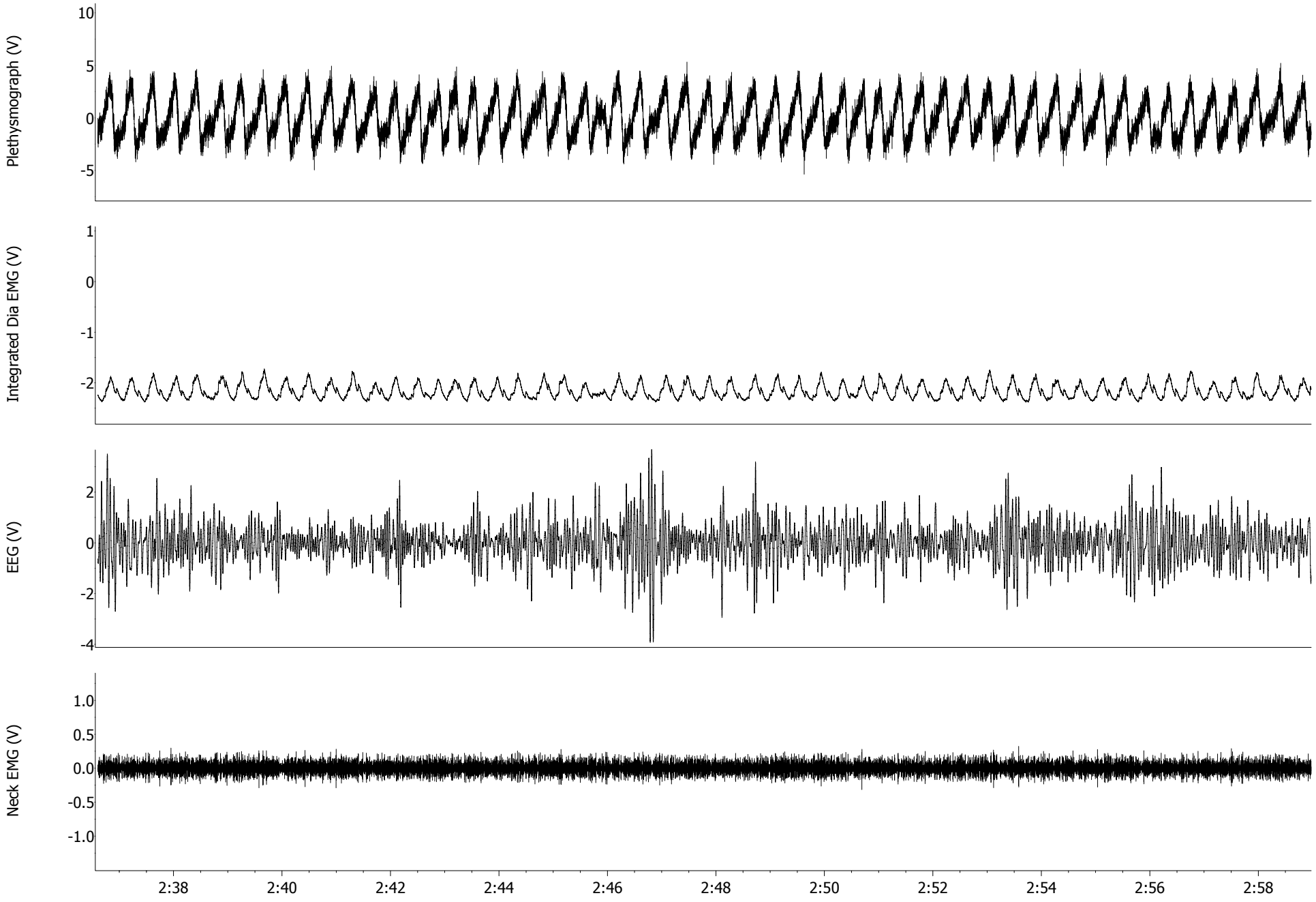

DAY4 Post-injection

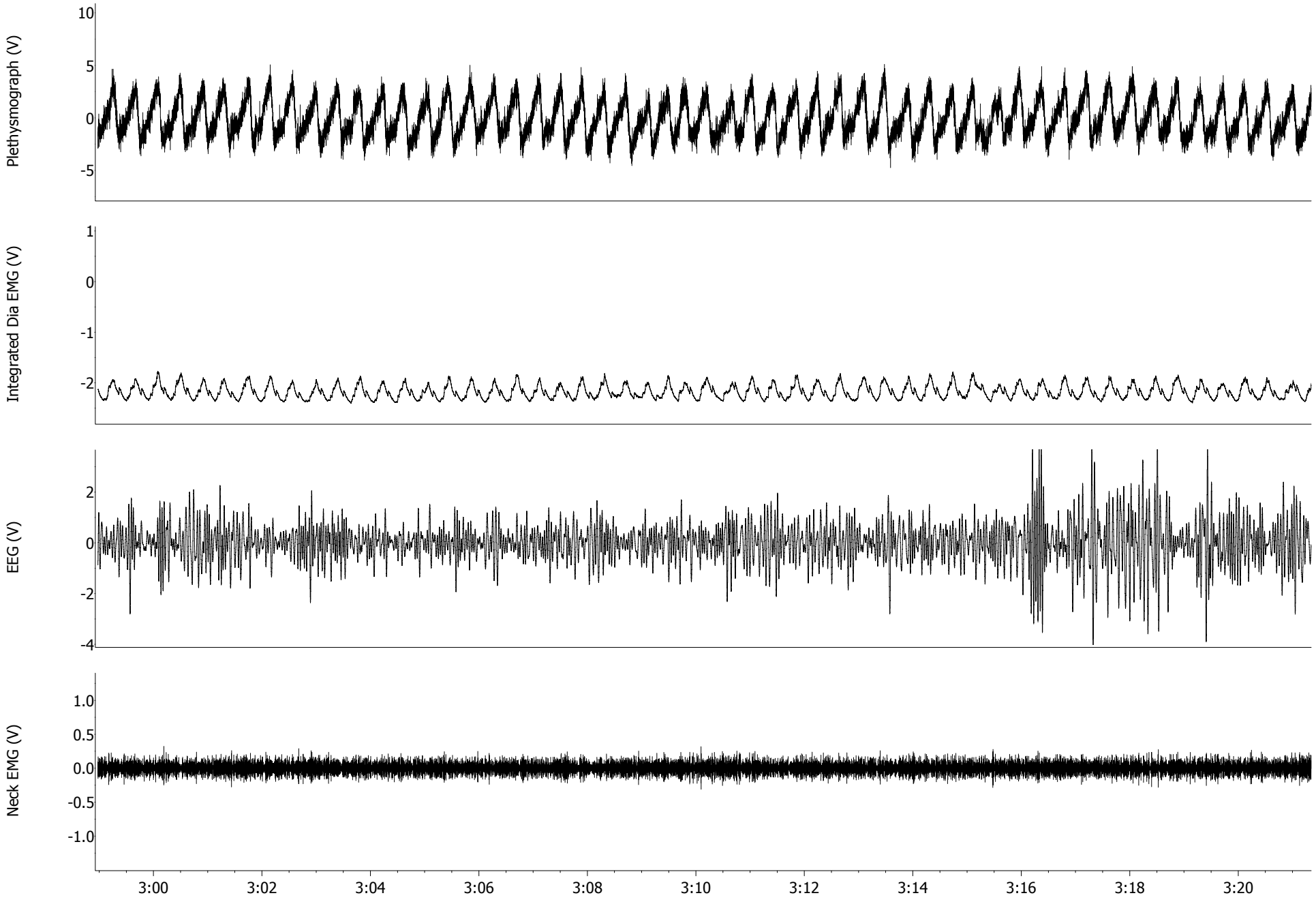

DAY4 Post-injection

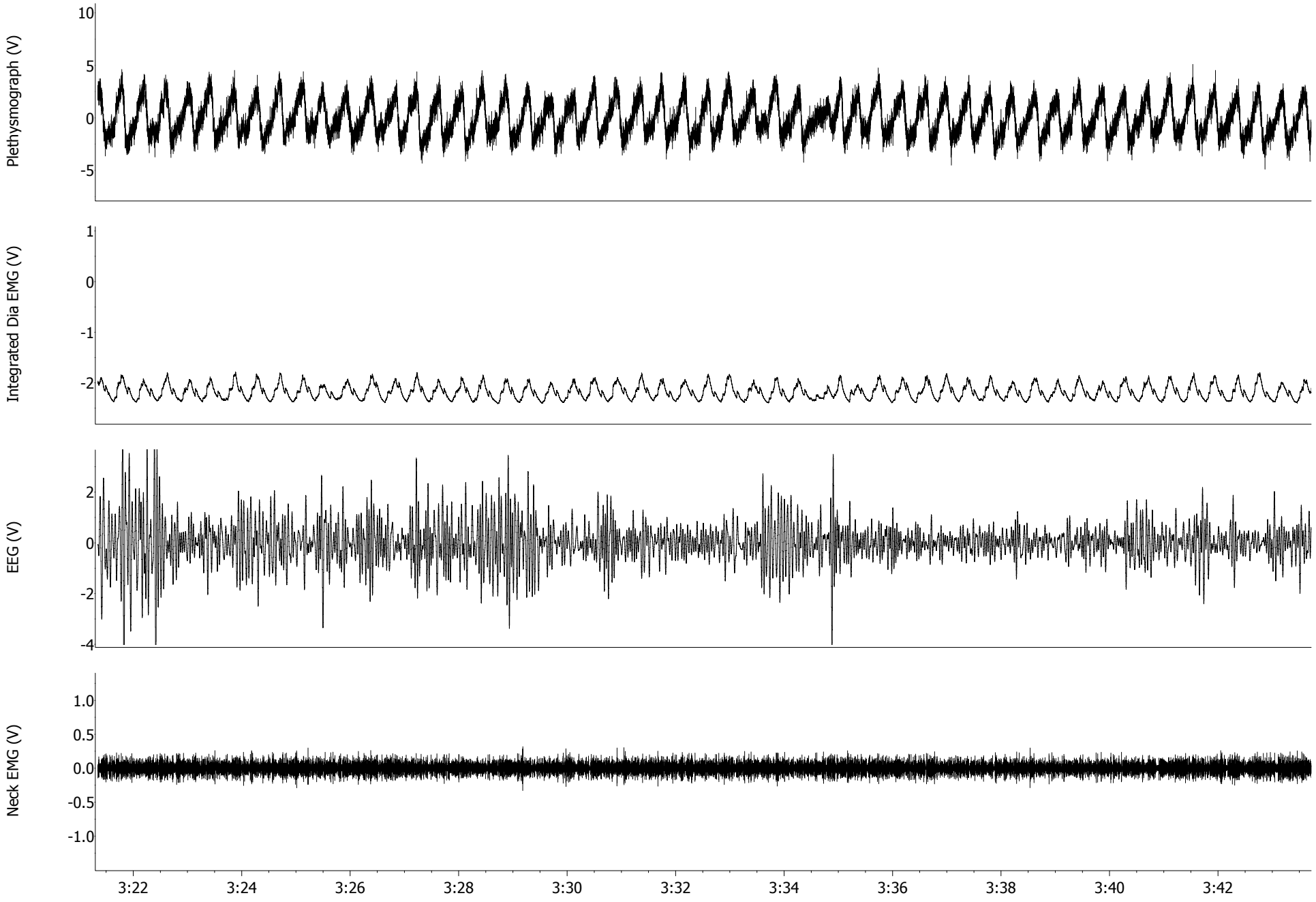

DAY4 Post-injection

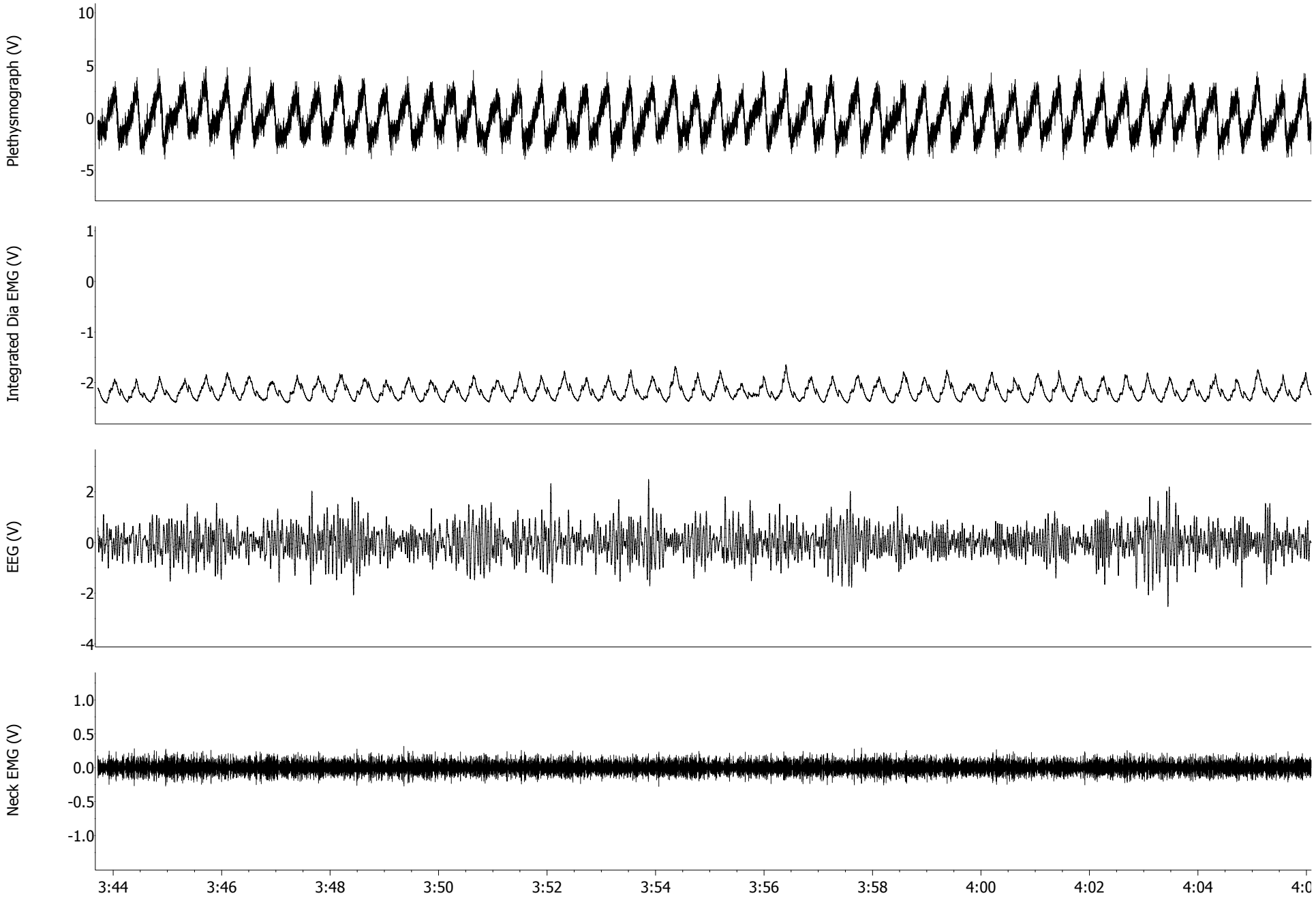

DAY4 Post-injection

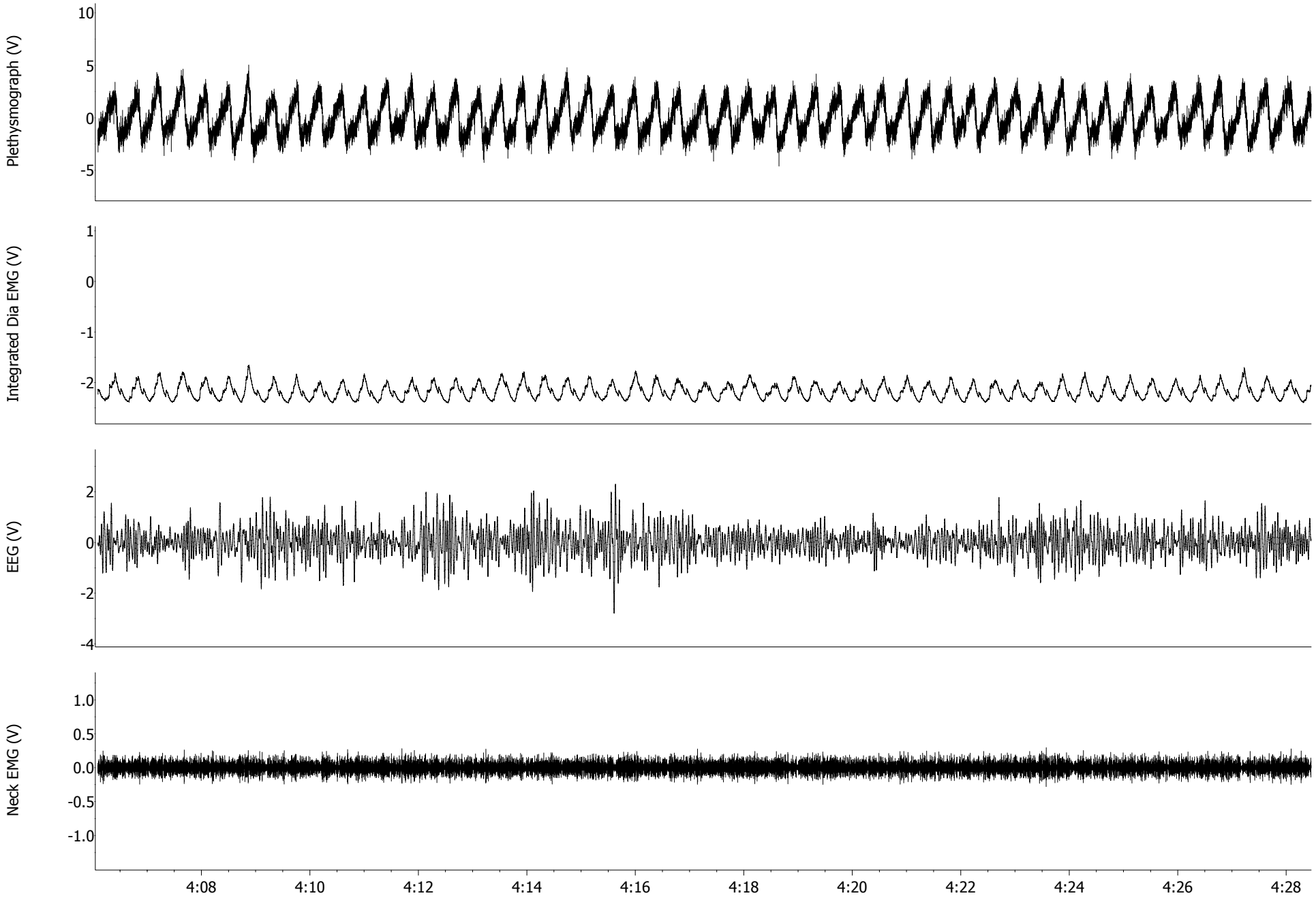

DAY4 Post-injection

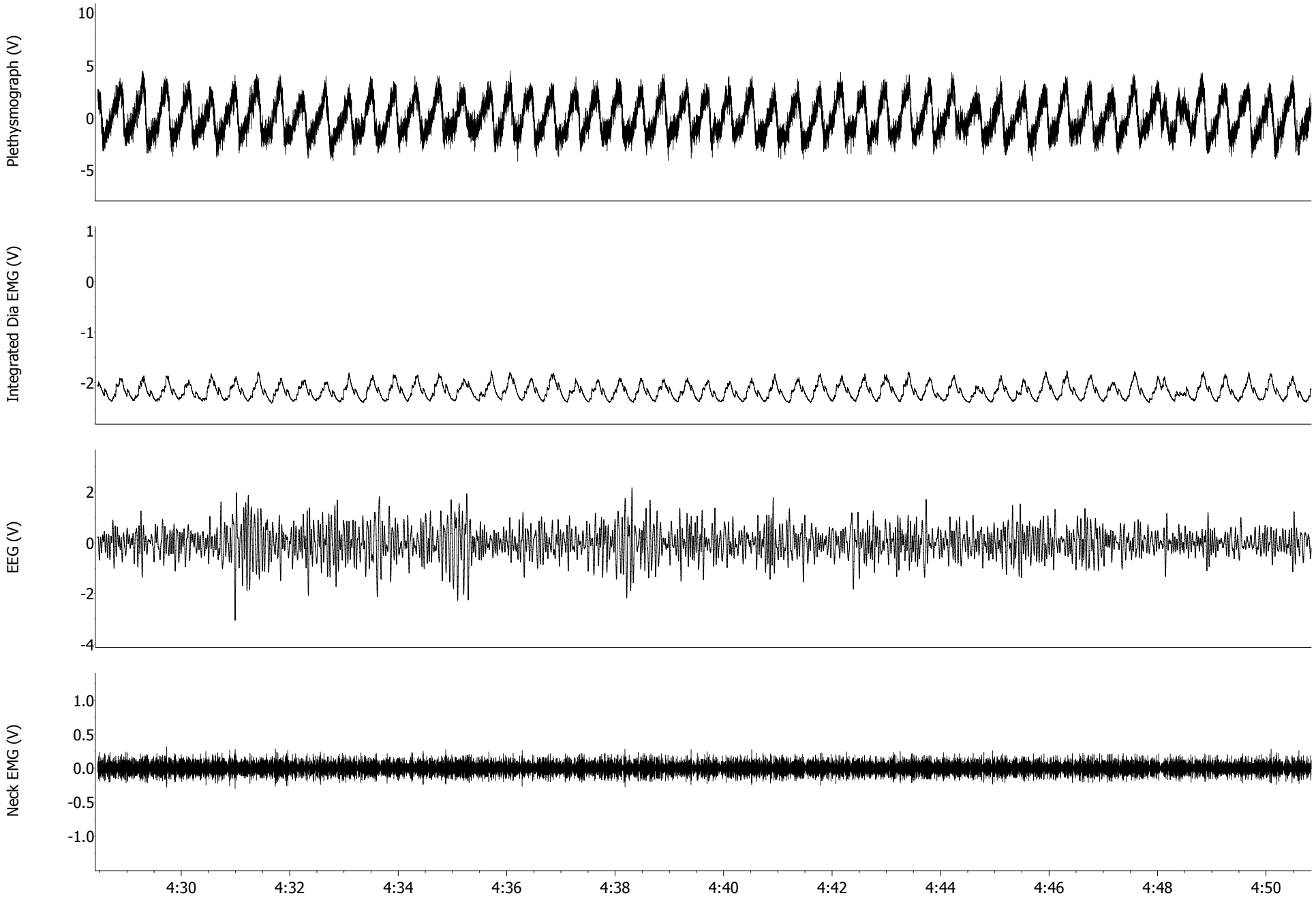

DAY4 Post-injection

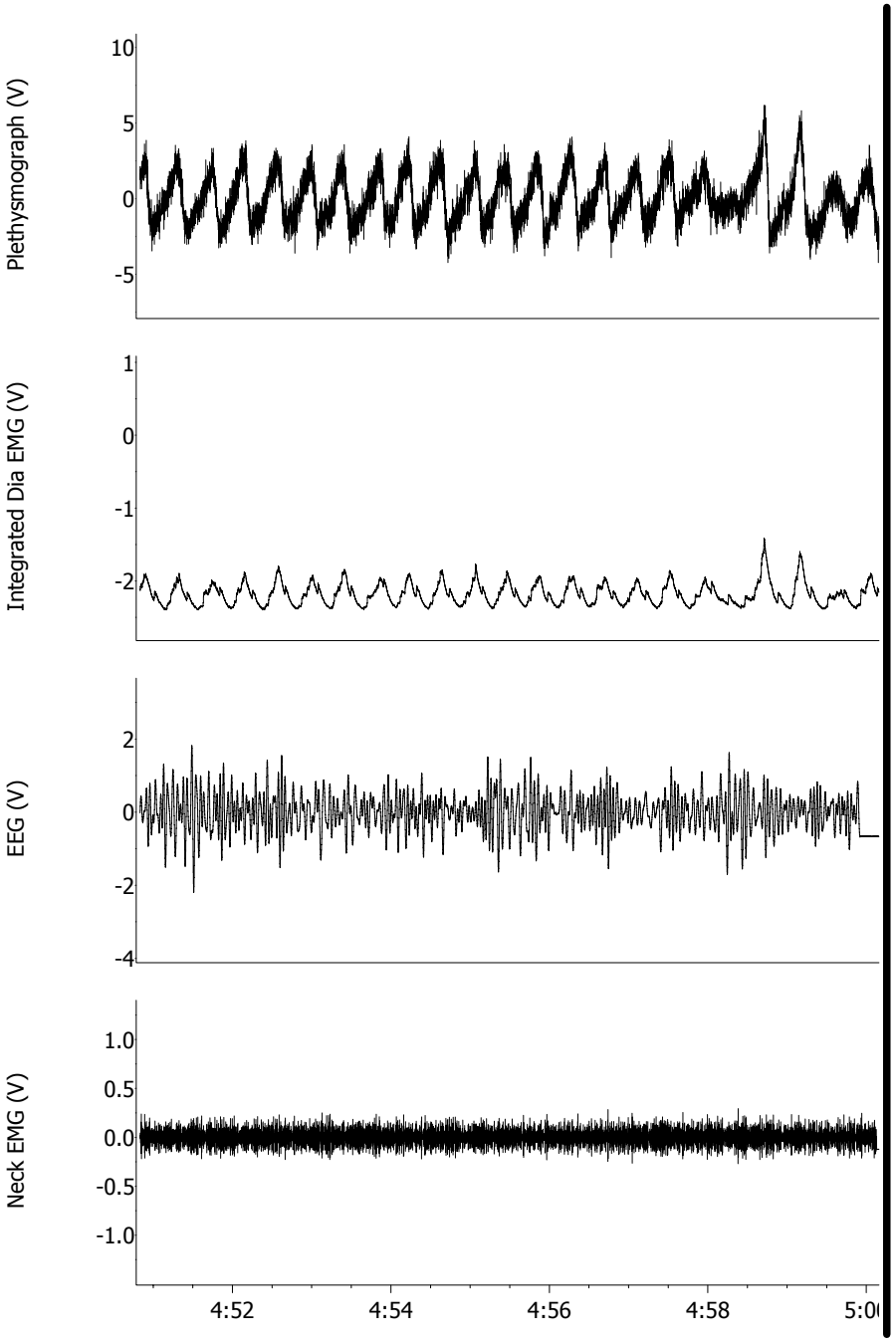

Supplementary Figure 3: Continuous 5 minute physiological recordings on day 4 post-injection. Tracings as in *Supplementary Fig. 2*. Respiratory disturbances increased in number and duration during REM sleep. During NREM and wakefulness, breathing was similar to pre-injection.

DAY6 Post-injection

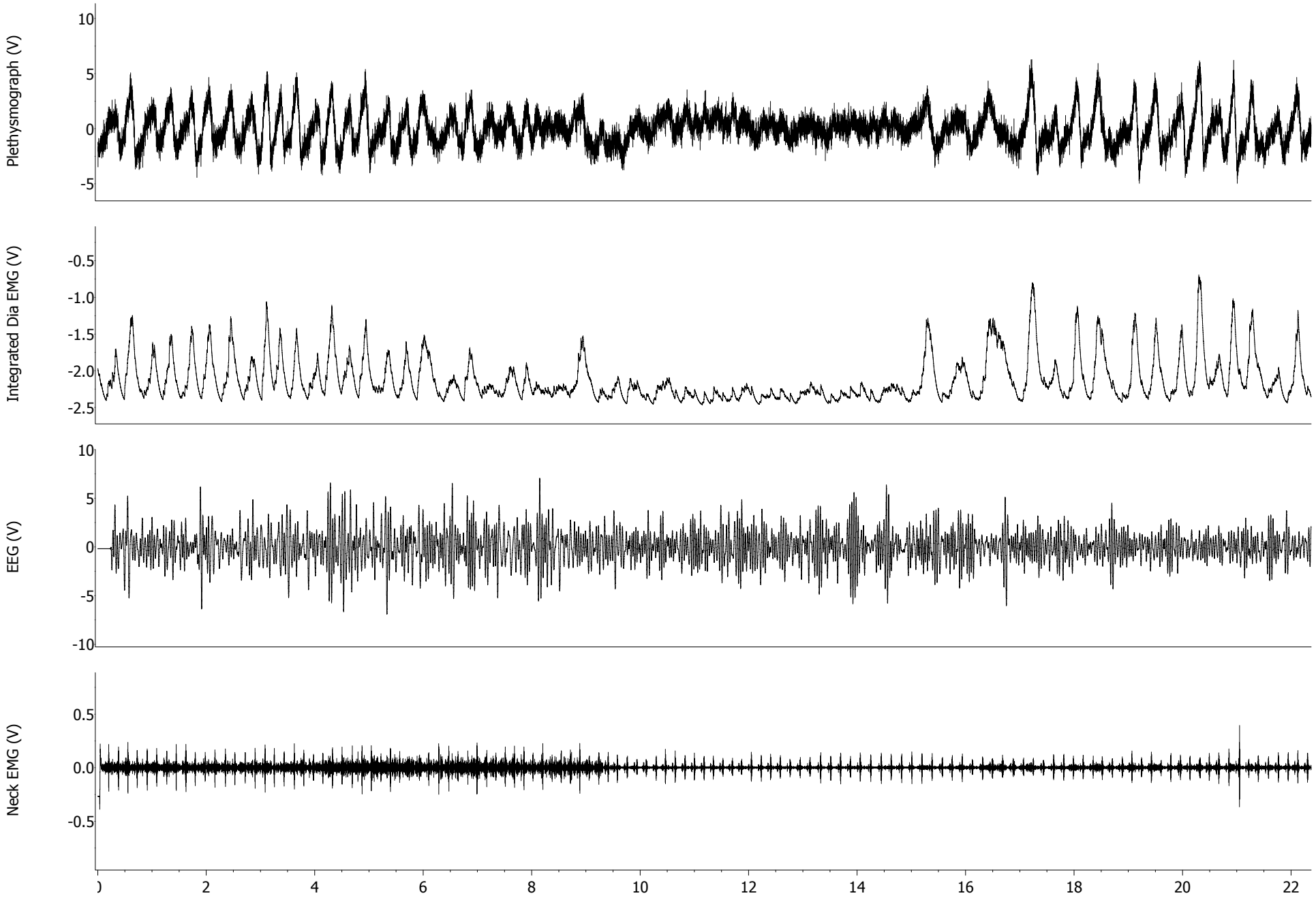

DAY6 Post-injection

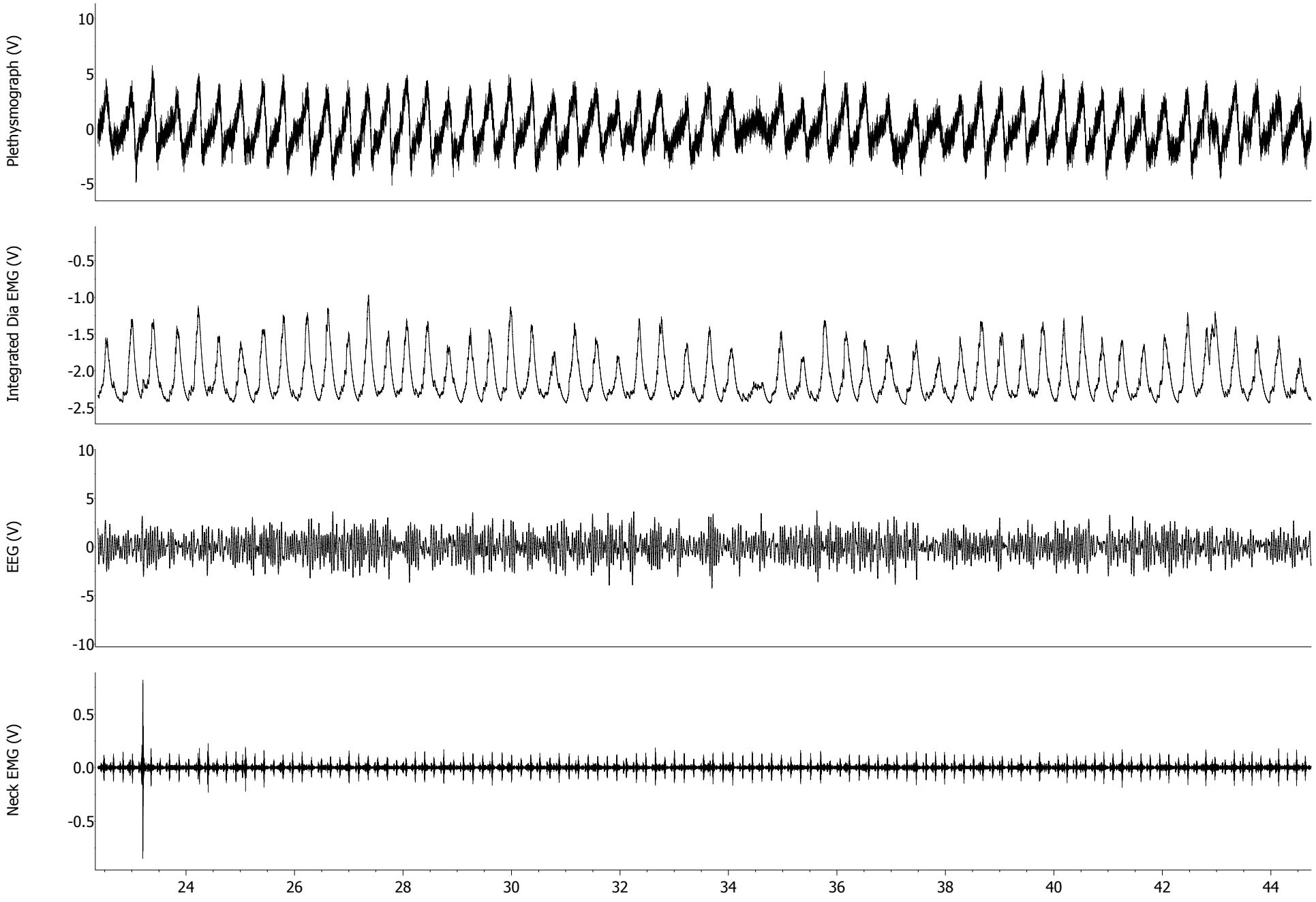

DAY6 Post-injection

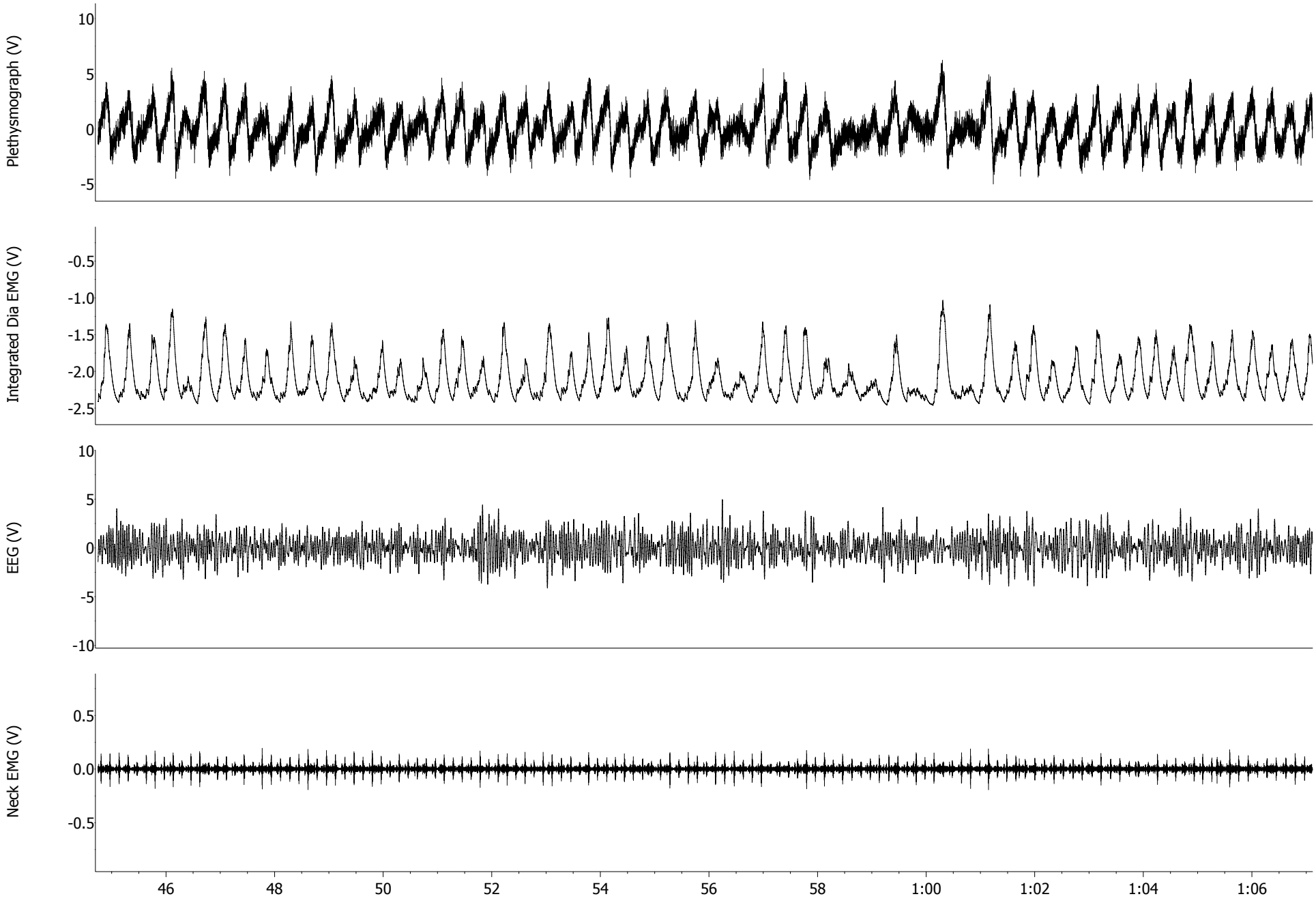

DAY6 Post-injection

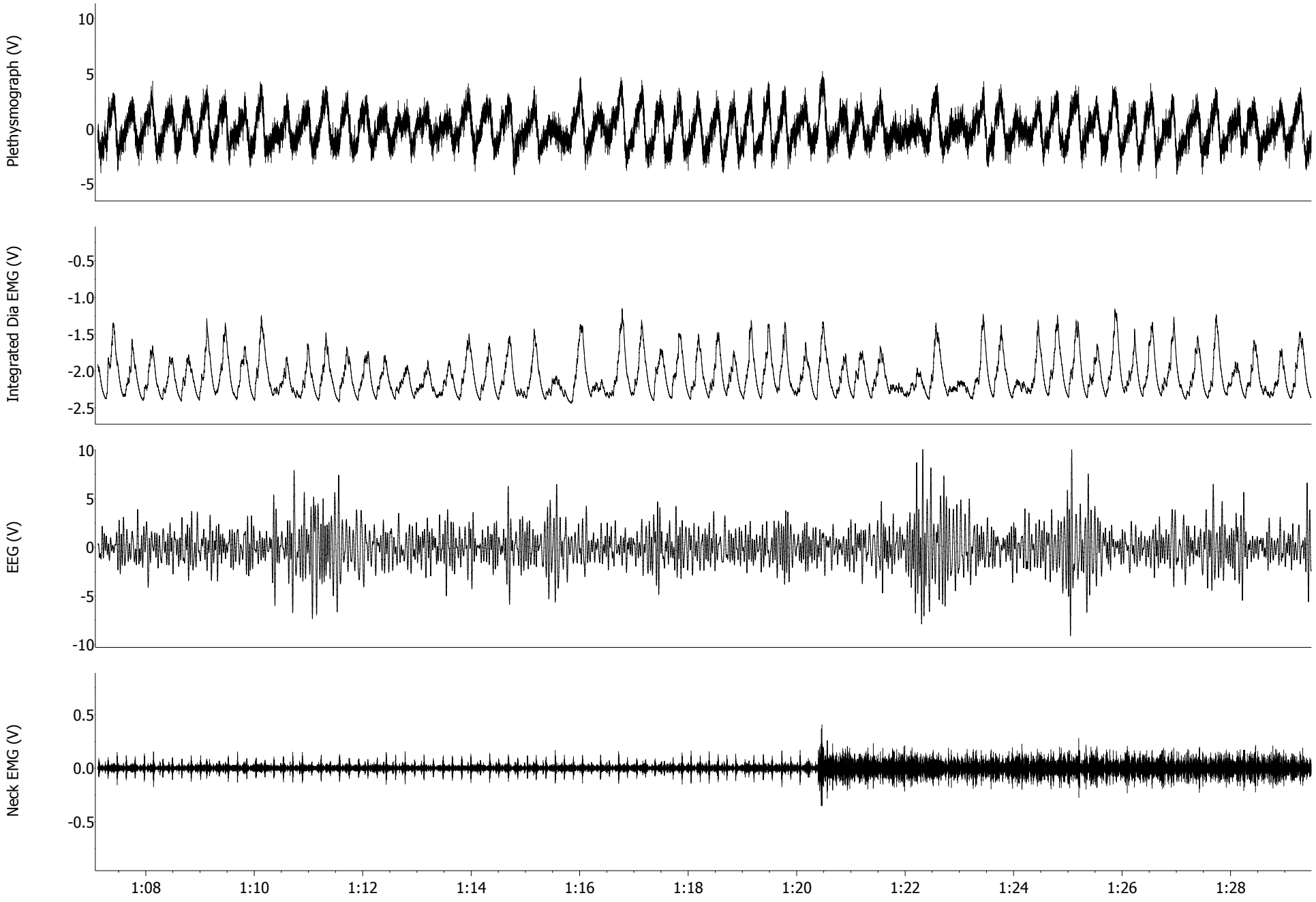

DAY6 Post-injection

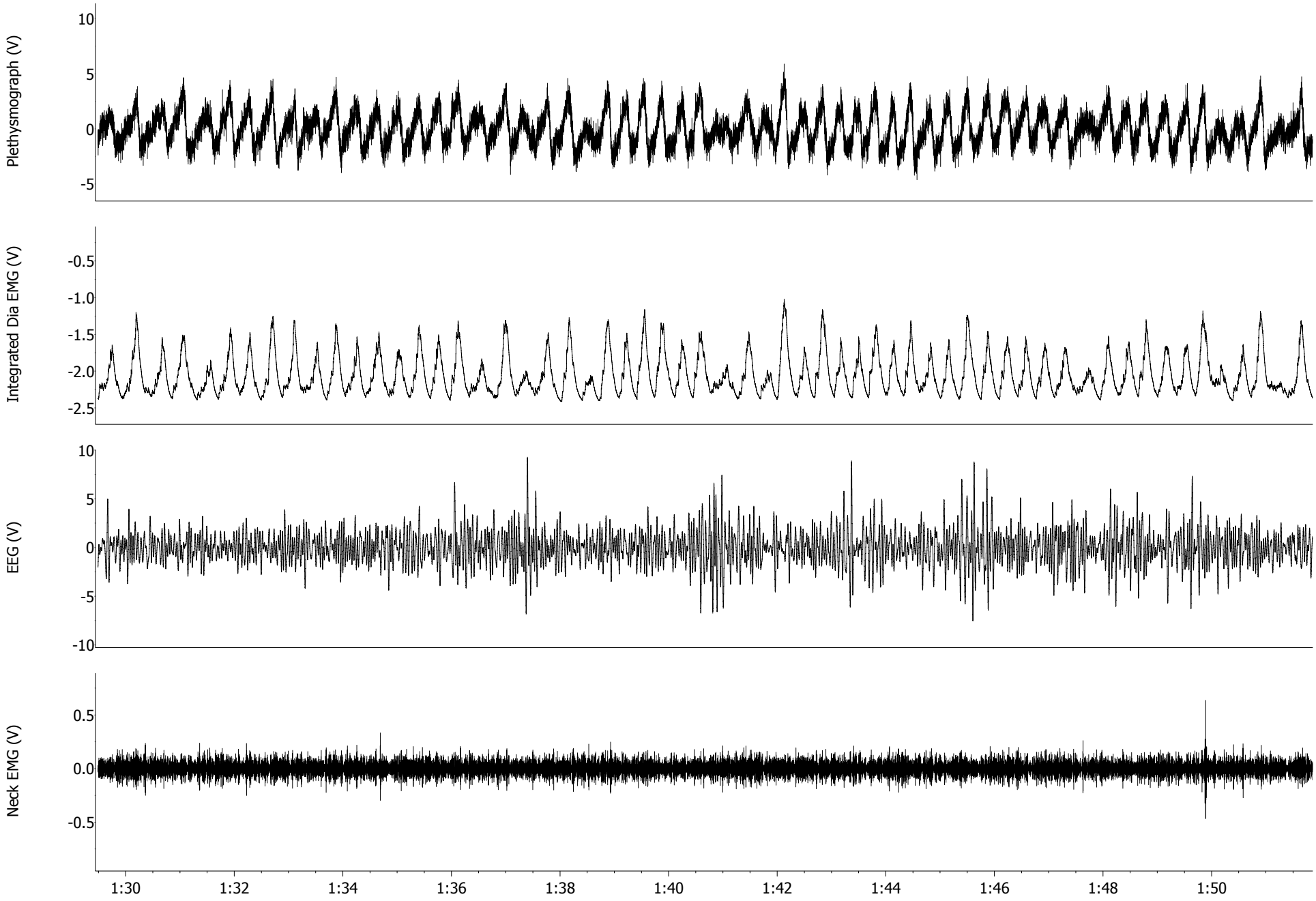

DAY6 Post-injection

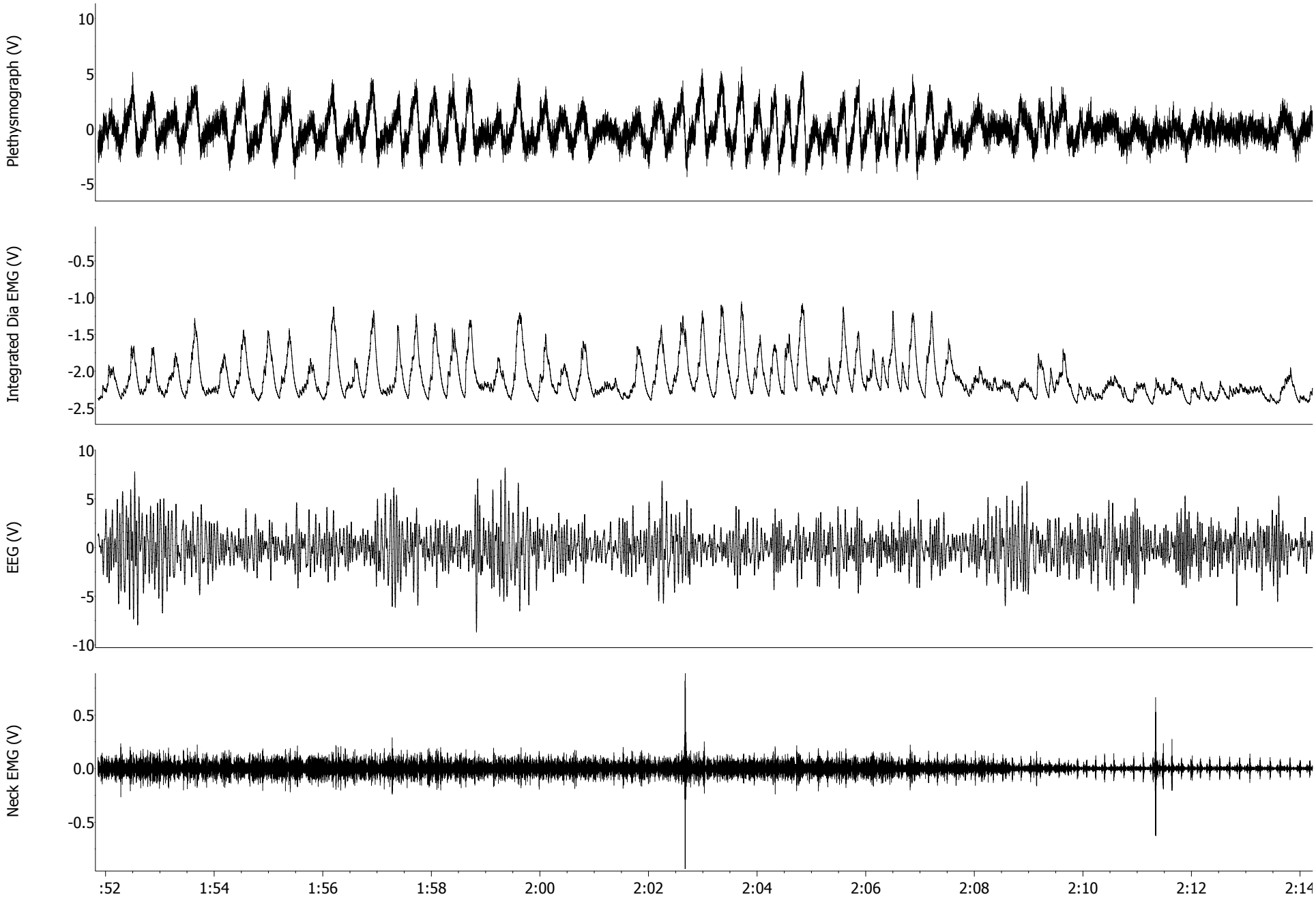

DAY6 Post-injection

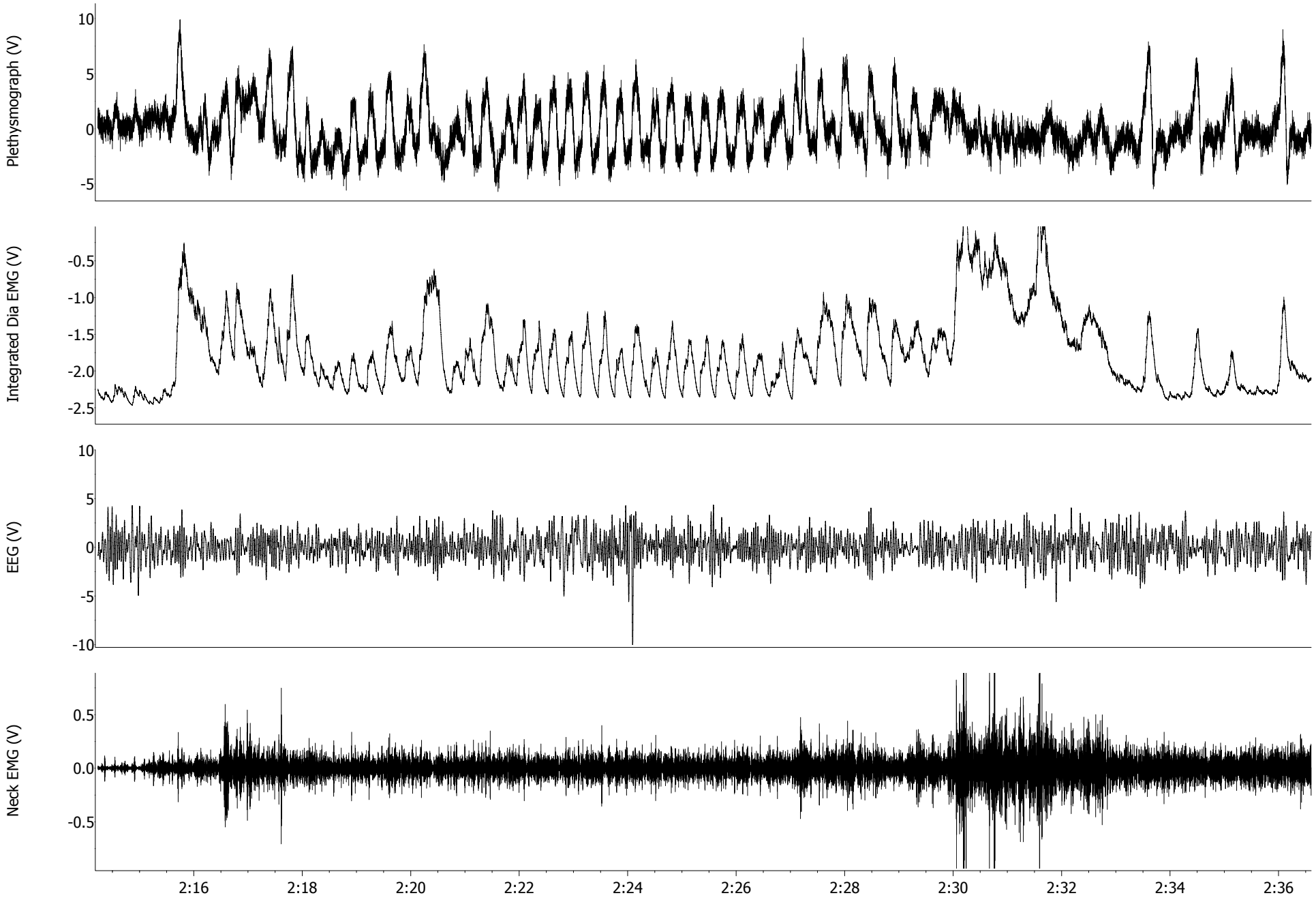

DAY6 Post-injection

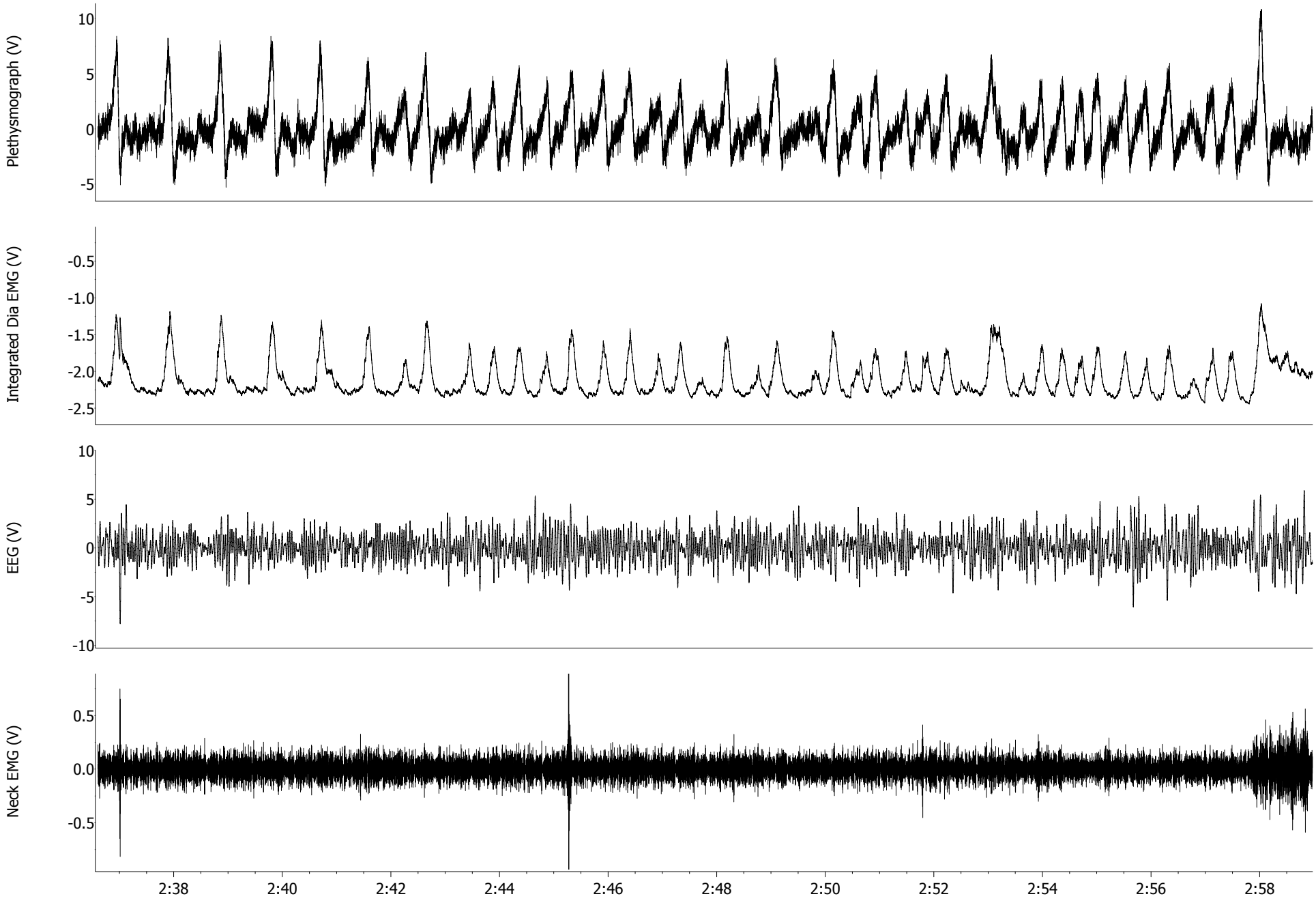

DAY6 Post-injection

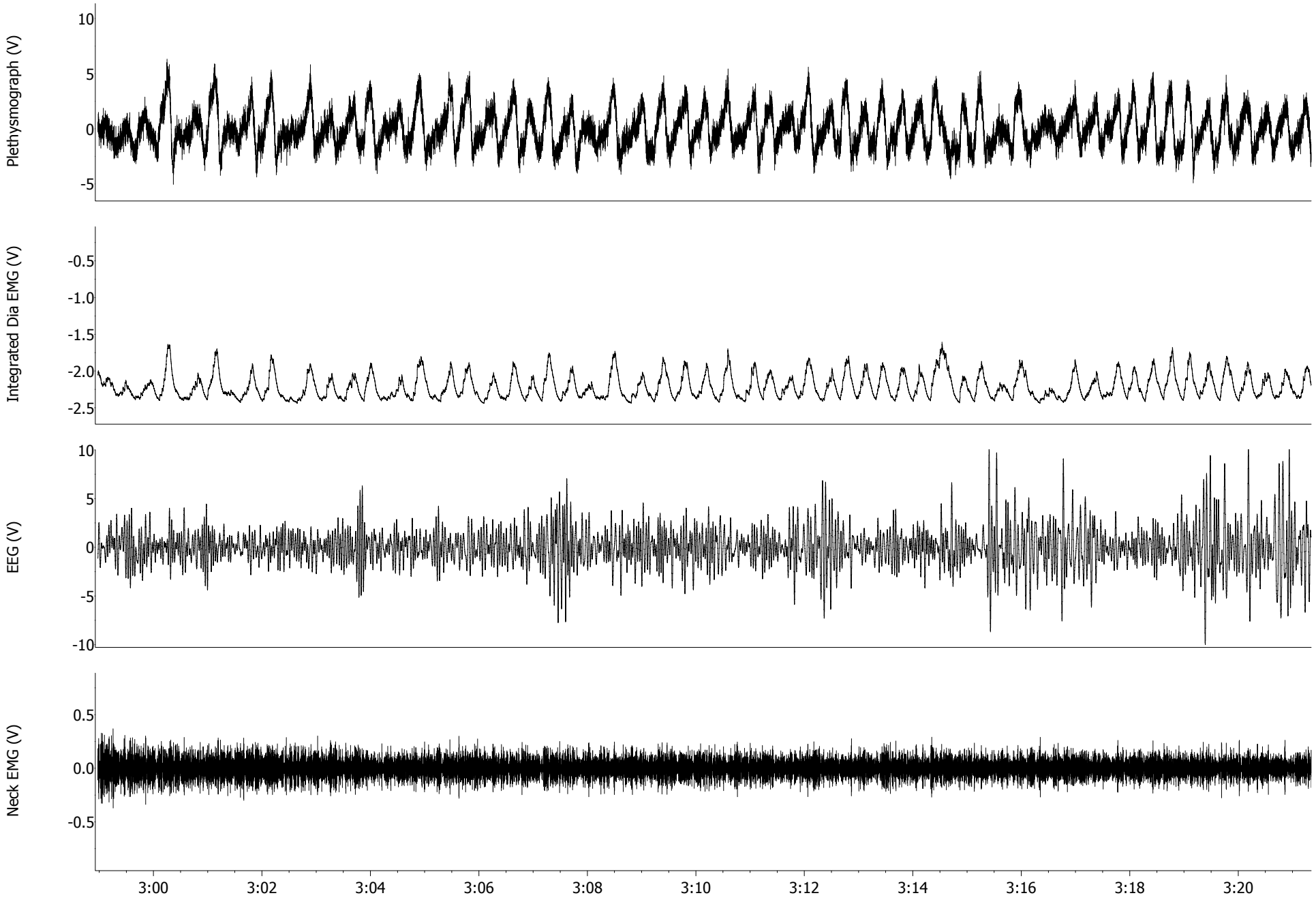

DAY6 Post-injection

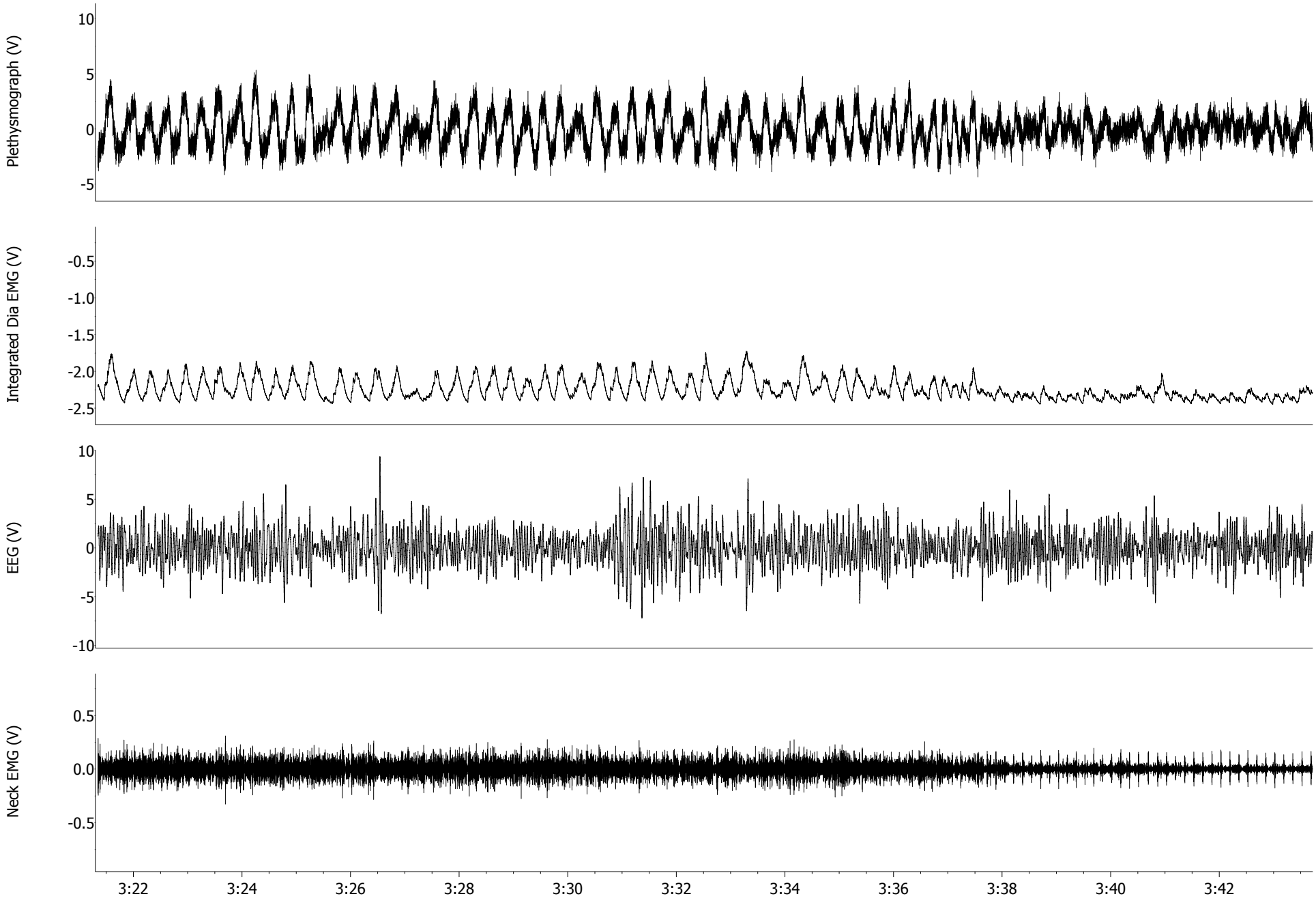

DAY6 Post-injection

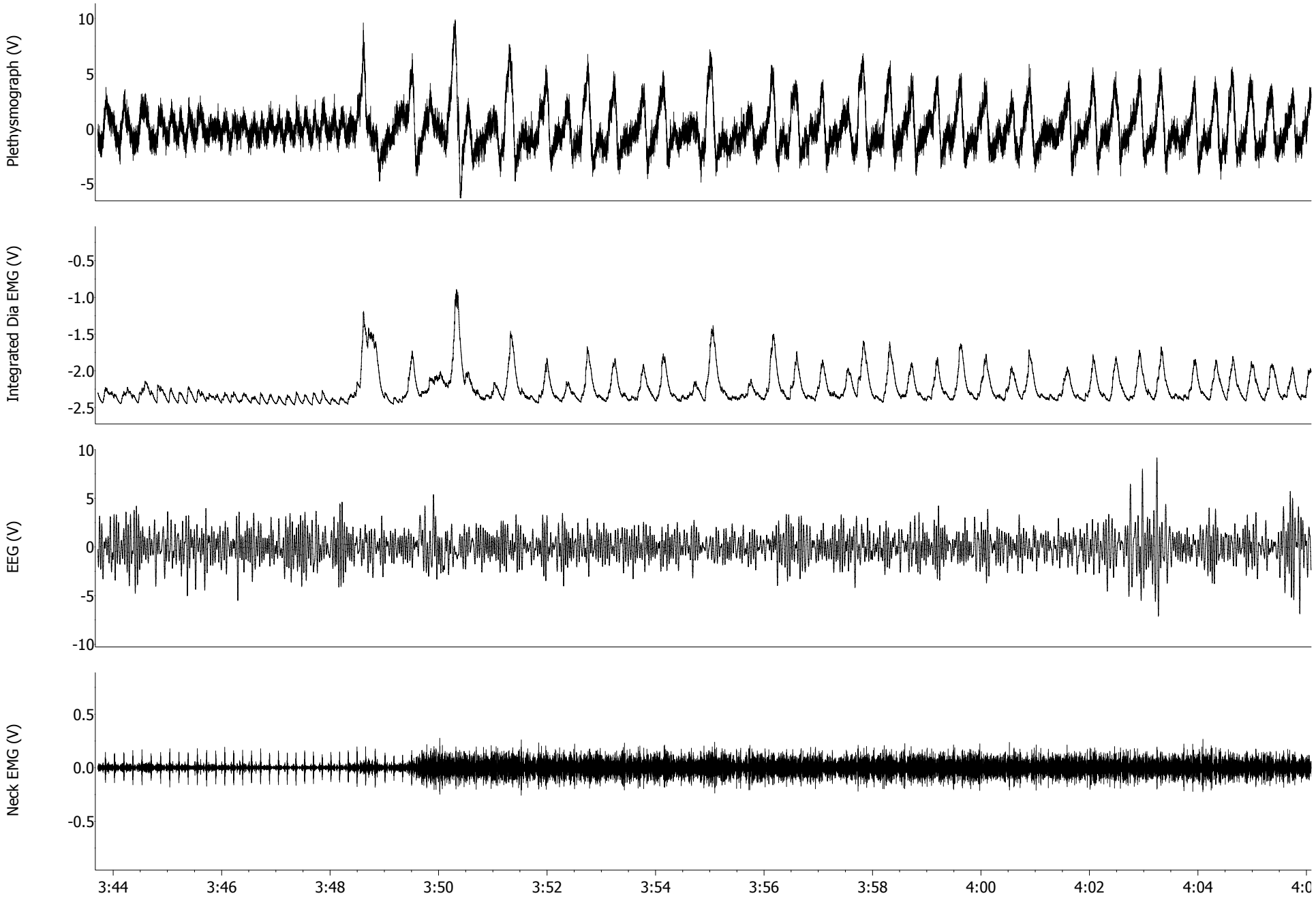

DAY6 Post-injection

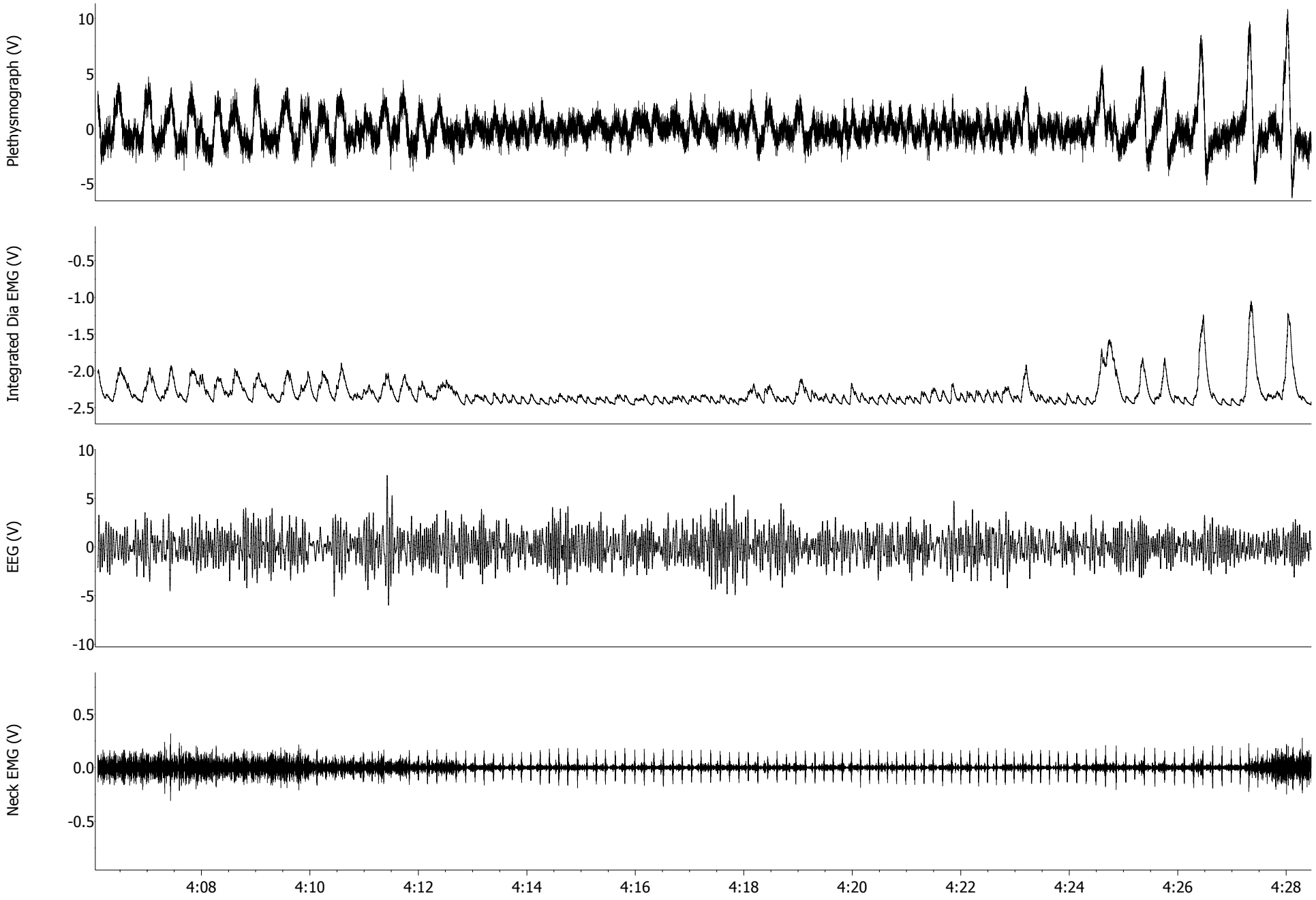

DAY6 Post-injection

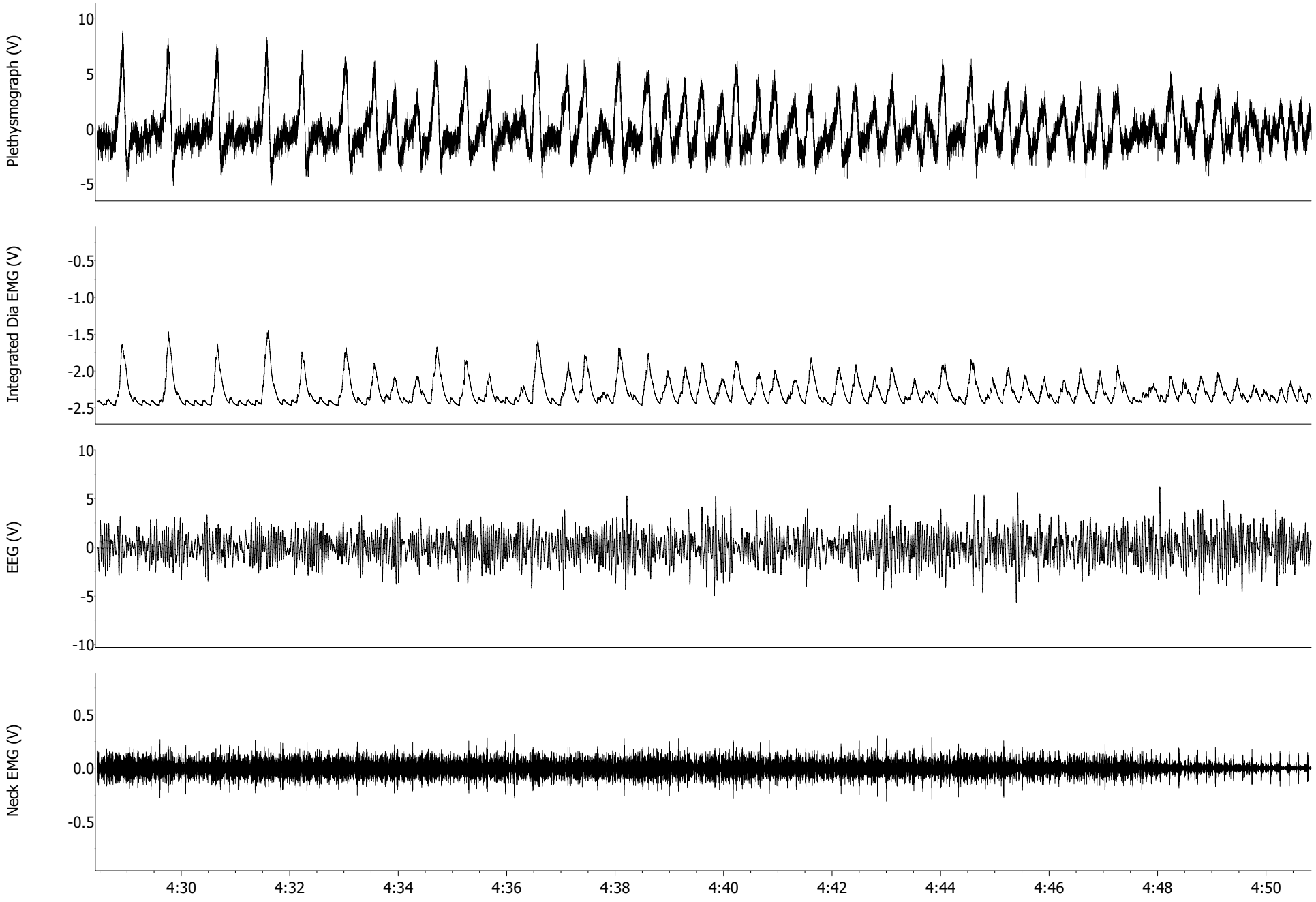

DAY6 Post-injection

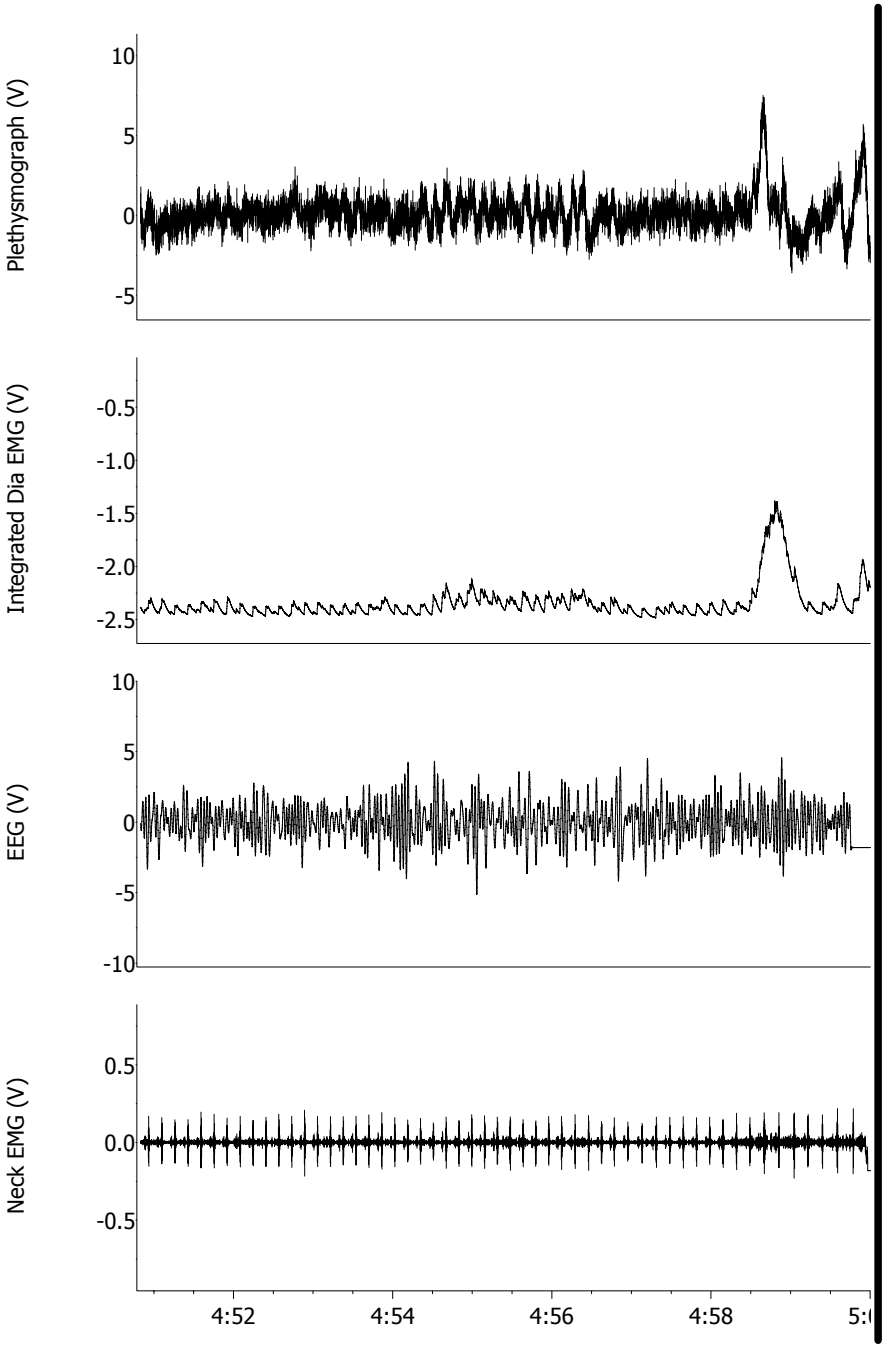

Supplementary Figure 4: Continuous 5 minute physiological recordings on day 6 post-injection. Tracings as in *Supplementary Fig. 2*. Respiratory disturbances during REM increased in frequency and duration; during NREM there was a smaller but significant increase; and during wakefulness, short periods of abnormal breathing, characterized by increased frequency and brief apneas, became more frequent.

DAY8 Post-injection

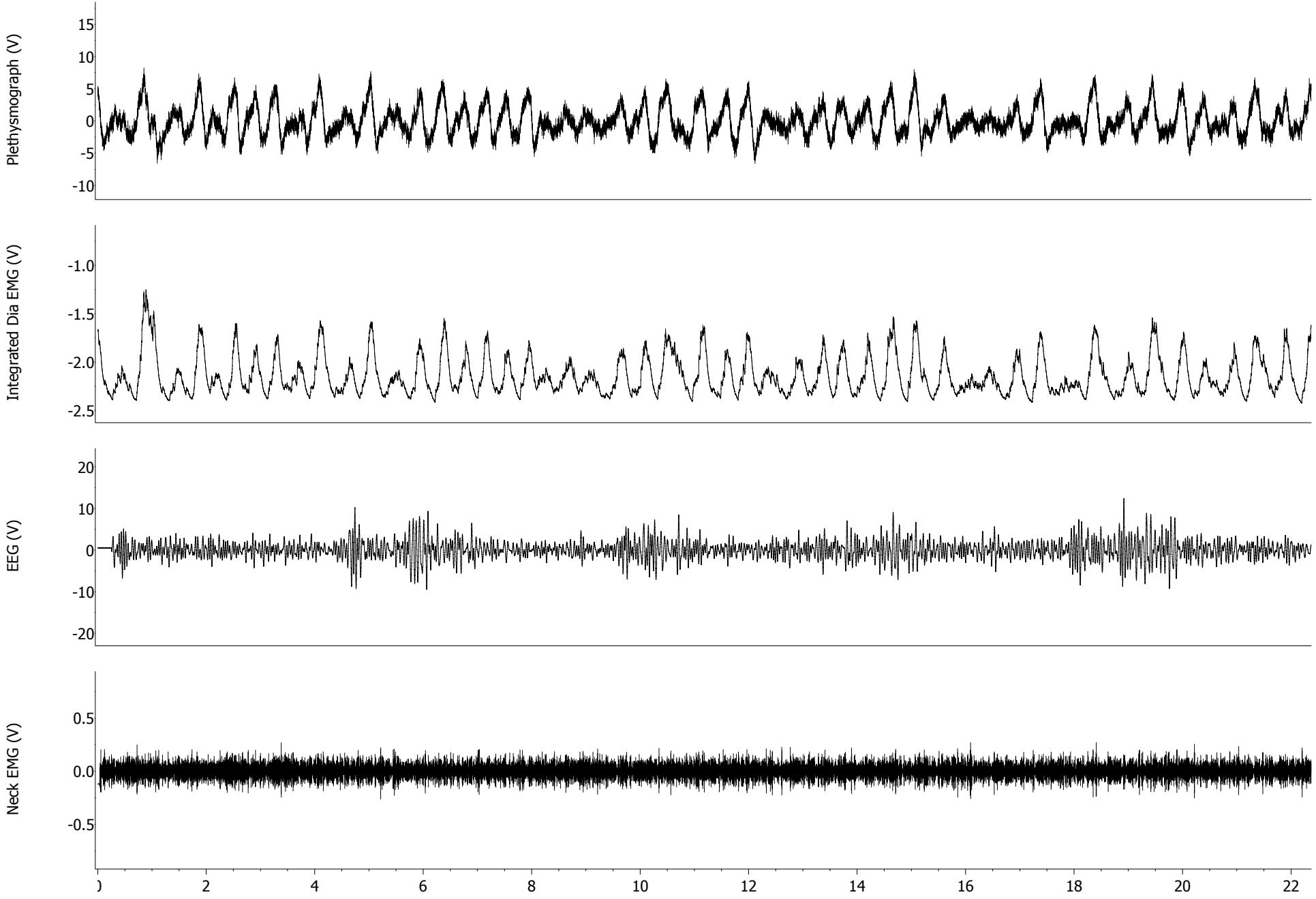

DAY8 Post-injection

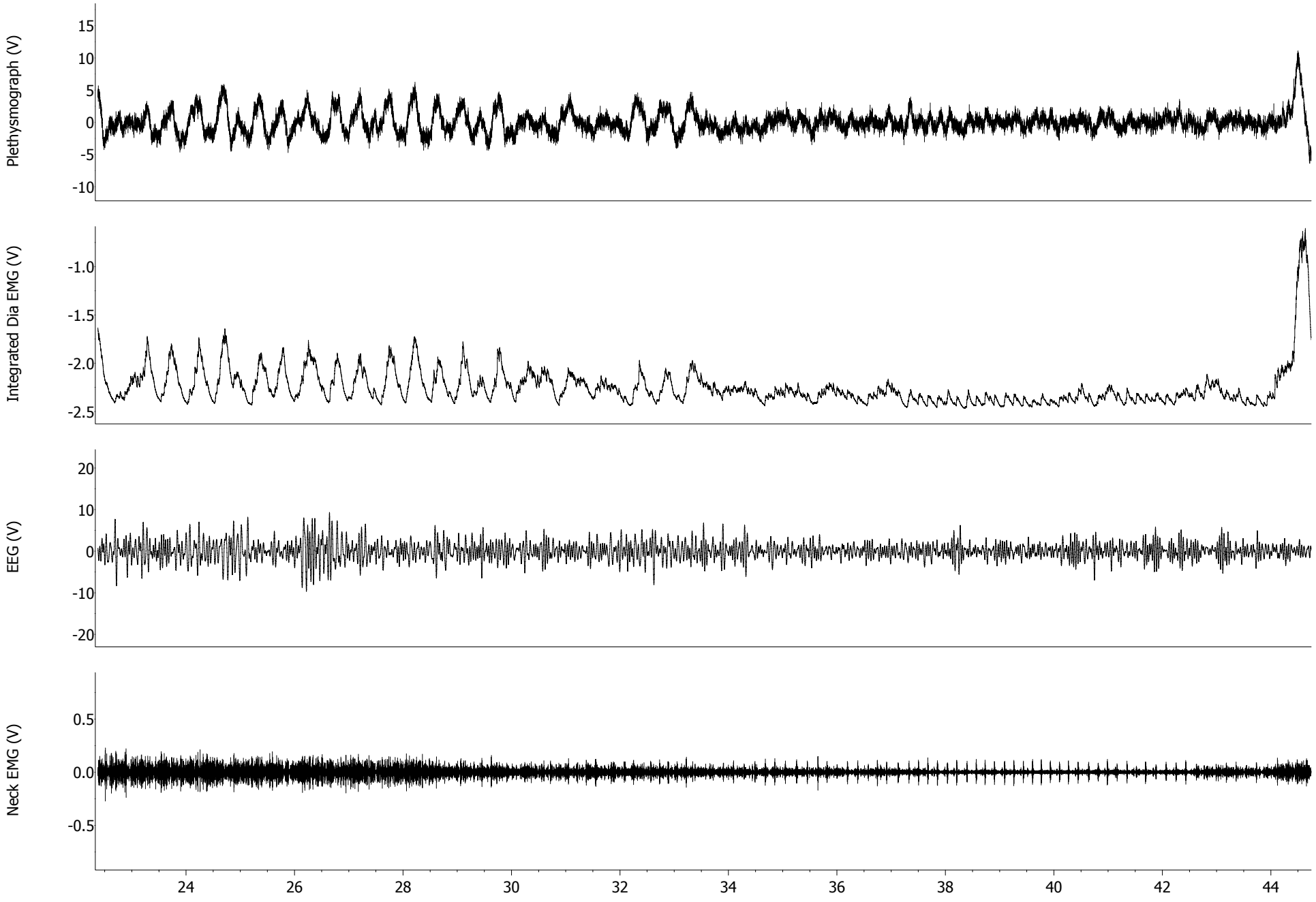

DAY8 Post-injection

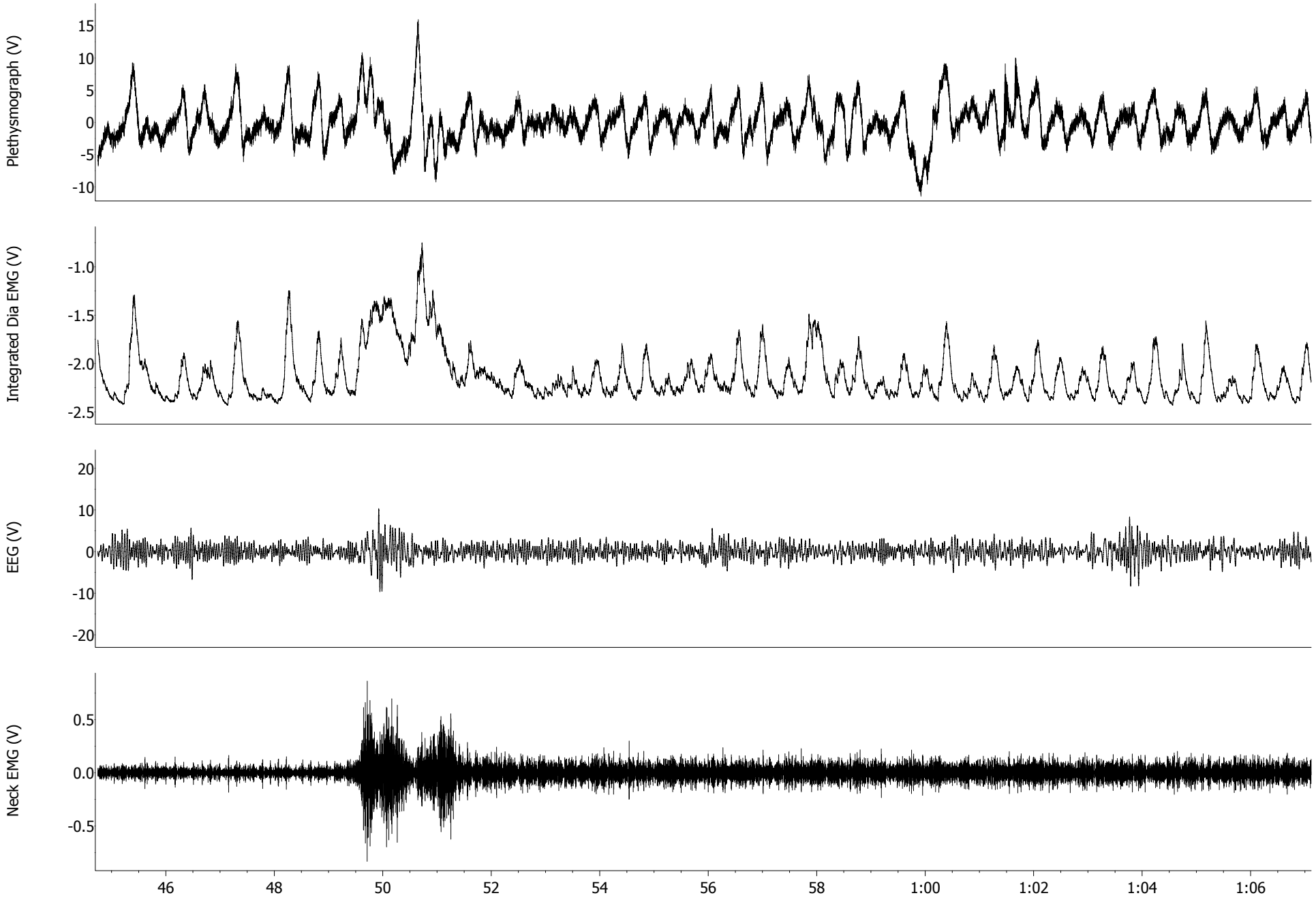

DAY8 Post-injection

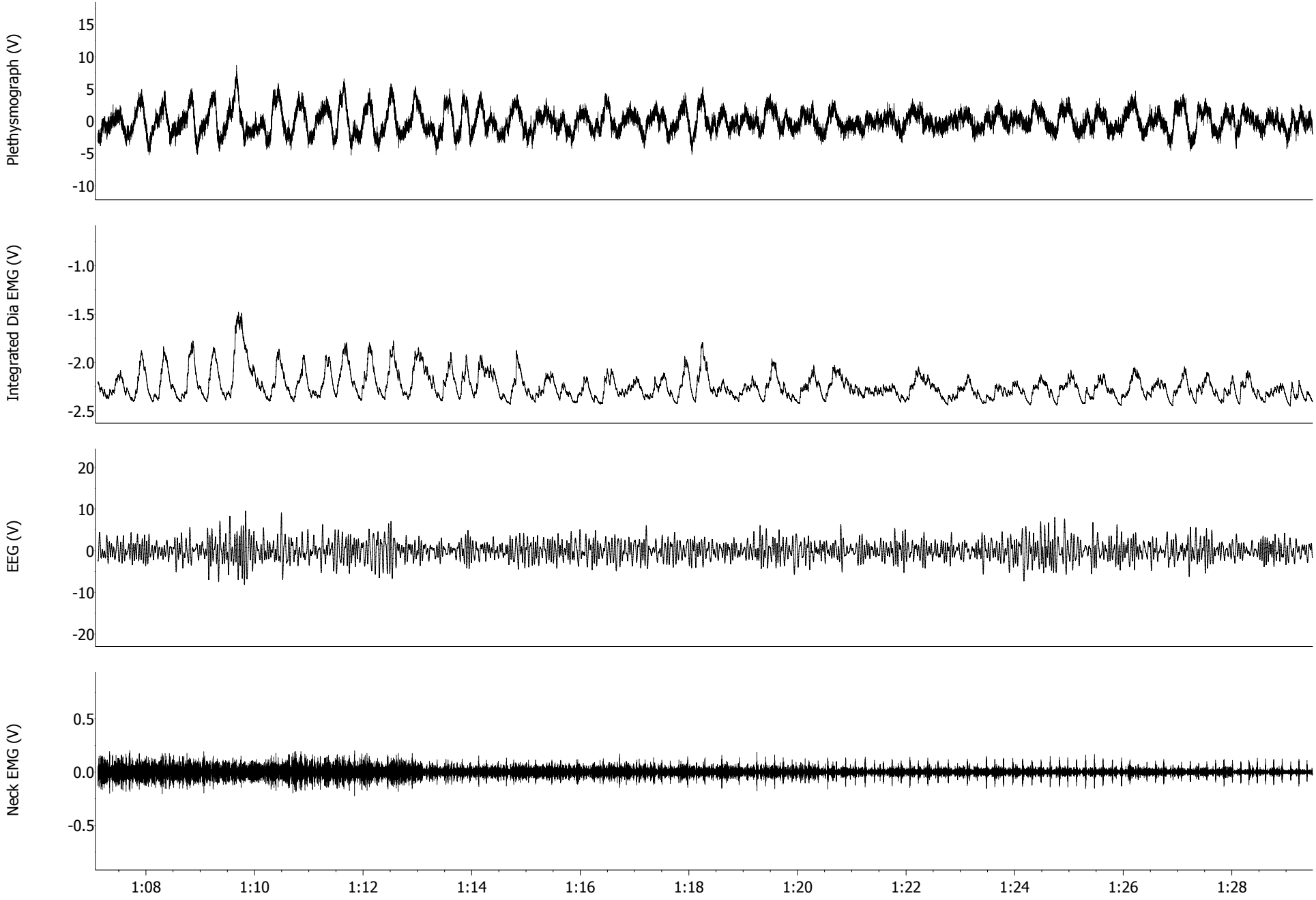

DAY8 Post-injection

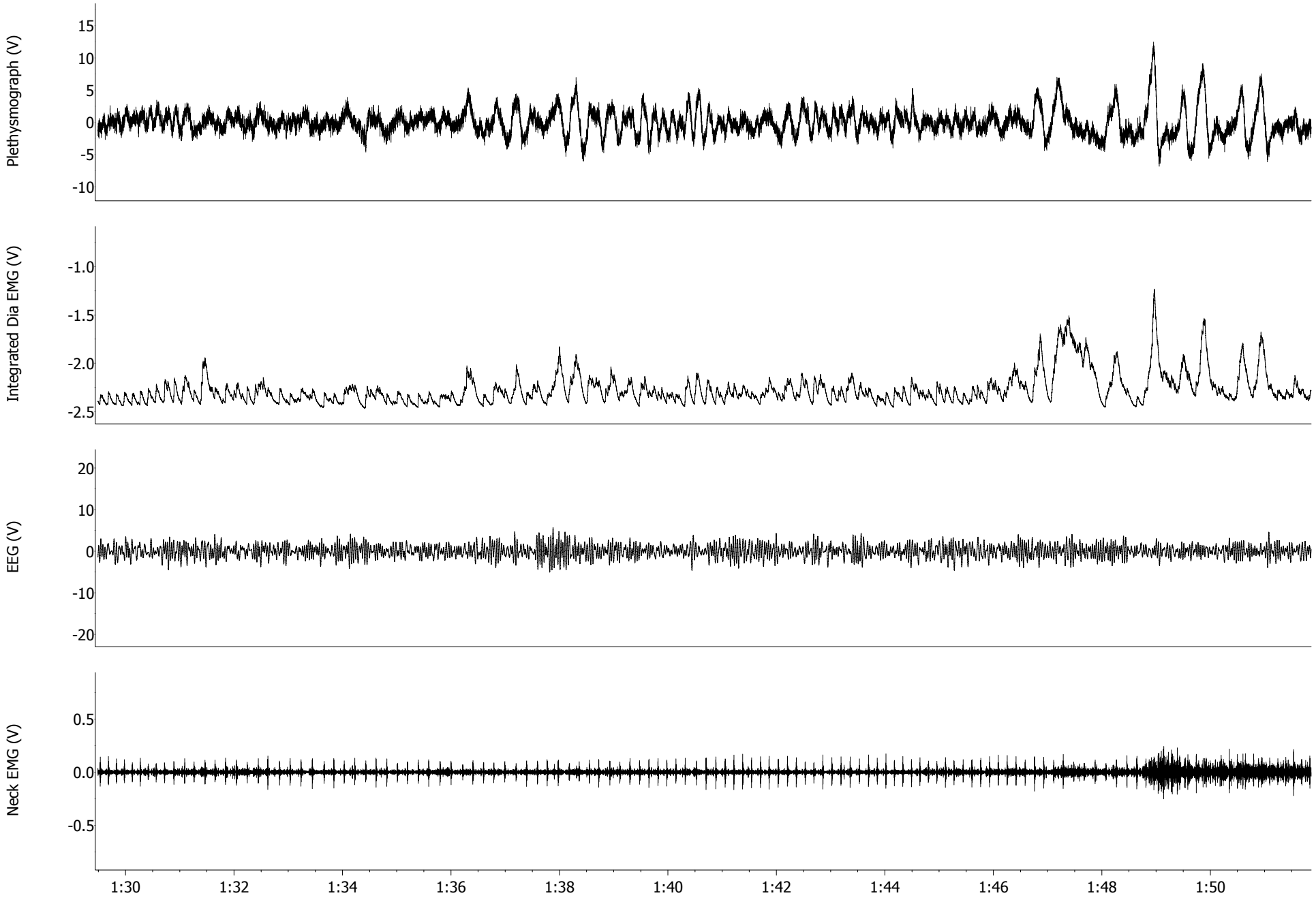

DAY8 Post-injection

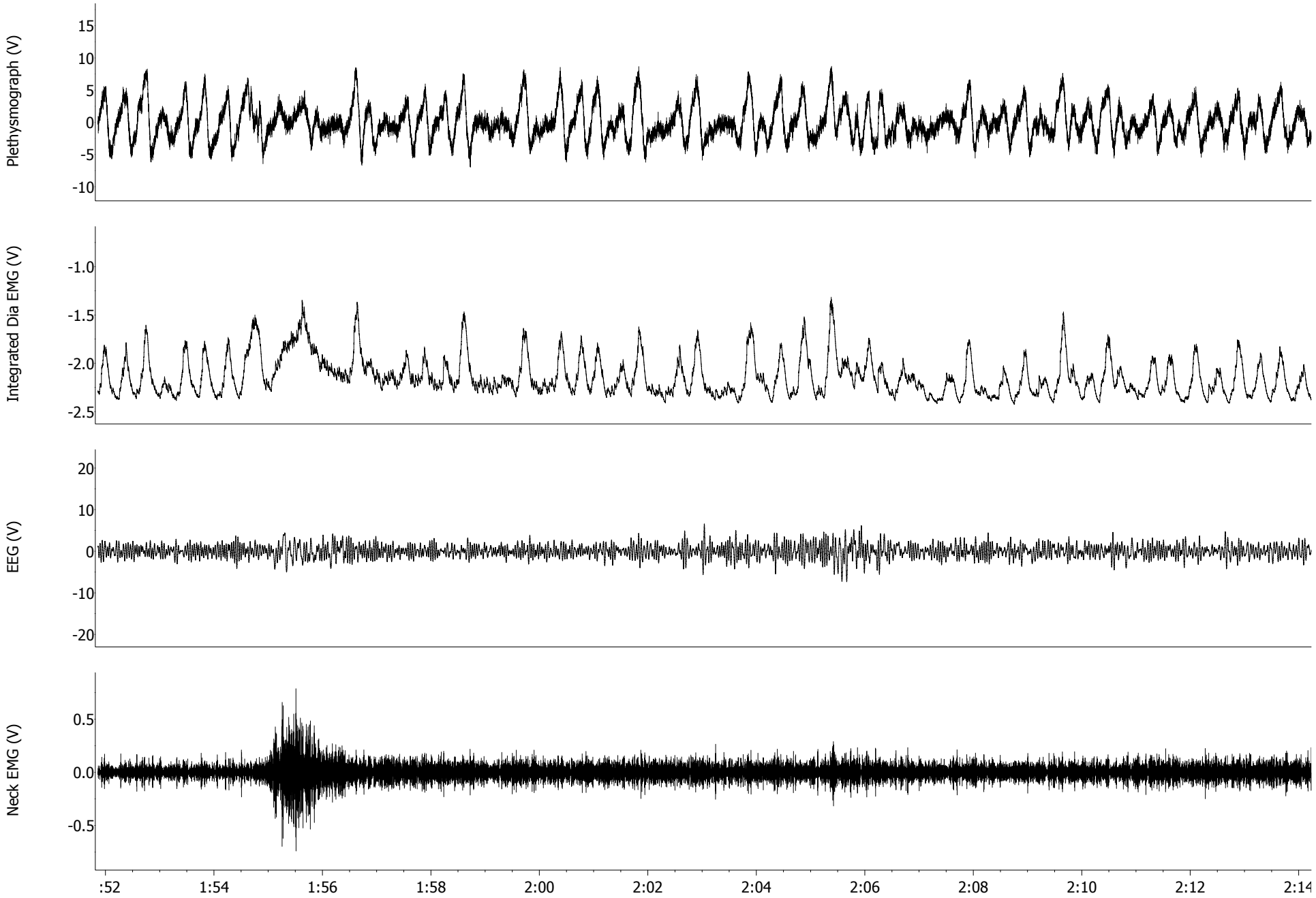

DAY8 Post-injection

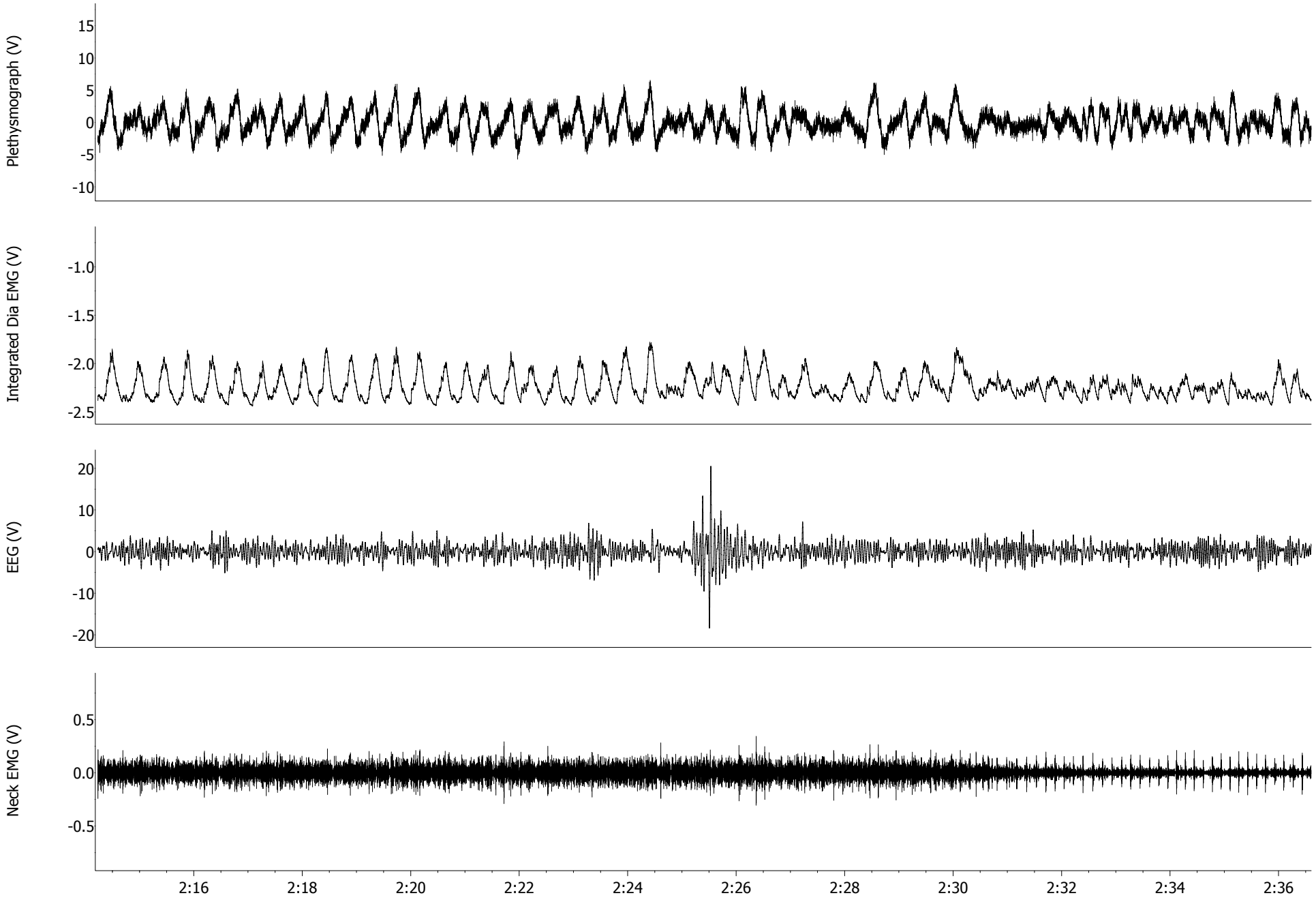

DAY8 Post-injection

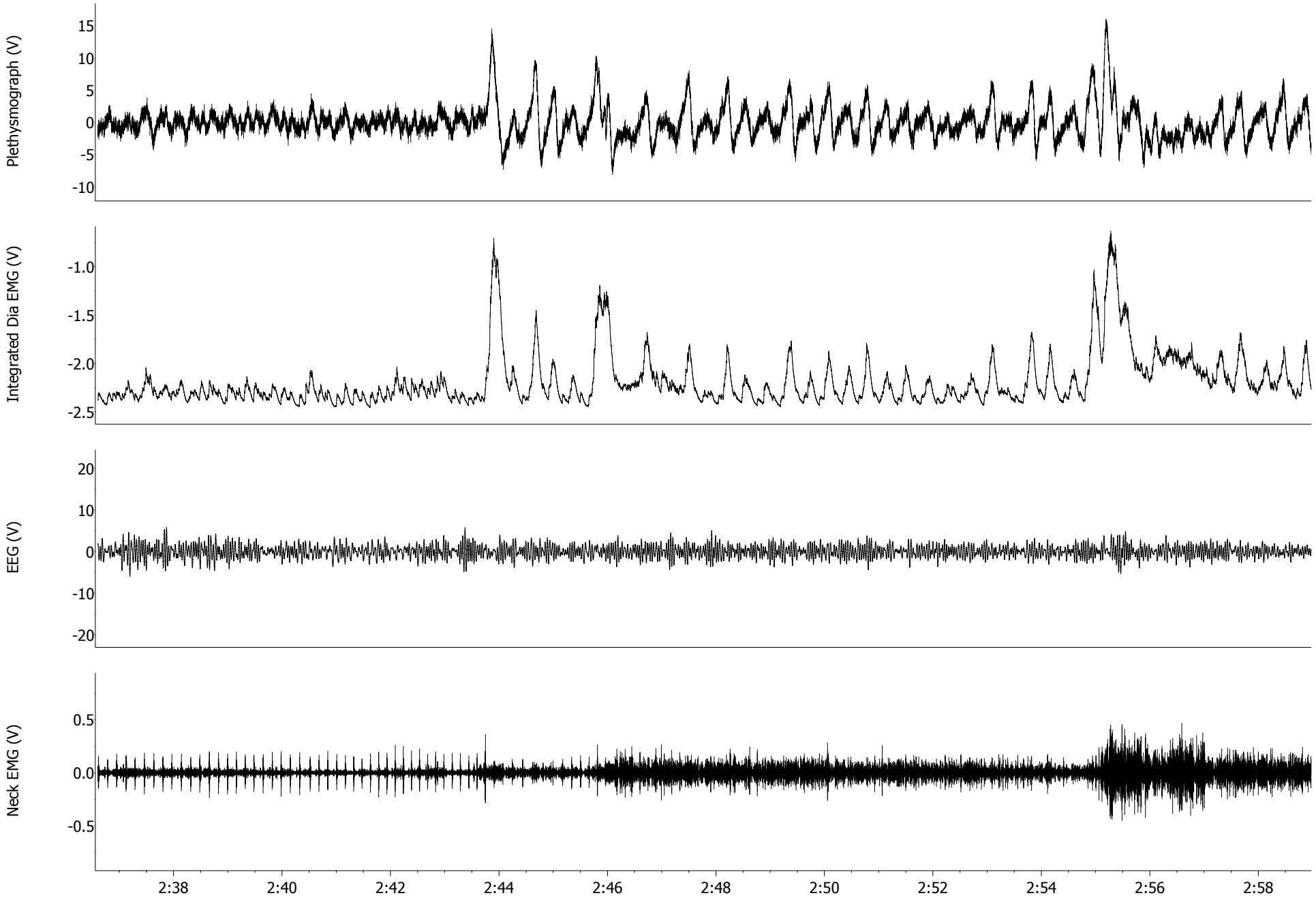

DAY8 Post-injection

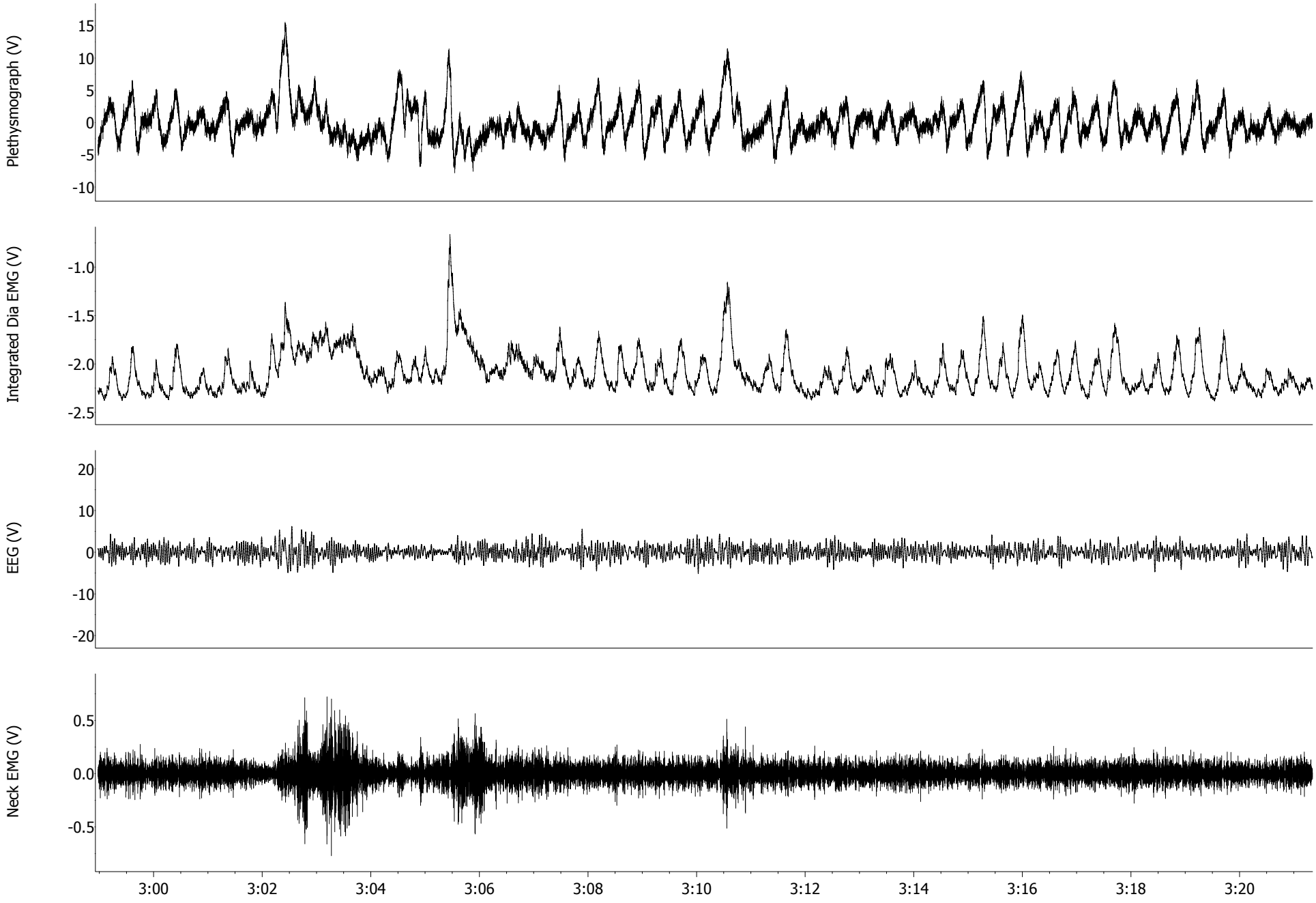

DAY8 Post-injection

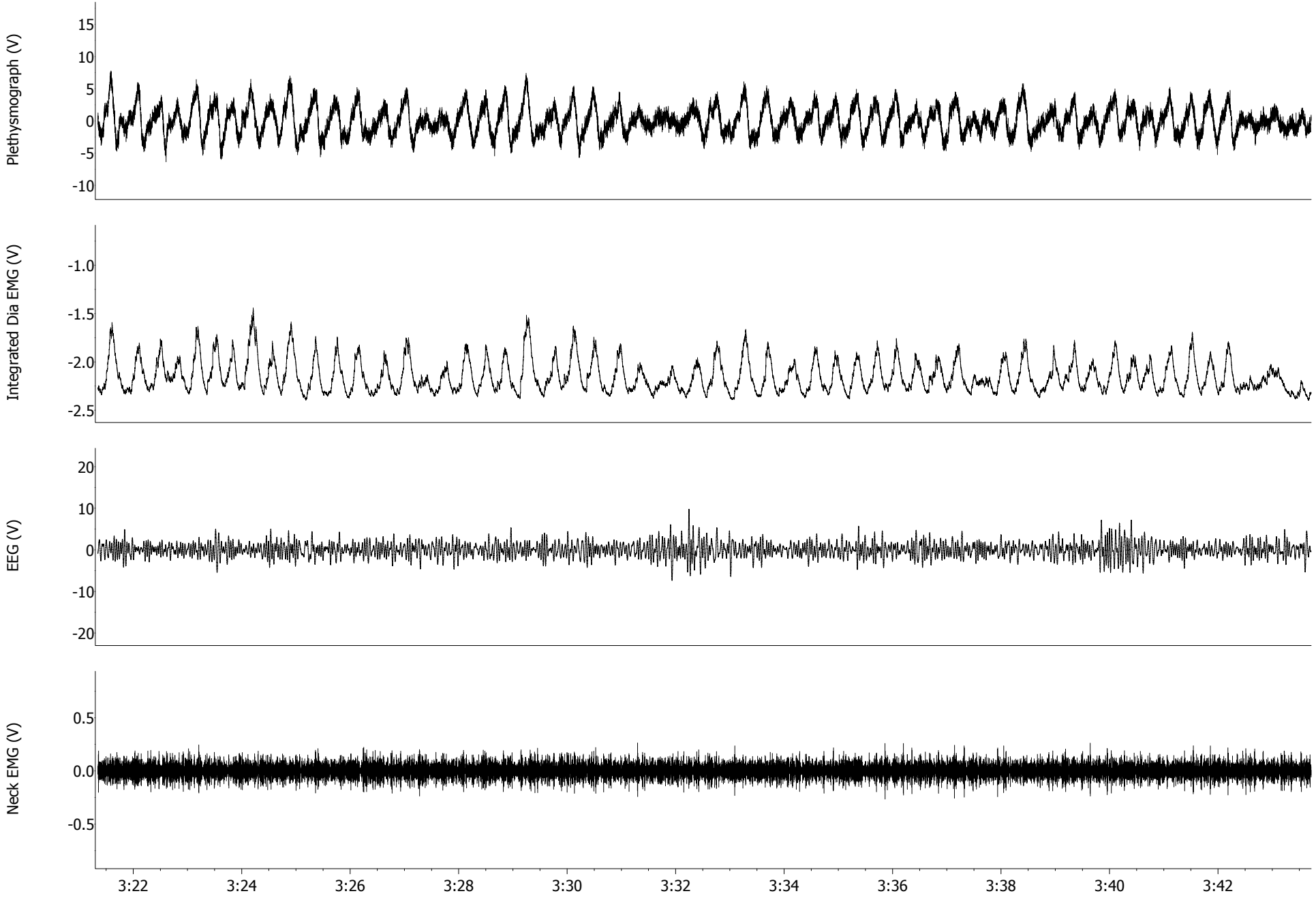

DAY8 Post-injection

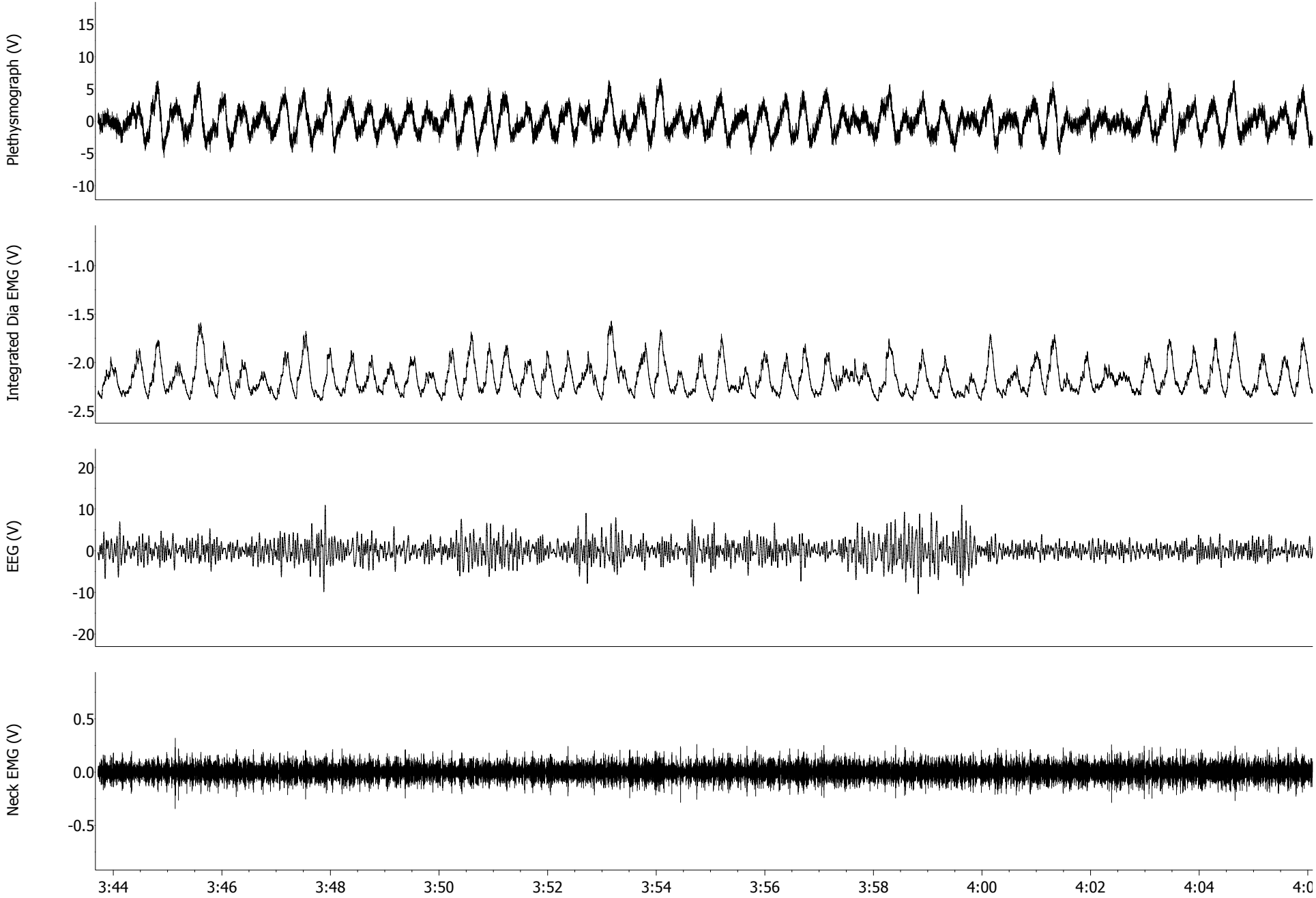

DAY8 Post-injection

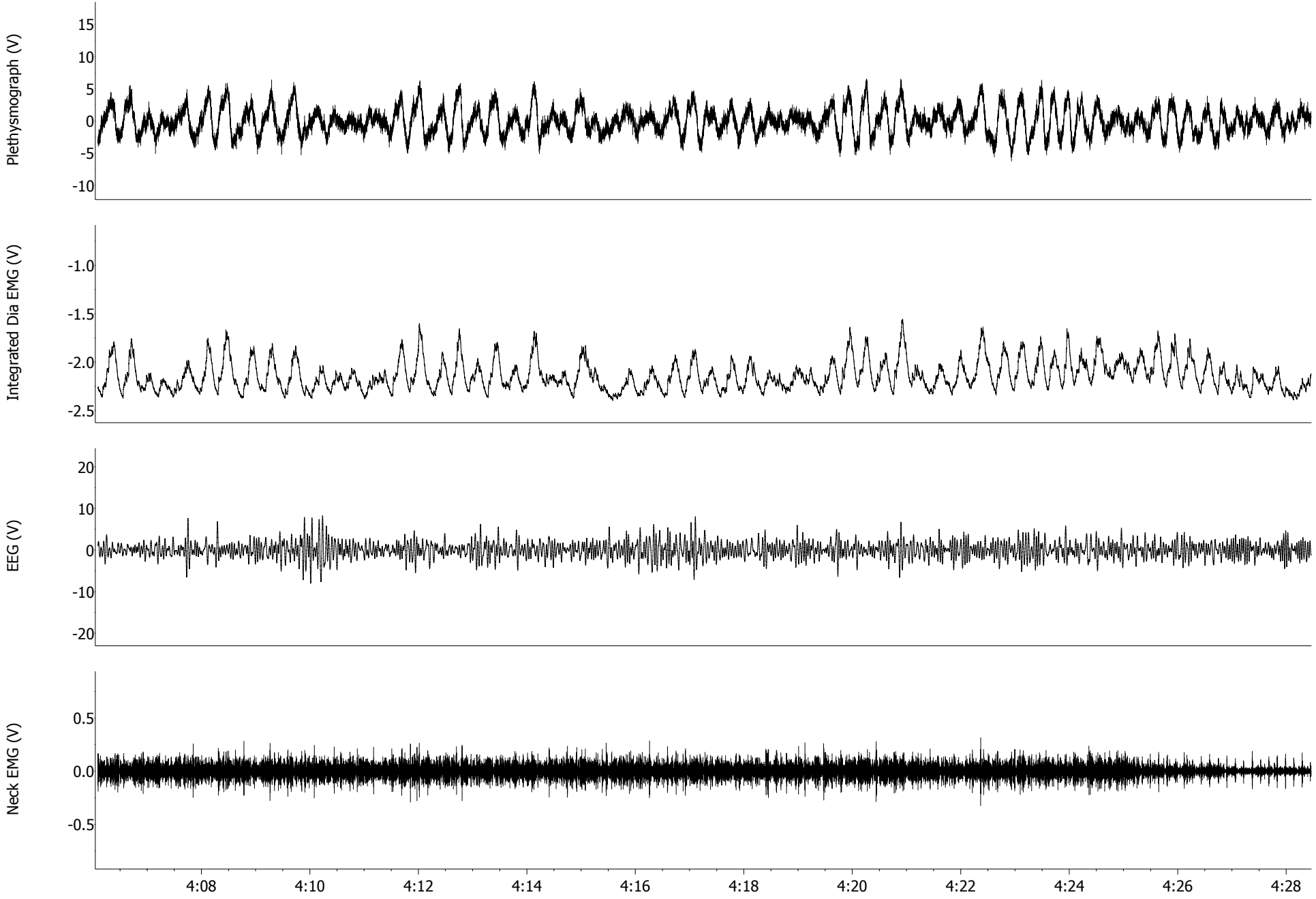

DAY8 Post-injection

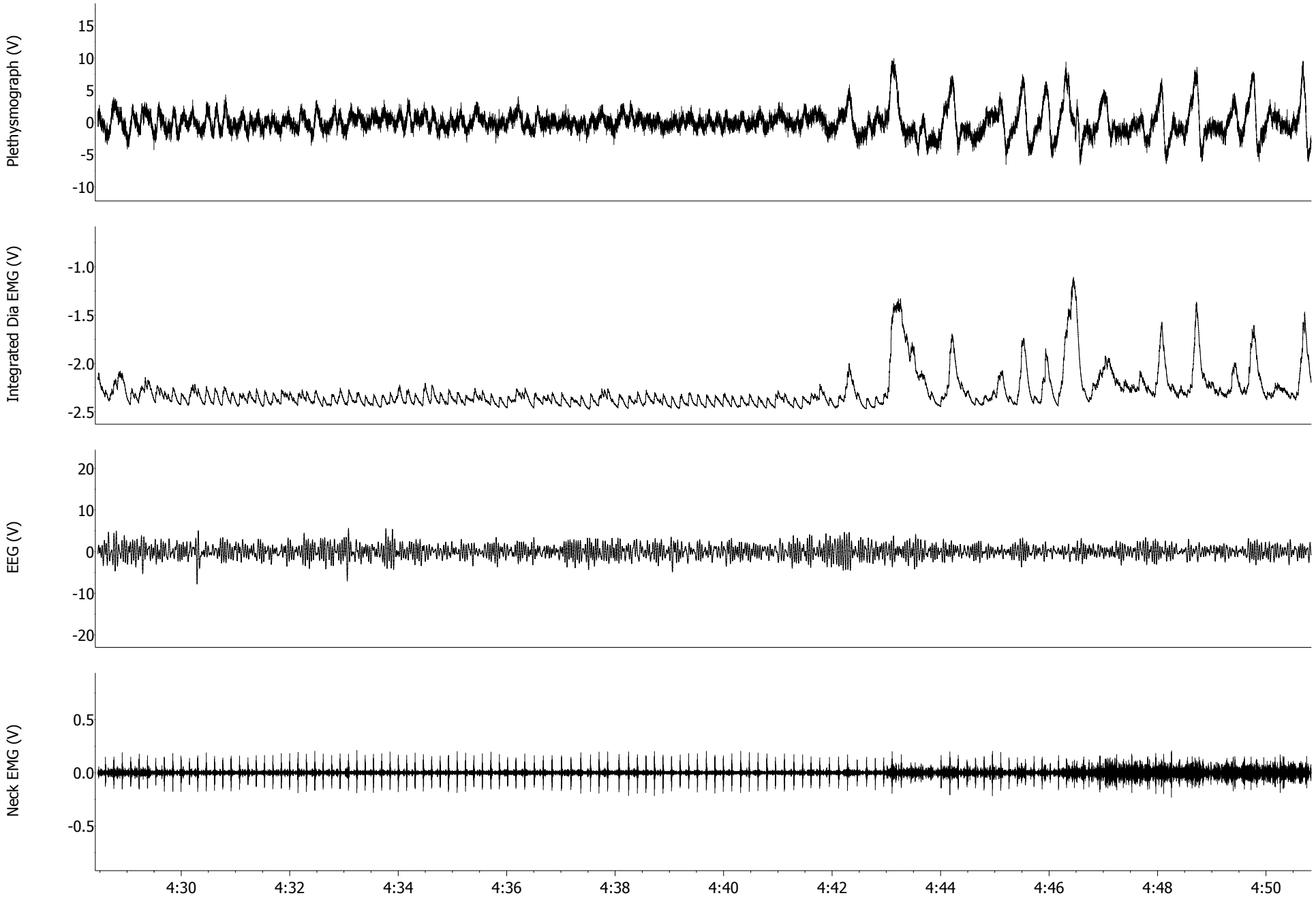

DAY8 Post-injection

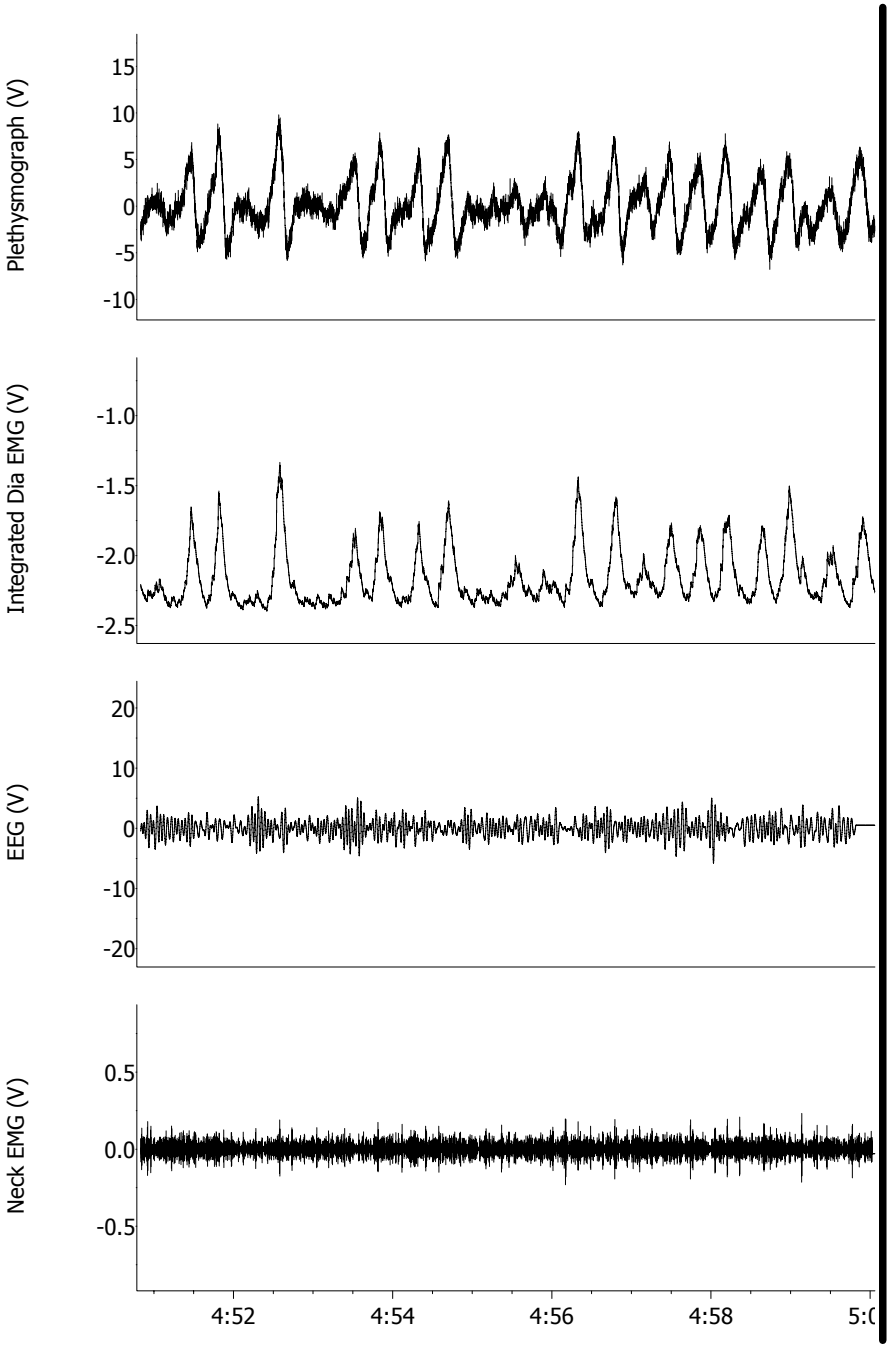

Supplementary Figure 5: Continuous 5 minute physiological recordings on day 8 post-injection. Tracings as in *Supplementary Fig. 2*. Rats were rarely able to complete a sleep cycle without a striking respiratory disturbance. During NREM, respiratory disturbances, characterized by hypopnea, dramatically increased in frequency, with apnea developing upon transition to REM and breathing only resuming upon waking. During wakefulness, breathing became increasingly irregular compared to that seen pre-injection, with larger, high frequency breaths interspersed with hypopnea and short apneas.

DAY10 Post-injection

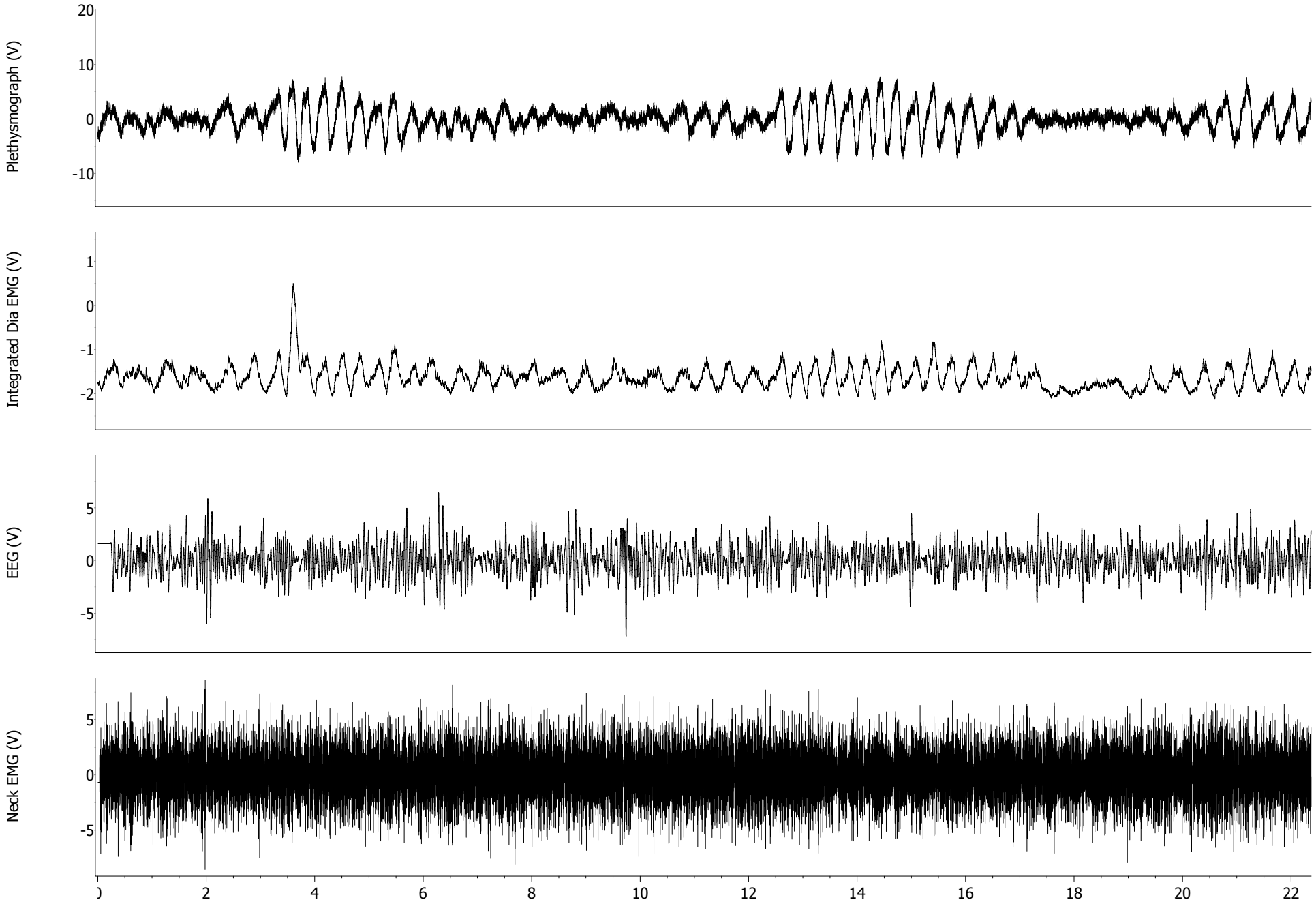

DAY10 Post-injection

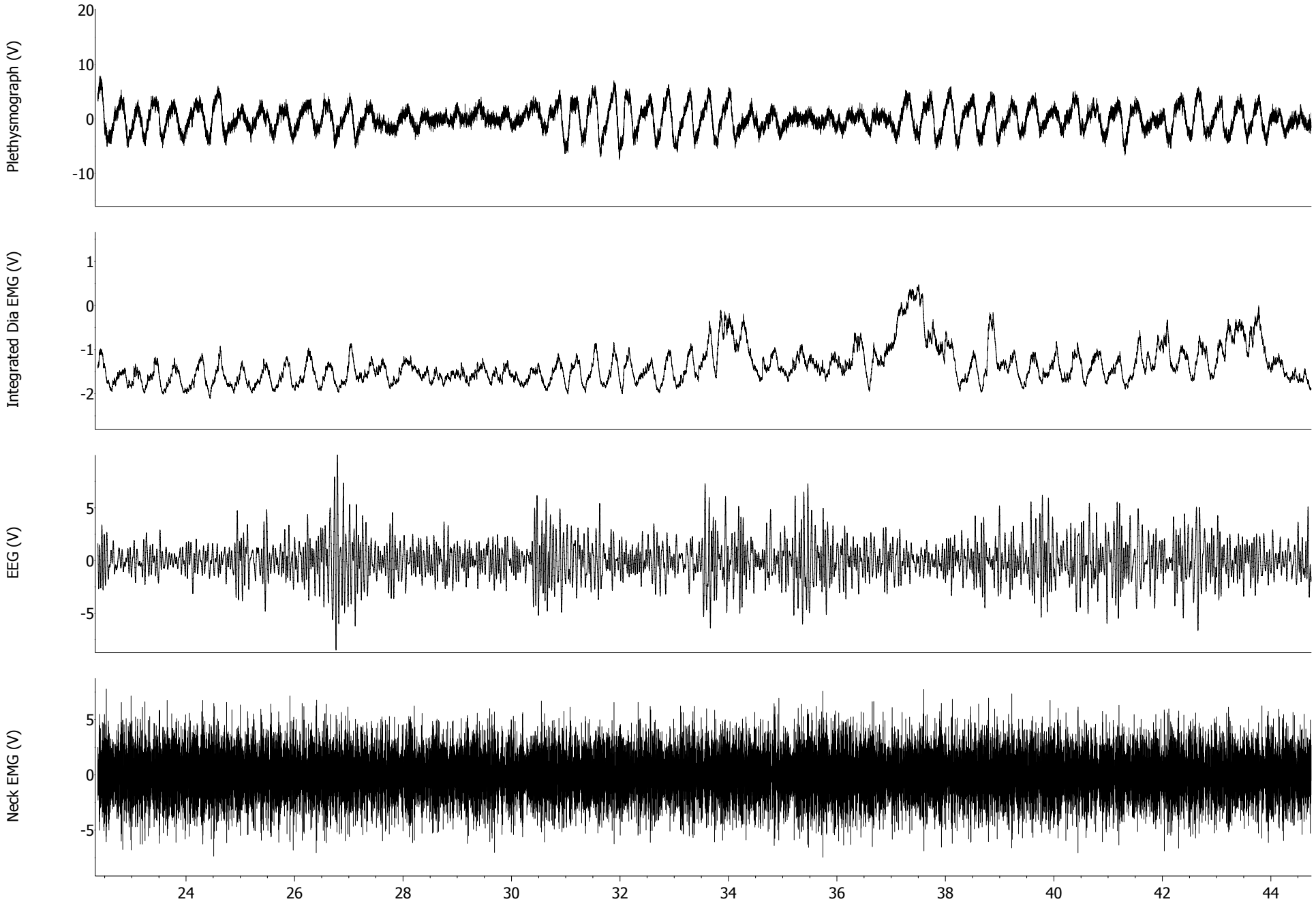

DAY10 Post-injection

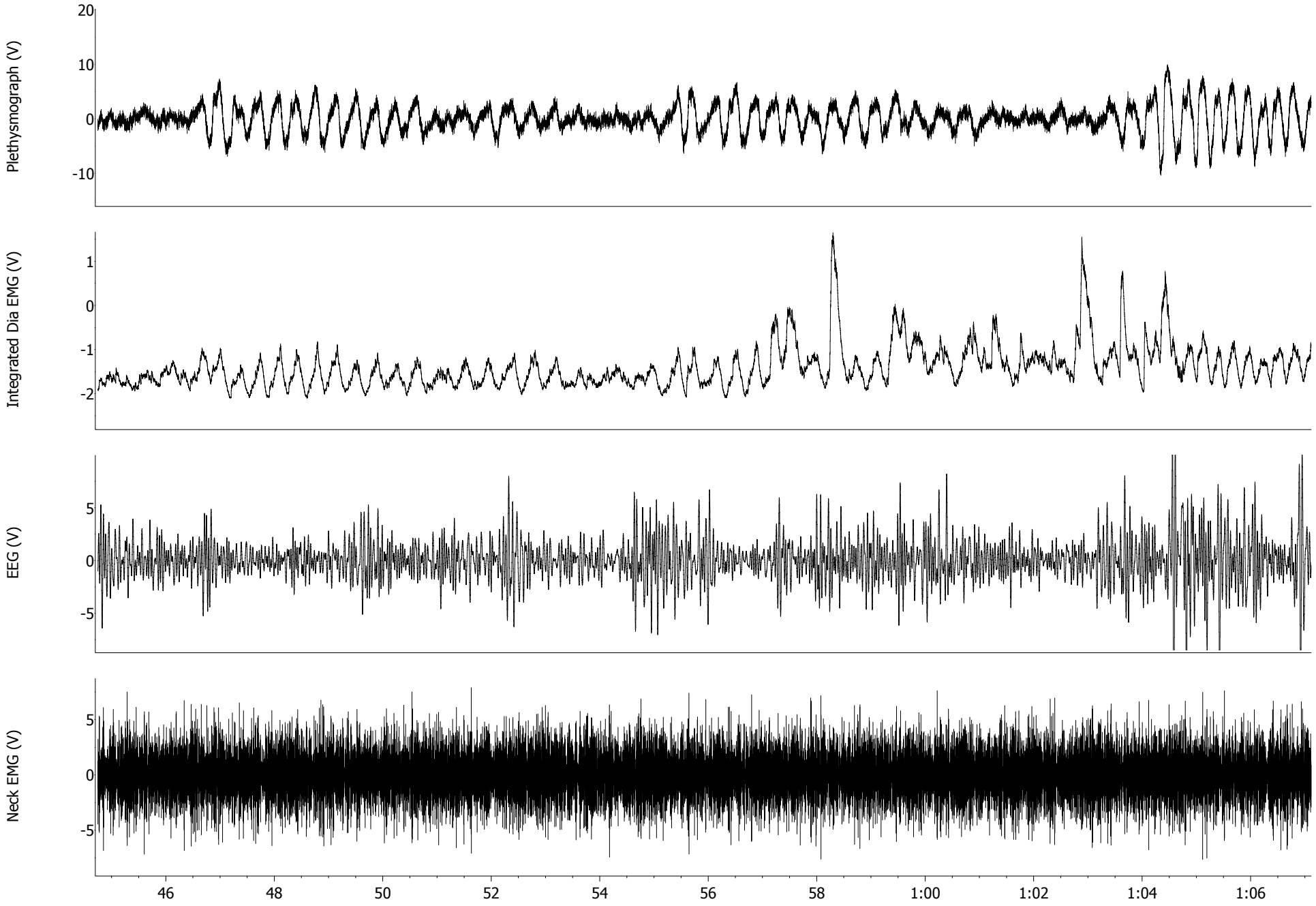

DAY10 Post-injection

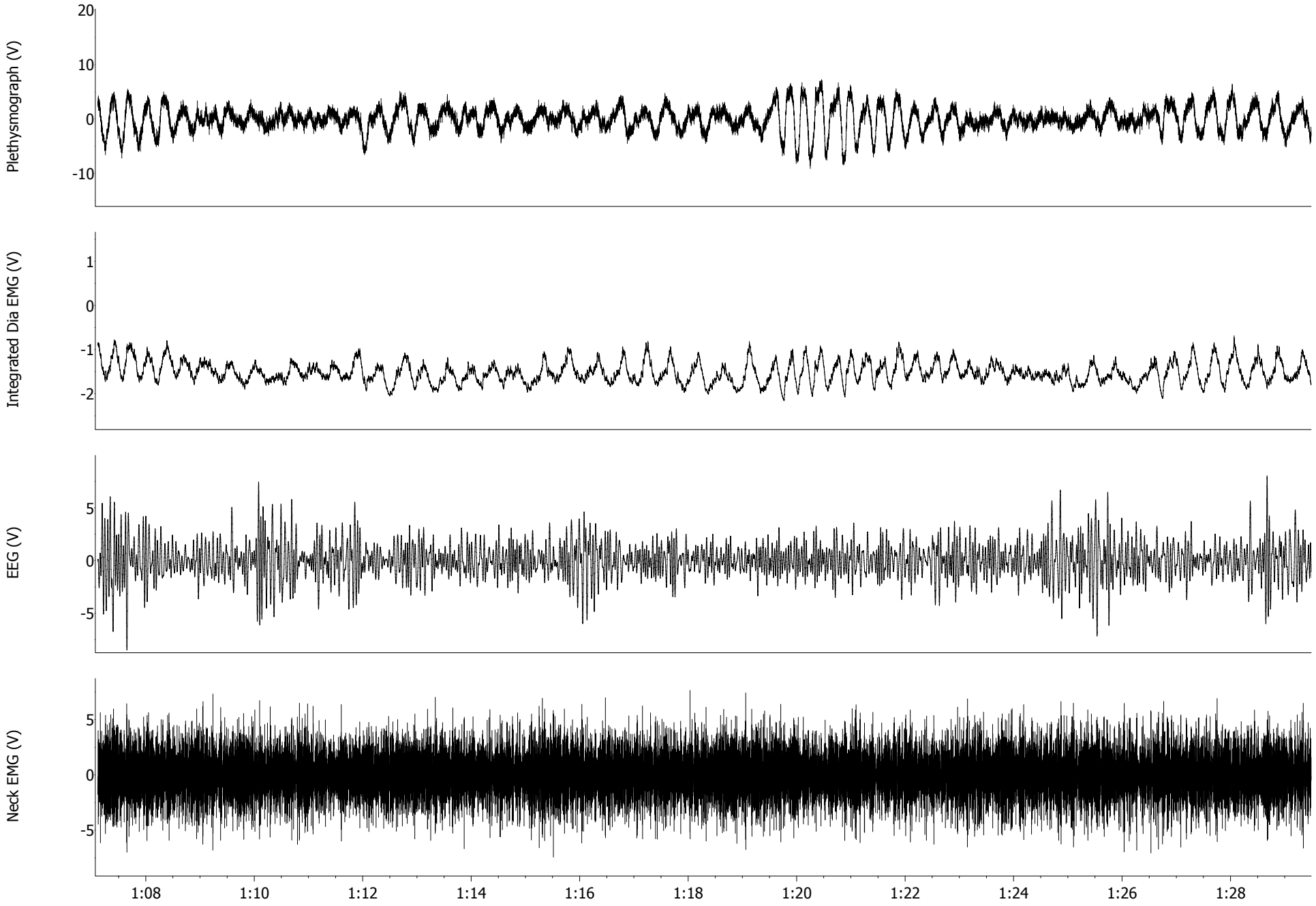

DAY10 Post-injection

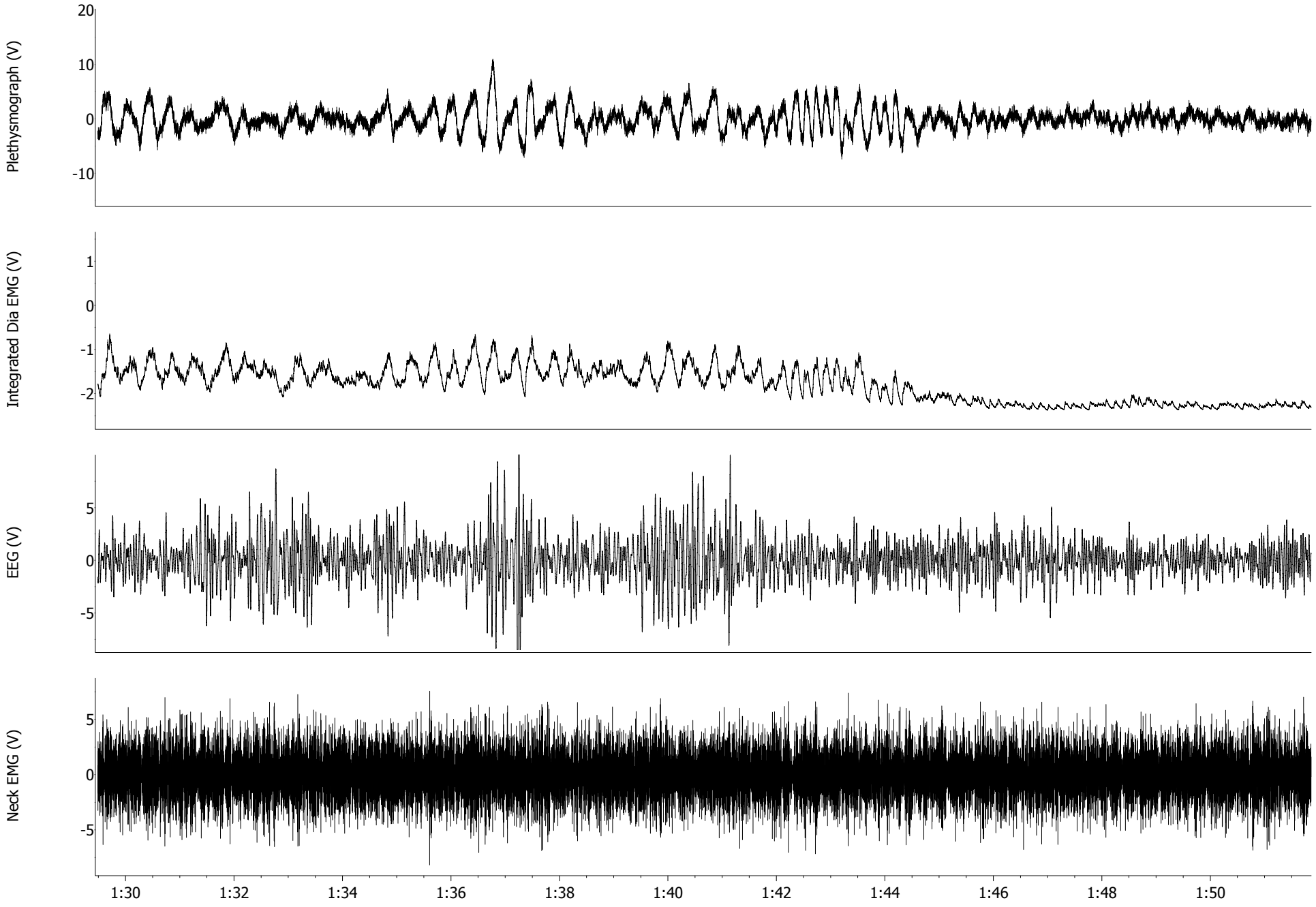

DAY10 Post-injection

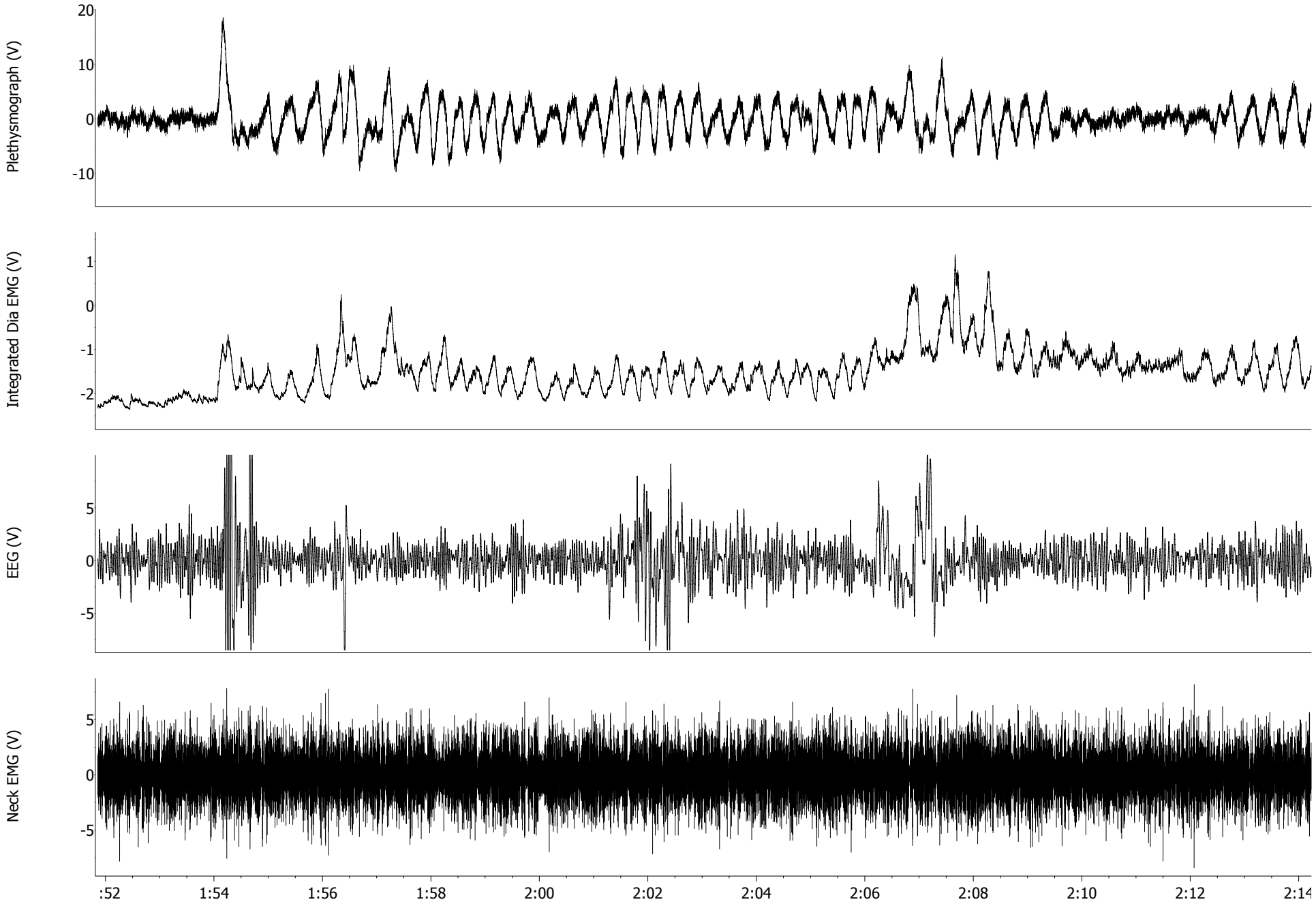

DAY10 Post-injection

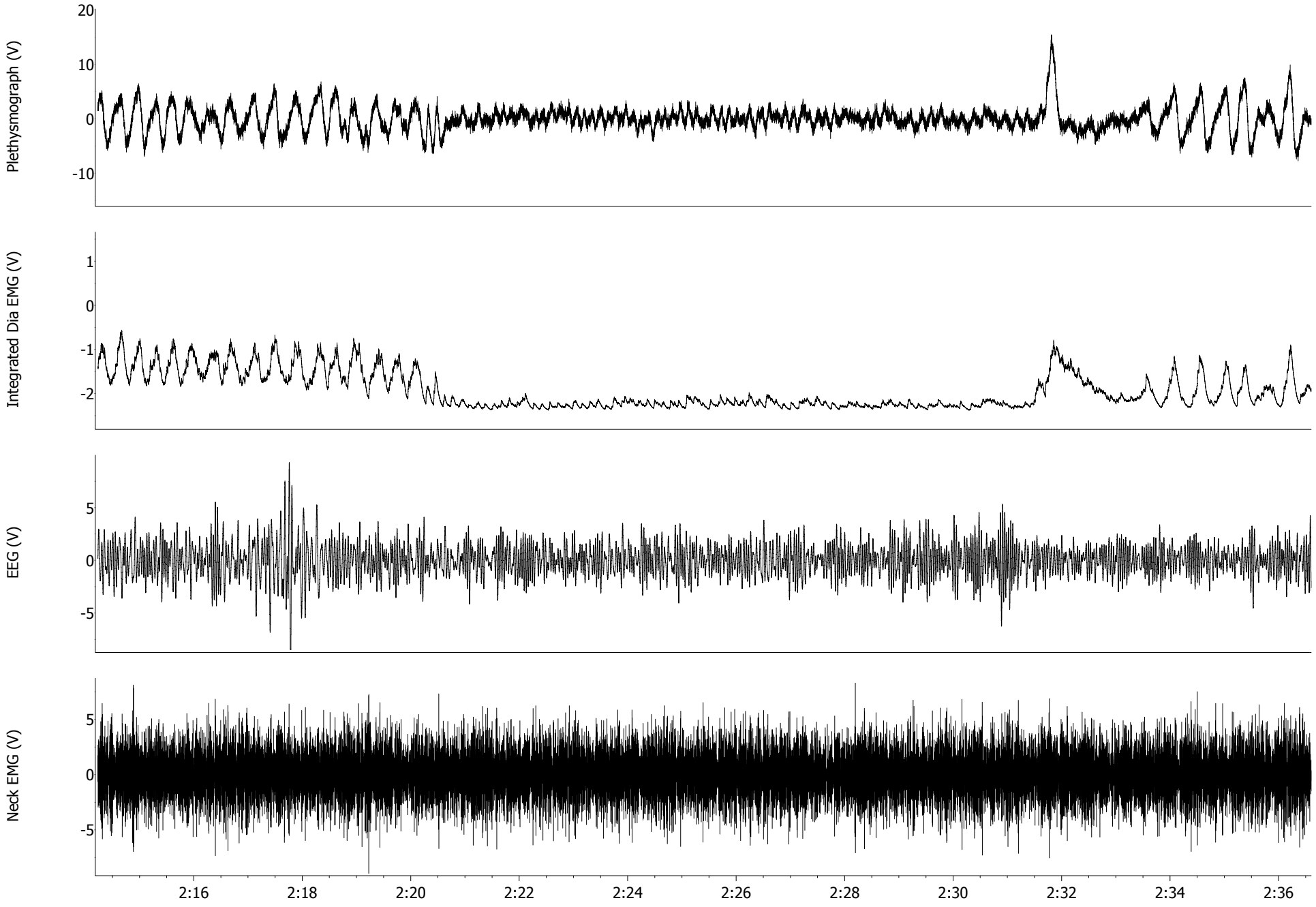

DAY10 Post-injection

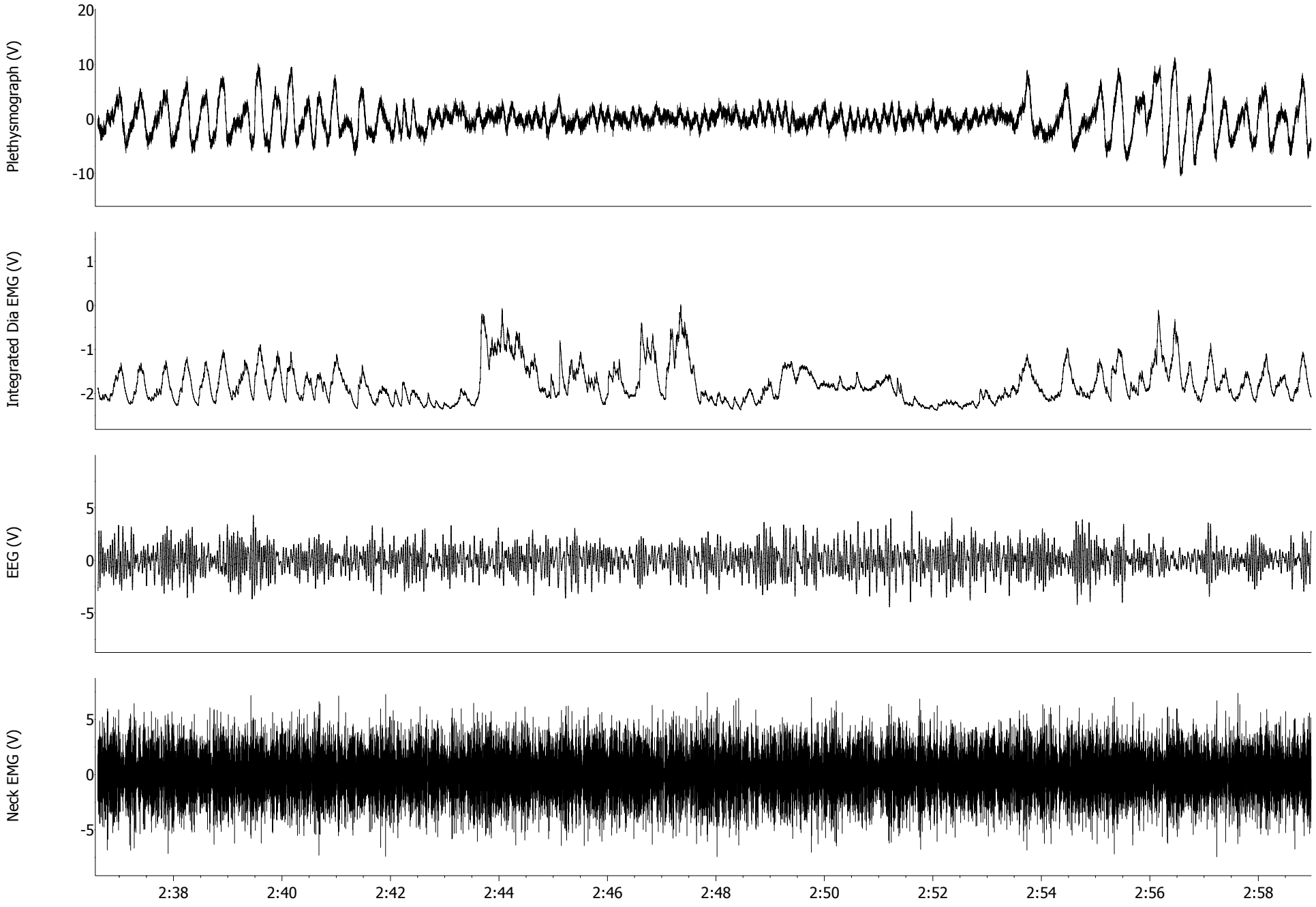

DAY10 Post-injection

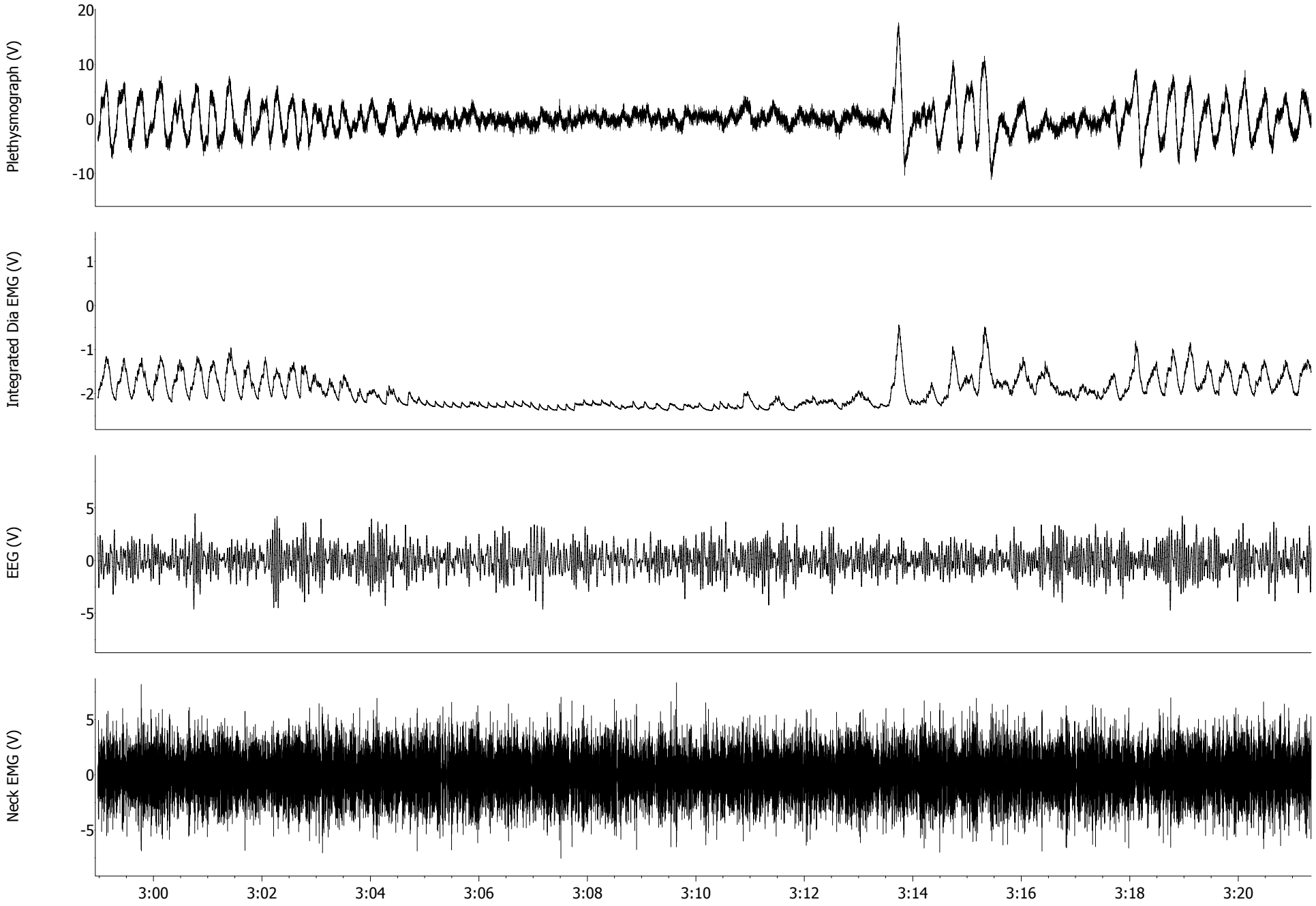

DAY10 Post-injection

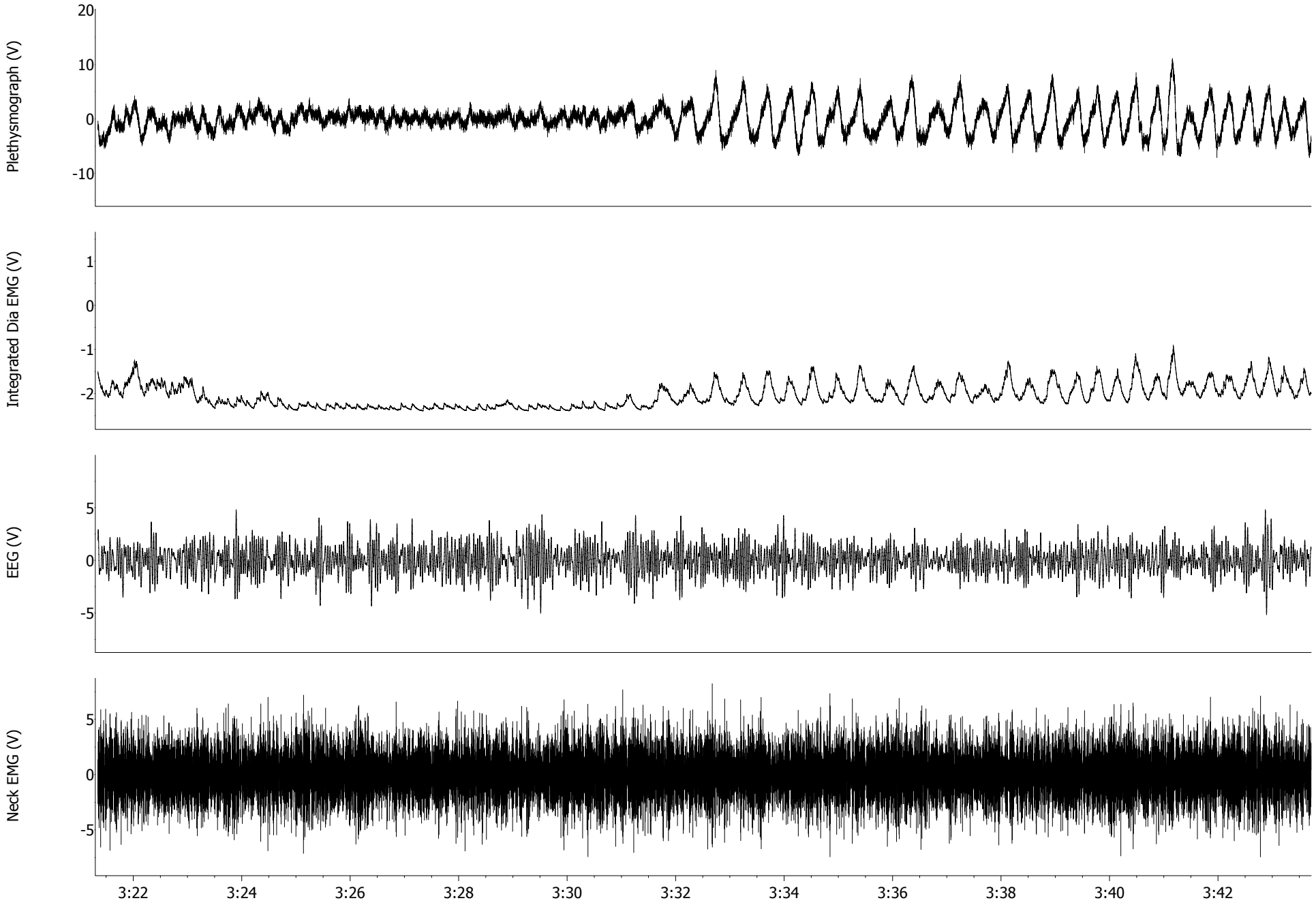

DAY10 Post-injection

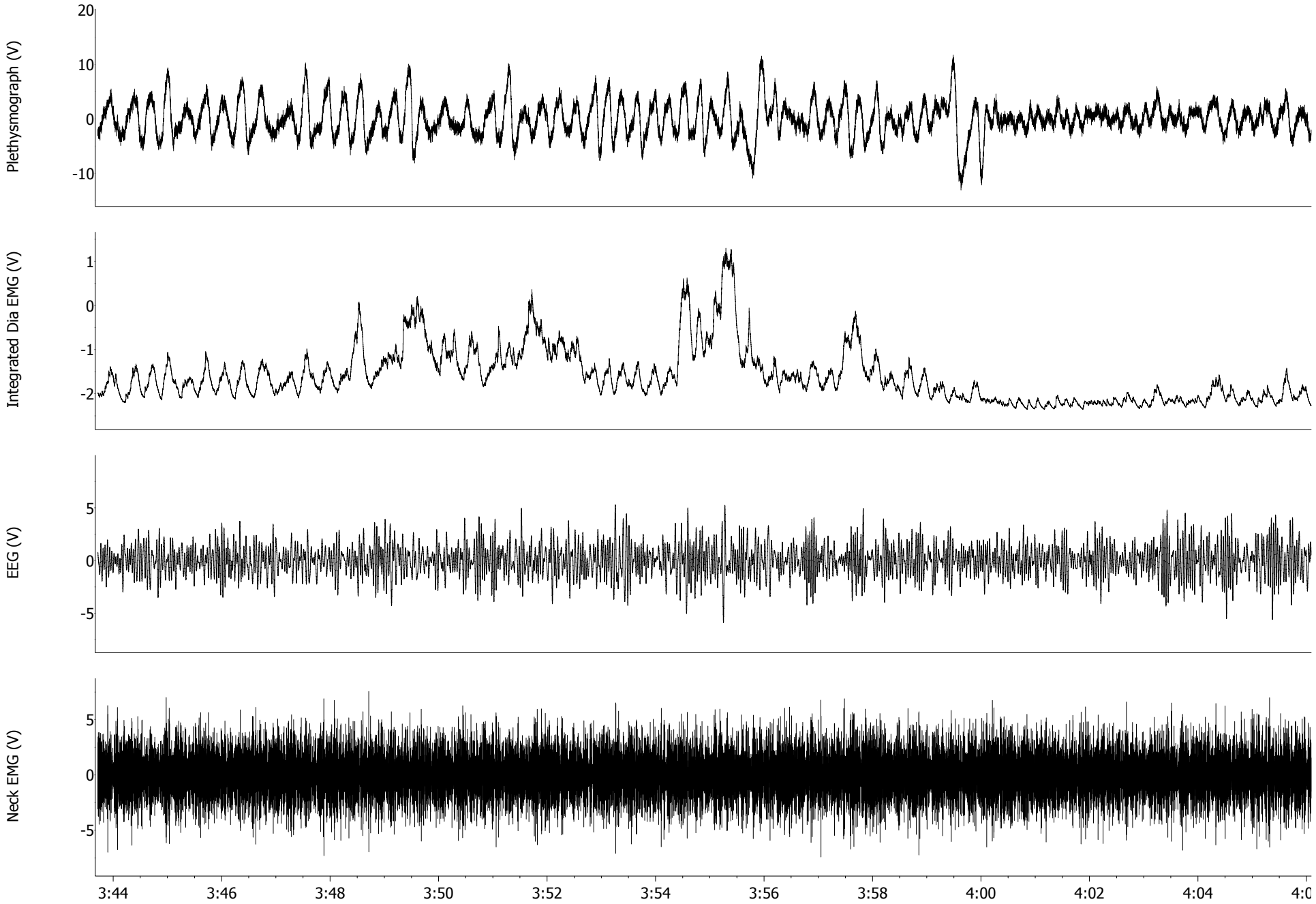

DAY10 Post-injection

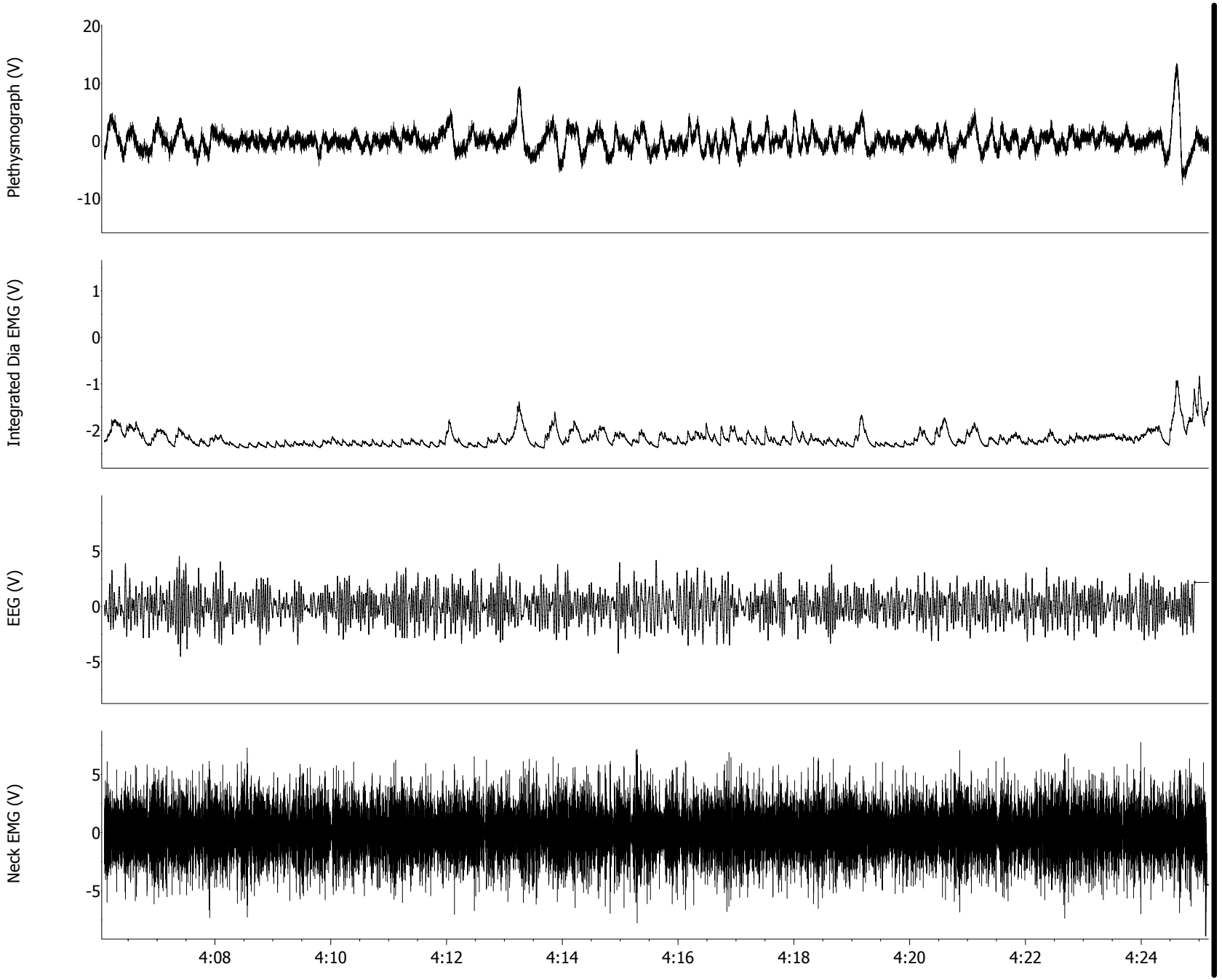

Supplementary Figure 6: Continuous 5 minute physiological recordings on day 10 post-injection. Tracings as in *Supplementary Fig. 2*. A stereotypical ataxic breathing pattern developed during wakefulness, consisting of an irregular sequence of high frequency, large breaths interspersed with numerous hypopneas and apneas. Breathing terminated immediately upon sleep onset and did not start until the rat (abruptly) awakened. A periodic Cheyne-Stokes-like pattern was intermingled with the ataxic breathing pattern.

Supplementary Methods

Surgical Procedures

All experimental procedures were approved by the Chancellor's Animal Research Committee at the University of California Los Angeles (protocol #1994-159-31E). Male Sprague-Dawley rats (*n*=12, 250-350g) were anaesthetized with Ketamine (100 mg/kg) and Xylazine (10 mg/kg) injected intraperitoneally, and if required Isoflurane (1-2%; Abbott laboratories, Il, USA) in 100% O_2 during surgery. Pairs of electrodes, made from insulated stainless steel wire (Cooner wire, Chatsworth, USA) with the last 2 mm uninsulated, were implanted to record: diaphragm electromyography (EMG); neck EMG; electrocardiogram (ECG); and electroencephalography (EEG; electrodes screwed into the skull, one over the frontal cortex: 2 mm anterior to bregma and 2 mm to the right of midline; a second over the parietal cortex: 3 mm posterior to bregma and 2 mm to the left of midline; and a third ground electrode). These wires were tunnelled subcutaneously to a 12-pin socket secured with a skin baton between the shoulder blades.

Two weeks later a second surgery was performed to stereotaxically inject either the toxin substance P conjugated to saporin (SP-SAP; 100-150 nl; 6.7 ng; Advanced Targeting Systems, CA, USA), which selectively ablates neurons expressing NK1Rs[18,19] (*n*=8), or, as a control, SP mixed with SAP, i.e., unconjugated, which does not ablate neurons (*n*=4), bilaterally into the preBötC. Bregma was positioned 5 mm below lambda, the dorsal surface of the brainstem exposed and the position of the preBötC identified (0.9 mm rostral, 2 mm lateral and 2.7 mm ventral to the calamus scriptorius (obex)).

Microinjections from a glass capillary tube with a 40 μm tip diameter of the toxin SP-SAP were made into the left preBötC, resulting in a sigh and a slight transient increase in respiratory frequency, followed by an identical injection into the right preBötC, that slowed and in some cases transiently stopped breathing. A second pair of microinjections was made just caudal to the first pair, eliciting similar responses. Mechanical ventilation was used when necessary; spontaneous breathing typically resumed within 5-15 minutes. The electrodes were left in place for 5 minutes after each injection to minimize backflow of the toxin up the electrode track. To identify the injection site, fluorescent microspheres (Molecular Probes, OR, USA) were added to the toxin solution. Post-operatively, rats received buprenorphine analgesic (0.1 mg/kg i.p., followed by 3 more injections at 12 hour intervals) and Cefipime antibiotics (6 mg/kg i.p.) for 5 days. For the first 2 days post-injection, rats appeared lethargic, with shallow breathing.

Experimental Protocol

Rats were housed in a room with a 12-hour light/dark cycle (light period from 0930-2130). During periods of data collection, rats were monitored within a plethysmograph, allowing the rats to move freely, with food and water available *ad libitum.* Post-injection, data were acquired for 9 hours/day (1000-1900) during the light cycle. The rats were monitored for any weight loss or infection; rats showing such signs were euthanized by a fatal injection of pentobarbitone (80 mg/kg i.p.).

Data analysis

Data were acquired using Chart 5 software (Powerlab 16SP, AD Instruments, USA), amplified (Grass Model P511K, Grass Instrument Co., and Animal Bioamp ML136, AD Instruments, CO, USA), filtered (EEG: 0.3-50 Hz, EMG: 10-100 Hz, ECG: 10-100 Hz) and sampled at 1000 Hz. Data acquired within a 2 hour period (between 1500 and 1800) every day post injection were analyzed. Sleep and wakefulness were determined from visual inspection, and analysis of neck EMG activity and the fast Fourier transform of the EEG signal in 5 s epochs at delta (0.3-5 Hz), theta (6-9 Hz) and sigma (10-15 Hz) frequency bands, based on the criteria defined by Benington *et al.,*[20,21]. In the awake state (WAKE) the EEG is a low amplitude, high frequency signal, low delta power, low theta*sigma power and high EMG activity; in nonREM (NREM) sleep the EEG signal is a high amplitude, low frequency signal, high delta power, moderate theta*sigma power and low EMG activity; in REM sleep the EEG is a low amplitude, high frequency signal, low delta power, high theta*sigma power and low to absent EMG activity. Data during periods of movement, which distorts the signals and prevents reliable measurements, were not analyzed; only data when the rat was asleep and in quiet wakefulness were analyzed.

Changes in breathing frequency and amplitude were measured on a breath-by-breath basis using whole body plethysmography (Buxco Electronics Inc., NY, USA). A constant airflow (1.5 l/min) was delivered through the plethysmograph chamber and respiratory parameters quantified by recording pressure fluctuations relative to a reference chamber, with a differential pressure transducer (DRAL501, Honeywell Data Instruments), that are

proportional to tidal volume. Inspiratory amplitude was calculated from the pressure signal output; control (pre-injection) data were normalized to 1 arbitrary volume unit (a.u.) and all data acquired on subsequent days were rescaled relative to control. Spontaneous respiratory disturbances were defined as hypopnea when inspiratory amplitude <0.5 a.u. and an apnea when there were no breathing movements >2s (~3 missed regular breaths). Respiratory disturbances are expressed as number of episodes normalized to 1 hour each of WAKE, NREM, and REM. All data are expressed as mean ± S.E.M. Statistical analysis were performed using Student's paired t-tests to compare means post-injection with means pre-injection, differences were regarded as significant if $p<0.05$.

Histology

Rats were anaesthetised with pentobarbitone, then transcardially perfused with 4% paraformaldehyde. The brain tissue (40 μm slices) underwent free-floating immunohisto-chemistry procedures to stain for NK1Rs (see[18]). Under light microscopy (Zeiss, Axioplan2, Carl Zeiss, USA) the extent of each lesion was determined by counting cells within a circle of 600 μm diameter enclosing the preBötC and in a larger rectangle (1600 x 1070 μm) enclosing this circle, as previously described by Gray[18].

Supplementary References

1. Morrell, M. J. et al. *Sleep Med* **4**, 451-4 (2003).
2. Macey, P. M. et al. *Am J Respir Crit Care Med* **166**, 1382-7 (2002).
3. Cohen-Zion, M. et al. *J Am Geriatr Soc* **49**, 1622-7 (2001).

4. Salorio, C. F., White, D. A., Piccirillo, J., Duntley, S. P. & Uhles, M. L. *J Clin Exp Neuropsychol* **24**, 93-100 (2002).

5. Ancoli-Israel, S. et al. *Sleep* **19**, 277-82 (1996).

6. Nogues, M. et al. *Neurology* **52**, 1777-83 (1999).

7. Arnulf, I. et al. *Am J Respir Crit Care Med* **161**, 849-56 (2000).

8. Barthlen, G. M. & Lange, D. J. *Eur J Neurol* **7**, 299-302 (2000).

9. Ferguson, K. A., Strong, M. J., Ahmad, D. & George, C. F. *Chest* **110**, 664-9 (1996).

10. Munschauer, F. E., Loh, L., Bannister, R. & Newsom-Davis, J. *Neurology* **40**, 677-9 (1990).

11. Guilleminault, C., Briskin, J. G., Greenfield, M. S. & Silvestri, R. *Sleep* **4**, 263-78 (1981).

12. Cormican, L. J., Higgins, S., Davidson, A. C., Howard, R. & Williams, A. J. *Eur Respir J* **24**, 323-5 (2004).

13. Maria, B. et al. *Respir Med* **97**, 1151-7 (2003).

14. Apps, M. C., Sheaff, P. C., Ingram, D. A., Kennard, C. & Empey, D. W. *J Neurol Neurosurg Psychiatry* **48**, 1240-5 (1985).

15. Efthimiou, J., Ellis, S. J., Hardie, R. J. & Stern, G. M. *Adv Neurol* **45**, 275-6 (1987).

16. Tsuda, T., Onodera, H., Okabe, S., Kikuchi, Y. & Itoyama, Y. *Ann Neurol* **52**, 367-71 (2002).

17. Onodera, H., Okabe, S., Kikuchi, Y., Tsuda, T. & Itoyama, Y. *Lancet* **356**, 739-40 (2000).

18. Gray, P. A., Janczewski, W. A., Mellen, N., McCrimmon, D. R. & Feldman, J. L. *Nat Neurosci* **4**, 927-30. (2001).

19. Mantyh, P. W. et al. *Science* **278**, 275-9. (1997).

20. Benington, J. H., Kodali, S. K. & Heller, H. C. *Sleep* **17**, 28-36. (1994).

21. Nattie, E. E. & Li, A. CO2 dialysis in the medullary raphe of the rat increases ventilation in sleep. *J Appl Physiol* **90**, 1247-57 (2001).

22. Guyenet, P. G., Sevigny, C. P., Weston, M. C. & Stornetta, R. L. *J Neurosci* **22**, 3806-16 (2002).

Note: Studies of clinical relevance to our findings.

Sleep-disordered breathing can result in intermittent episodes of hypoxia, the cumulative effect of which includes the possible loss of brain gray matter [1,2], impaired cognitive function [3,4], and increased mortality [5]. Here, preBötC neuronal loss caused multiple repeated episodes of (apnea-induced) hypoxia that would likely have caused further neuronal loss [1,2]. We suggest that this effect was minor during the early stages of sleep-disordered breathing, i.e., days 3-6, because the disturbances were limited in total duration, so the initial changes in breathing pattern were the direct effect of NK1R preBötC neuron loss. Beyond this point, however, the cumulative effect of intermittent hypoxia resulting from prolonged apneas could have induced neuronal death, not necessarily restricted to the preBötC, further disrupting respiratory pattern during sleep and wakefulness.

Adults with syringobulbia (with brainstem symptoms or MRI evidence of medullary syrinx) breathe relatively normally during wakefulness but during sleep, breathing patterns are severely disrupted by the occurrence of central apneas or severe hypopneas[6]. Respiratory disorders in sleep are common in patients with some neurodegenerative diseases e.g., amyotrophic lateral sclerosis (ALS)[7-9], multiple systems atrophy (MSA)[10-12], or Parkinson's disease (PD)[13-15], while breathing during wakefulness is considered otherwise normal. Many of these patients die suddenly during sleep[7,10,13]. Additionally, patients with MSA or PD also have impaired chemosensitivity to hypoxia[16,17], which in rats can result from loss of preBötC neurons[18].